Holocene and Last Glacial Maximum (paleo-) productivity off Morocco: Evidence from benthic foraminifera and stable carbon isotopes

(Paläo-) Produktivität im Holozän und Letzten Glazialen Maximum vor Marokko aus benthischen Foraminiferen und stabilen Kohlenstoffisotopen

---

Astrid Eberwein

Ber. Polarforsch. Meeresforsch. xxx (2006)
ISSN 1618-3193

Astrid Eberwein
Alfred Wegener Institute for Polar and Marine Research
Am Alten Hafen 26
27568 Bremerhaven
Germany
e-mail: aeberwein@awi-bremerhaven.de

Die vorliegende Arbeit ist die inhaltlich unveränderte Fassung einer kumulativen Dissertation, die im Juni 2006 dem Fachbereich Geowissenschaften der Universität Bremen vorgelegt wurde.

Table of contents

Abstract

I used the distribution and composition of benthic foraminiferal faunas as well as the stable carbon isotopic signals of benthic foraminiferal tests as proxy in determining and reconstructing (paleo-) productivity during the Holocene and the Last Glacial Maximum (LGM). The investigation area is located between Cape Yubi (27.5°N) and Cape Ghir (31°N) off Morocco (NW-Africa). Present chloropyll-*a* distributions in surface waters inferred from satellite imagery indicate that the investigated stations cover different productivity regimes. First, benthic foraminifera were calibrated as proxy regarding productivity. In this context, the influence of different environmental parameters on live (Rose Bengal stained) and dead species in sediment surface samples (0 – 1 cm) was examined. Furthermore, the impact of organic carbon fluxes on the microhabitat distribution of live benthic foraminifera (0 – 10 cm) was investigated. Finally, the potential of benthic foraminifera as productivity proxy was used to reconstruct paleoproductivity during the LGM.

The results revealed a high productivity variability in the upwelling region off Morocco in the Holocene and during the LGM. Generally, the local productivity during the LGM was more heterogeneous than presently. It turned out that productivity, and the resulting organic matter export to the sea-floor, are the most important factors controlling the horizontal as well as vertical distribution and composition of Holocene benthic foraminiferal faunas. In the cape regions, identical live and dead assemblages, high standing stocks, and low species $\delta^{13}C$ values reflect the highly productive Cape Ghir and Cape Yubi filaments. The faunal succession from the shelf to the deep sea, the decrease in total standing stocks and the increase of the average living depth of *Globobulimina affinis* reflect the decrease in organic matter fluxes. By contrast, the area between the capes is characterised by differently composed live and dead faunas, low standing stocks, and higher $\delta^{13}C$ values, thus reflecting low to slightly seasonally varying productivity in the Holocene.

During the LGM, paleoproductivity was higher in the area between the capes than in the Holocene, whereas paleoproductivity was comparably high off the capes. Four major regions with characteristic productivity regimes were distinguished: (1) the region off Cape Yubi was characterised by highest paleoproductivity; (2) west and southwest off Cape Ghir moderate to high, seasonally fluctuating paleoproductivity was predominant; (3) the region southwest off Cape Yubi was characterised by moderate, highly seasonally varying paleoproductivity; and (4) the region further offshore Cape Ghir was characterised by highest seasonally varying paleoproductivity.

Zusammenfassung

Im Rahmen dieser Studie diente die faunistische Zusammensetzung und Verbreitung benthischer Foraminiferen, sowie die stabilen Kohlenstoff-Isotopenverhältnisse ihrer Gehäuse als Indikatoren zur Erkennung der Primärproduktion im Holozän und zur Rekonstruktion der Paläoproduktion während des Letzten Glazialen Maximums (LGM). Das Arbeitsgebiet befindet sich zwischen Kap Ghir (31°N) und Kap Yubi (27.5°N) vor der marokkanischen Küste (NW-Afrika). Rezente Chlorophyll-*a* Gehalte im Oberflächenwasser verdeutlichen, dass die analysierten Proben unterschiedliche Produktivitätsregime abdecken. Benthische Foraminiferen wurden zunächst bezüglich der Produktivität geeicht, um sie anschliessend als leistungsfähigen Paläoproduktivitätsproxy für das LGM einzusetzen. Für diese Kalibrierung wurde der Einfluss unterschiedlicher Umweltparameter auf die Zusammensetzung und Verteilung der Lebend- und Totfauna und die Auswirkung von organischen Kohlenstoffflüssen auf die Mikrohabitatverteilung lebender benthischer Foraminiferen des Holozäns untersucht.

Die Ergebnisse bestätigen, dass das Auftriebsgebiet vor Marokko im Holozän durch starke Produktivitätsunterschiede gekennzeichnet ist und verdeutlichen, dass die regionale Produktivitätsvariabilität im LGM deutlich stärker ausgeprägt war. Es wurde gezeigt, dass der entscheidendste Faktor, der die holozäne horizontale und vertikale Verteilung und Zusammensetzung benthischer Foraminiferenfaunen bestimmt, die Primärproduktion und der Export von organischer Substanz zum Meeresboden ist. In den Kapregionen wird die hohe Produktivität der Kap Ghir und Kap Yubi Filamente durch identische Lebend- und Totfaunen, hohe Siedlungsdichten sowie niedrige $\delta^{13}C$ Werte reflektiert. Die Abfolge der benthischen Foraminiferenvergesellschaftungen entlang des Transekts vom Schelf zur Tiefsee, die Abnahme der Siedlungsdichten und die Zunahme der mittleren Lebenstiefe von *Globobulimina affinis* zeigen den abnehmenden Export organischen Materials an. Im Gegensatz dazu ist die Region zwischen den beiden Kaps durch niedrige bis saisonal schwankende Primärproduktion charakterisiert. Dies spiegelt sich in unterschiedlichen Lebend- und Totfaunen, niedrigen Siedlungsdichten sowie höheren $\delta^{13}C$ Werten wider.

Im LGM war die Paläoproduktivität im Gebiet zwischen den Kaps erhöht im Vergleich zum Holozän, wohingegen sie vor den Kaps vergleichbar war. Im LGM lassen sich vier Regionen mit charakteristischen Paläoproduktivitätsregime unterscheiden: (1) Die Region vor Kap Yubi zeichnete sich durch höchste Paläoproduktivität aus; (2) in der Region vor Kap Ghir war moderate bis hohe, saisonal schwankende Paläoproduktivität vorherrschend; (3) die Region südwestlich von Kap Yubi war durch moderate, saisonal stark variierende Paläoproduktivität charakterisiert; und (4) in der Region vor Kap Ghir existierte die am stärksten saisonal variierende Paläoproduktivität.

Danksagung

Mein erster Dank gilt meinem Doktorvater Prof. Dr. Andreas Mackensen für die Vergabe und Betreuung dieser Arbeit. Ich danke Dir für die enthusiastische Diskussionsbereitschaft und konstruktive Kritik, die mich immer wieder motiviert haben, sowie die Unterstützung bei der Teilnahme an Expeditionen und Konferenzen. Vielen herzlichen Dank für Deine Unterstützung und Prioritätensetzung bei der Umsetzung meiner Pläne in der Endphase! Herrn Prof. Dr. Gerold Wefer danke ich für die Übernahme des Zweitgutachtens.

Ich danke der Besatzung des Forschungsschiffes *Meteor* für ihre ausgezeichnete Arbeit während der Expeditionen, die erst die Bearbeitung des Probenmaterials im Rahmen dieser Dissertation ermöglicht hat, sowie die angenehme Atmosphäre.

Für die exzellente technische Unterstützung, vielfältige und geduldige Hilfe im Labor und am REM, das Suchen und Finden diverser Proben danke ich Ute Bock, Volker Diekamp, Beate Hollmann, Gerd Kuhn, Almuth Maschner, Günther Meyer, Birgit Meyer-Schack, Maike Scholz, Monika Segl, Susanne Wiebe und Alexius Wülbers.

Viele Kollegen haben durch ihr Interesse, ihre Diskussionsbereitschaft und das Bereitstellen von Rohdaten zum erfolgreichen Gelingen dieser Arbeit beigetragen. Ich danke Sylvia Brückner, Catalina Gebhardt, Helena Filipsson, Tim Freudenthal, Peer Helmke, David Heslop, Claus-Dieter Hillenbrand, Ulrike Holzwarth, Sabine Kasten, Holger Kuhlmann, Laetitia Licari, Helge Meggers, Susanne Neuer, Gerhard Schmiedl, Stefanie Schumacher, Dorit Siggelkow, Silke Steph, Julia Thiele und Michelle Zarrieß.

Meinen Freunden einen ganz lieben und herzlichen Dank für die vielen schönen und lustigen Freizeitaktivitäten und die Sonnennachmittage und -abende am Deich, insbesondere in der Endphase der Promotion, die mir immer wieder positive Energie gegeben haben und mir gezeigt haben, dass DAS LEBEN LACHT! Ich habe wieder mehr Zeit für‘s Powershoppen und hoffe, Ihr kommt alle mit nach Dubai :-) Meiner Familie gilt ein ganz spezieller Dank für die Unterstützung in vielerlei Hinsicht. ‘Jedem Anfang wohnt ein Zauber inne‘ (Hermann Hesse).

1. INTRODUCTION

Ocean margins are high-production systems and, therefore, provide high resolution sedimentary archives, in which significant information of Earth's climate history is stored. Coastal upwelling areas are of particular interest, since the biological production accounts for 80 % of the total marine new production (Berger et al., 1989). This marine production is affected by the global and, particularly, regional atmospheric and oceanographic circulation. Enhanced atmospheric circulation is suggested to be responsible for stronger upwelling, which in turn increases the primary productivity in surface waters. Amongst other factors, organic matter production is considered to control the exchange of the greenhouse gas carbon dioxide between the atmosphere and ocean, which in turn causes present and past climate variations.

Benthic foraminifera are a valuable proxy for paleoceanographic reconstructions, since they have a long geological record, an ubiquitous distribution and their calcareous tests have a high fossilisation potential. Distinct benthic foraminiferal faunal compositions and the stable isotopic composition of their calcareous tests in Recent sediments provide substantial information about the association with present environmental conditions. In this context, the attention is focused on benthic foraminifera as a useful proxy for the export production to the sea floor, bottom and pore water oxygen concentrations and bottom water mass circulation.

It is important to increase our knowledge about the influence of productivity on the distribution and composition of modern benthic foraminiferal faunas and the stable isotopic composition of their tests, since this knowledge serves as basis for a detailed reconstruction of paleoproductivity, which allows conclusions about past climate changes. In this context, it is essential to conduct spatially highly resolved investigations to detect local heterogeneities and to reliably reconstruct paleoproductivity. Therefore, I focus on the characterisation of modern benthic foraminifera and their preferences regarding productivity and its influence on the stable carbon isotopic composition of their tests in a regionally restriced area within the upwelling region off Morocco (NW-Africa). Subsequently, benthic foraminifera are used as proxy for a detailed reconstruction of past productivity conditions during the Last Glacial Maximum (LGM).

1.1 Investigation area

The investigation area is located in the upwelling region off Morocco at the NW-African continental margin. Cape Ghir (31°N) and Cape Yubi (27.5°N) restrict this area in the north and south, respectively. The Canary Islands, which are located 100 to 600 km off the African coast at a latitude of 28° - 29°N, form the western boundary. The broad Moroccan continental shelf is characterised by an extension between 30 km and 100 km. A relatively narrow shelf with an extension of 25 km off Cape Ghir and a broader shelf with an extension of 75 km off Cape Yubi was observed (Summerhayes et al., 1976).

1.1.2 Present-day conditions

The study area is part of the large-scale N-Atlantic recirculation system, which combines the Gulf Stream via the Azores Current (AC) and the Canary Current (CC) with the North Equatorial Current. The AC splits into three branches south of the Azores Islands, of which the eastern most branch, the southwards directed CC, has a major influence on the coastal upwelling off Morocco. The flow path of the CC either through the Canary Islands or along the Moroccan coast is seasonally variable (Stramma and Siedler, 1988; Knoll et al., 2002) and it increases during summer and fall (Knoll et al., 2002). The well-mixed surface layer is underlein by the southward directed North Atlantic Central Water (NACW) down to 600 m. Below the NACW the southward directed Mediterranean Outflow Water (MOW), occurs between 600 m - 1700 m and is characterised by high salinity. Between 600 m - 1000 m depth the northward flowing nutrient-enriched Antarctic Intermediate Water was observed close to the coast (Knoll et al., 2002; Llinás et al., 2002). The southward directed nutrient-depleted North Atlantic Deep Water (NADW) occurs between 1700 m and 4000 m and the northward directed nutrient-enriched Antarctic Bottom Water (AABW) below 4000 m (Sarnthein et al., 1982).

The NW-African–Iberian upwelling region, belongs to one of the four major eastern boundary upwelling systems of the world (Hagen, 2001; Carr, 2002) and is characterised by high marine production. The high primary production is reflected by enhanced chlorophyll-*a* concentrations in surface waters as inferred from satellite imagery (Fig. 1).

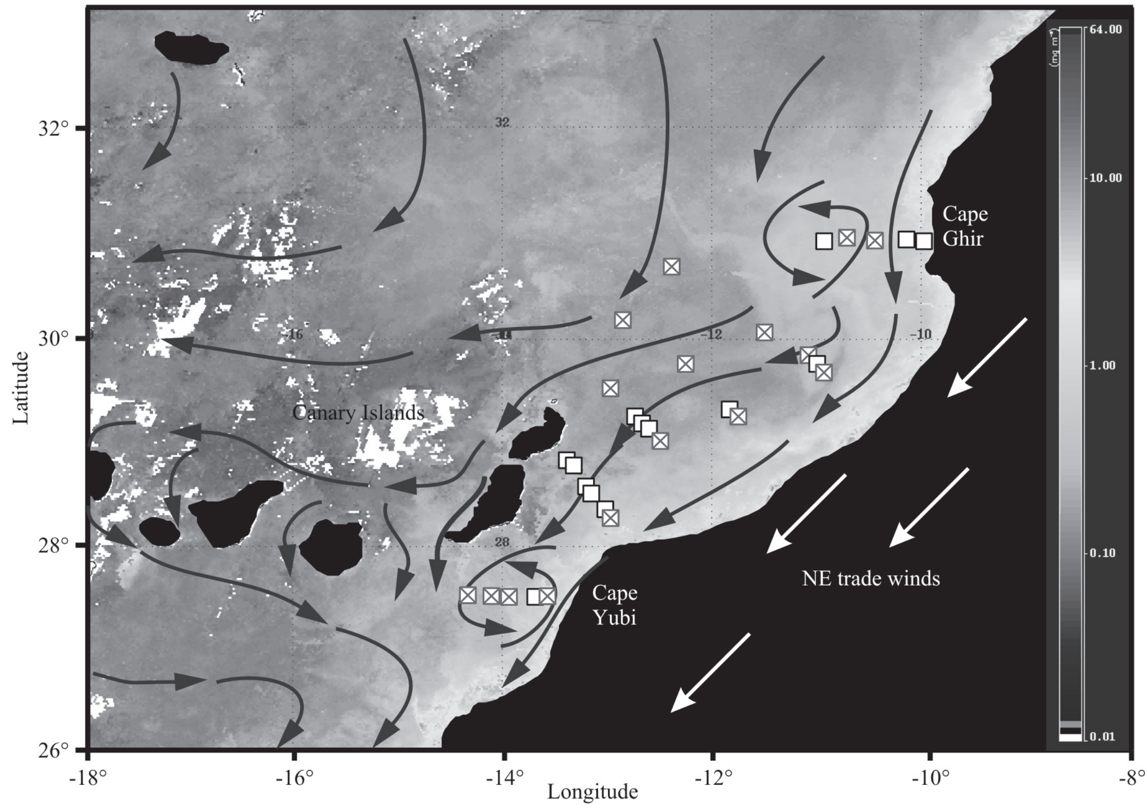

Fig. 1: Study area with chlorophyll-*a* distributions (mean March 1998; Helmke, pers. comm) in surface waters. Direction of surface currents (= Canary Current) after Mittelstaedt (1991) and NE trade winds are indicated by arrows. Squares mark investigated Holocene and LGM (squares with crosses) sample locations.

Primary productivity is linked to the interaction of the CC, the coastal morphology and variations in NE trade wind intensity. Coastal upwelling is coupled to the latitudinal northwards shifts of the subtropical high (Azores High) and tropical low pressure areas connected to the migration of the Inter Tropical Convergence Zone. North of 25°N seasonal upwelling is observed with strongest upwelling events in boreal summer and fall (Mittelstaedt, 1991; Van Camp et al., 1991; Nykjaer and van Camp, 1994). Off Morocco, upwelling of NACW is restricted to a maximum offshore extent of 70 km (Mittelstaedt, 1991; Hernández-Guerra and Nykjaer, 1997; Hagen, 2001). However, particularly, at cape locations the development of filaments is observed, which are characterised by high nutrient concentrations. The filaments can be advected several hundred kilometers into the open ocean (Van Camp et al., 1991; Nykjaer and van Camp, 1994; Hagen et al., 1996; Hernández-Guerra and Nykjaer, 1997; Parrilla et al., 1999), and thus are an important transport mechanism of nutrients into the oligotrophic open ocean.

1.1.3 Past conditions

During the last glacial / interglacial transition the trade wind belt had almost the identical latitudinal extension as today (Sarnthein et al., 1981; Hooghiemstra et al., 1987; Hooghiemstra, 1989). However, the trade wind intensity was considered to be enhanced compared to modern conditions as a result of the stronger atmospheric temperature and pressure gradient (Sarnthein et al., 1981; Hooghiemstra et al., 1987; Hooghiemstra, 1989). During the LGM, the sea level was by about 120 m lower than presently (Fairbanks, 1989). The influence of sea level changes on the productivity record has been recently discussed. Martinez et al. (1999) and Bertrand et al. (2000) showed that sea level changes are responsible for zonal shifts of upwelling centers, which in turn control productivity. The assumption that the NW-African upwelling region is the prime example of generally enhanced producitvity during glacial times (Sarnthein et al., 1982) has to be reconsidered. Cape Blanc (21°N), the today's centre of year-round upwelling activity was characterised by lower productivity during the LGM (Bertrand et al., 1996; Martinez et al., 1999; Zhao et al., 2000; Sicre et al., 2001). In contrast, higher glacial productivity seemed to have been geographically restricted to the northern part of the NW-African upwelling system. Enhanced productivity was observed at 25°N (Abrantes, 2000; Sicre et al., 2000; Ternois et al., 2000; Zhao et al., 2000), and in the Canary Islands region (Freudenthal et al., 2002; Henderiks et al., 2002; Moreno et al., 2002; Kuhlmann et al., 2004). Therefore, the NW-African margin has been described as a region with intense productivity variations of regional significance during glacials (Bertrand et al., 1996; Martinez et al., 1999; Sicre et al., 2001).

1.2 Brief overview of benthic foraminiferal research

Benthic foraminifera (Order FORAMINIFERIDA Eichwald 1830) are eukaryotic, single-celled, and mostly multiple chambered organisms (Sen Gupta, 1999). Presently, about 1000 living genera and approximately 6000 extant species are described (Loeblich and Tappan, 1988), and the first occurence of test fragments was accounted for Cambrian sediments. Benthic foraminifera inhabitat all aquatic environments and are major contributors of the meiofaunal (> 50%) and macrofaunal biomass (Gooday et al., 1992). They are known to have a wide range of different diets (Lipps, 1983; Caralp, 1989a; 1989b; Murray, 1991; Bernhard and Bowser, 1992; Gooday et al., 1992; Gooday, 1994). Benthic foraminiferal tests are either composed of calcite, constructed from foreign particles or organic material by the foraminifera itself (Gooday, 2001). Particularly, the calcareous specimens have a great fossilisation potential at least above the calcite compensation depth.

The first classification of benthic foraminifera was carried out by d'Orbigny (1826) and was followed by extensive and long-lasting taxonomic work (e.g. Brady, 1879; Brady, 1881; Brady, 1884; Cushman, 1918-1931; Heron-Allen and Earland, 1922; Cushman, 1948; Phleger and Parker, 1951). Subsequently, descriptions of the bathymetrical and geographical distribution patterns of benthic foraminifera species were conducted (e.g. Phleger, 1960; Lutze, 1980) and a correlation between benthic foraminifera and physicochemical water mass characteristics was suggested (Streeter, 1973; Schnitker, 1974; Schnitker, 1979; Schnitker, 1980; Murray et al., 1986). The staining method with Rose Bengal invented by Walton (1952) enabled to distinguish between tests containing protoplasm and those being empty.

It was shown that benthic foraminifera live above (truely epibenthic) (Lutze and Thiel, 1989), on (epibenthic) and within (endobenthic) the sediment (Corliss, 1985; Gooday 1986) with clear microhabitat preferences (Mackensen and Douglas, 1989; Rathburn and Corliss, 1994; Mackensen et al., 2000; Schmiedl et al., 2000). This distinct vertical zonation is predominantly influenced by the organic carbon flux and dissolved bottom water oxygen concentrations (Jorissen et al., 1995). In this context some species have been identified to track distinct redox boundaries in the porewater (Corliss and Emerson, 1990; Jorissen et al., 1998; Fontanier et al., 2002; Licari et al., 2003). It is generally accepted that the organic carbon flux is the essential parameter in controlling the benthic foraminifera community (e.g. Corliss and Emerson, 1990; Loubere, 1991), as long as the bottom water or pore water oxygen concentration does not fall below the critical threshold, which has a considerable impact on the benthic foraminiferal occurence and distribution as well (Bernhard, 1992; Jorissen 1998; Loubere, 1994; Kaiho, 1994, 1999; Schönfeld, 2001; Geslin et al., 2004; Sen Gupta and Machain-Castillo, 1993) Quantity and mode of organic matter fluxes control the absence or presence of distinct species (e.g. Gooday, 1988; Rathburn and Corliss, 1994; Gooday, 1996; Jannink et al., 1998; de Rijk et al., 2000; Schmiedl et al., 2000; Morigi et al., 2001) as well as the benthic foraminiferal faunal composition and vertical stratification within the sediment (e.g. Jorissen et al., 1992; Mackensen et al., 1995; Loubere, 1997; Jorissen et al., 1998; Fontanier et al., 2002; Gooday and Hughes, 2002; Eberwein et al., subm). Furthermore, the benthic foraminiferal density is controlled by the organic carbon export (Lutze and Coulbourn, 1984; Altenbach, 1988; Gooday, 1994; Fontanier et al., 2002; Heinz et al., 2002).

The stable carbon isotopic composition of benthic foraminifera tests was a further focus in the researcher's intererest. In this context, the main emphasis in using these stable carbon isotopic compositions lies on productivity influence (Zahn et al., 1986; Loubere, 1987; Mackensen et al., 1993b; McCorkle et al., 1997; Mackensen and Licari, 2004), bottom-water mass characteristics (Woodruff et al., 1980; Graham et al., 1981), and bottom-water circulation changes (Duplessy et al., 1984; Curry et al., 1988; Sarnthein et al., 1994; Bickert and Wefer, 1996; Mackensen et al., 2001; Bickert and Mackensen, 2004; Curry and Oppo, 2005). The truely epibenthic foraminiferal species *Cibicidoides wuellerstorfi* usually reflects the $\delta^{13}C$ signal of the dissolved inorganic carbon (DIC) in the bottom water (Woodruff et al., 1980; Belanger et al., 1981; Graham et al., 1981; Duplessy et al., 1984; Zahn et al., 1986; Duplessy et al., 1988; McCorkle and Keigwin, 1994; Mackensen and Licari, 2004), whereas the $\delta^{13}C$ signal of endobenthic species reflect the productivity linked pore-water $\delta^{13}C$ gradient (Mackensen and Douglas, 1989; McCorkle et al., 1990; Loubere et al., 1995; Rathburn et al., 1996; McCorkle et al., 1997; Mackensen et al., 2000; Holsten et al., 2004; Mackensen and Licari, 2004; Schmiedl et al., 2004). Reconstruction of bottom water $\delta^{13}C_{DIC}$ using $\delta^{13}C$ values of *C. wuellerstorfi* was questioned, since productivity-linked lower $\delta^{13}C$ values of this species were observed (Sarnthein et al., 1988; Mackensen et al., 1993b; Sarnthein et al., 1994; Bickert and Wefer, 1999). More recently, however, no productivity influence was recorded (Mackensen and Licari, 2004; Corliss et al., 2006; Eberwein and Mackensen, 2006). It was shown that $\delta^{13}C$ values of all specimens of the same species vary little over the entire habitat depth in which they occur (Mackensen and Douglas, 1989; Rathburn et al., 1996; McCorkle et al., 1997; Mackensen et al., 2000; Mackensen and Licari, 2004; Schmiedl et al., 2004; Fontanier et al., 2006), which is important regarding paleoproductivity reconstructions. The approach of $\Delta\delta^{13}C$ offsets (difference between $\delta^{13}C$ values of epi- and endobenthic species) were used either to reconstruct (paleo-) productivity variations (Woodruff and Savin, 1985; Zahn et al., 1986; McCorkle et al., 1994; Fontanier et al., 2006) or assumed to indicate bottom-water oxygen concentrations (McCorkle et al., 1997; Fontanier et al., 2006; Schmiedl and Mackensen, in press).

The influence of carbonate ion undersaturated bottom water masses on benthic foraminiferal isotopic compositions is only marginally investigated (Bemis et al., 1998; Mackensen and Licari, 2004). Most recently, there is evidence that benthic foraminiferal ^{13}C is extremly depleted in methane enriched settings (Wefer et al. 1994; Rathburn et al., 2000; Hill et al., 2003; Kennett et al., 2003; Rathburn et al., 2003; Mackensen et al., 2006). Intense methane releases are considered to have caused rapid climate changes. It seems promising to use $\delta^{13}C$ values to detect methane flux variations and thus, to find out about their importance in climate changes. Summarizing I point out that benthic foraminifera provide a useful and reliable proxy in paleo-oceanographic reconstructions, although the involved and interacting biogeochemical processes need further investigations.

1.3 Aim of this thesis

This PhD thesis entitled 'Holocene and Last Glacial Maximum (paleo-) productivity off Morocco: evidence from benthic foraminifera and stable carbon isotopes' has been carried out within the subproject 'Characterisation of high-productivity regions using microfossils and organic compounds', which is part of the DFG Research Center Ocean Margins (RCOM).

The thesis has been divided into three main parts. The first part gives an introduction, which concentrates on the study area, its present and past climatic conditions as well as on a brief review of benthic foraminiferal research. The second and major part, which is composed of three manuscripts, focuses on the presentation and discussion of the results of the research conducted during this PhD thesis. The third part summarises the main conclusions of the second part and gives a perspective beyond outstanding problems.

1.3.1 Objectives

High-production systems, such as the NW-African coastal upwelling area are important regions concerning the organic carbon cycle. Particularly, glacial / interglacial variations in marine productivity are considered to determine atmospheric CO_2 concentrations. The primary objective of this PhD thesis is to assign and reconstruct (paleo-) productivity conditions with the aid of benthic foraminiferal species and their stable carbon isotopic composition in a geographically limited area within the upwelling region off Morocco (NW-Africa). The central questions arising from this background include the following aspects:

- Does the Recent benthic foraminiferal community reflect present productivity conditions?
- To what extent is the isotopic composition of Recent benthic foraminifera affected by productivity?
- Can benthic foraminifera be used as reliable proxy to reconstruct paleoproductivity and distribution of past bottom water masses?
- Did paleoproductivity during the Last Glacial Maximum change as compared to productivity in the Holocene?

In order to answer these questions three manuscripts have been prepared, all of which have been submitted to international journals. The main topics of these manuscripts are summarised in the following.

1.3.2 Overview of Research

Eberwein, A. and Mackensen, A. (2006). Regional primary productivity differences off Morocco (NW-Africa) recorded by modern benthic foraminifera and their stable carbon isotopic composition. (Deep-Sea Research I).

We examine the correlation of live and dead benthic foraminifera with different environmental parameters, such as chlorophyll-*a* concentrations in surface waters (indicative of primary productivity) as inferred from satellite imagery, bottom water mass characteristica and sediment type. The discussion focuses on the effect of primary productivity on the composition and distribution of benthic foraminiferal faunas as well as the stable carbon isotopic composition of the most common species. Therefore, this study was conducted with a high spatial resolution to obtain a detailed picture of the modern primary productivity conditions. We further discuss the factors determining the similarities and discrepancies between live and dead benthic foraminiferal assemblages, to assign fundamental ecological information, which is a prerequisite for paleoproductivity reconstruction.

Eberwein, A. Mackensen, A. and Davenport, R. (submitted, in revision). The influence of organic matter fluxes on the microhabitat distribution of live benthic foraminifera off Cape Ghir and Cape Yubi (NW-Africa). (Journal of Foraminiferal Research).

In order to assess the impact of organic matter fluxes on the benthic foraminiferal community and the microhabitat distribution seven sediment surface samples, four of them located under the Cape Ghir filament, three of them under the Cape Yubi filament, were investigated for their live benthic foraminiferal content. Furthermore, we discuss the interplay between the quantity of exported organic matter and bottom water oxygen concentration in relation to the vertical zonation of benthic foraminifera. In this context a special focus is set on the density and average living depth of the deep infaunal species *Globobulimina affinis*, since this species is considered to be tightly linked to the zone of zero oxygen concentrations.

Eberwein, A. and Mackensen, A. (submitted). Last Glacial Maximum productivity and water masses off NW-Africa: evidence from benthic foraminifera and stable isotopes. (Marine Micropaleontology).

We reconstruct paleoproductivity and stratification of water masses during the Last Glacial Maximum (LGM). The $\delta^{13}C$ of *Cibicidoides wuellerstorfi* and equilibrium adjusted $\delta^{18}O$ values of several species were used to determine the water mass stratification. Paleoproductivity was reconstructed with the aid of distinct assemblages and indicator species as well as the differences of $\delta^{13}C$ values between epi- and infaunal species. Based on these proxies the main emphasis lies on the reconstruction of paleoproductivity and its comparison with Holocene productivity patterns.

2.1 Manuscript 1

Regional primary productivity differences off Morocco (NW-Africa) recorded by modern benthic foraminifera and their stable carbon isotopic composition

Eberwein, A. & Mackensen, A.

Alfred Wegener Institute for Polar and Marine Research, Columbusstrasse, D-27568 Bremerhaven, Germany

Keywords: Benthic foraminifera; Chlorophyll-*a*; Stable carbon isotopes; Organic matter; NW-Africa

Abstract

The influence of different primary productivity regimes on live (Rose Bengal stained) and dead benthic foraminiferal distribution, as well as on the stable carbon isotopic composition of foraminiferal tests, was investigated in sediment surface samples ((0-1 cm)) from the upwelling region off Morocco between Cape Ghir (31°N) and Cape Yubi (27°N). A combination of factor analysis, detrended correspondence analysis (DCA) and canonical correspondence analysis (CCA) was applied to the benthic foraminiferal data sets. Five major assemblages for both the live and dead fauna were revealed by factor analysis. In the cape regions organic matter fluxes are enhanced by high chlorophyll-α concentrations in the overlying surface waters. Here, benthic foraminiferal faunas are characterized by identical live and dead assemblages, high standing stocks, and low species $\delta^{13}C$ values, indicating constant year-round high productivity. *Bulimina marginata* dominates the unique fauna at the shallowest station off Cape Ghir indicating highest chlorophyll-*a* concentrations. Off both capes, the succession of the *Bulimina aculeata* / *Uvigerina mediterranea* assemblage, the *Sphaeroidina bulloides* / *Gavelinopsis translucens* assemblage, and the *Hoeglundina elegans* assemblage from the shelf to the deep sea reflects the decrease in chlorophyll-*a* concentrations, hence the export flux. In contrast, the area between the capes is characterized by differently composed live and dead assemblages, low standing stocks, and less depleted $\delta^{13}C$ values, thus reflecting low primary productivity. High foraminiferal numbers of *Epistominella exigua, Eponides pusillus*, and *Globocassidulina subglobosa* in the dead fauna indicate a seasonally varying primary productivity signal. Significantly lower mean $\delta^{13}C$ values were recorded in *Bulimina mexicana*, *Cibicidoides kullenbergi*, *H. elegans, U. mediterranea* and *Uvigerina peregrina*. *Cibicidoides wuellerstorfi* is a faithful recorder of bottom water $\delta^{13}C$ in the Canary Islands regions. The mean $\delta^{13}C$ signal of this species is not significantly influenced by constant high organic matter fluxes. The species-specific offset between live and dead specimens is the same.

1. Introduction

Benthic foraminifera are an important proxy in reconstructing primary productivity changes and corresponding organic matter fluxes to the sea floor (Altenbach and Sarnthein, 1989; Loubere, 1991; Berger and Herguera, 1992; Linke and Lutze, 1993; De Rijk et al., 2000). The variation in primary productivity is responsible for the amount and quality of organic matter reaching the seafloor, which in turn influences the composition and standing stocks of benthic foraminiferal faunas (Lutze and Coulbourn, 1984; Caralp, 1989; Corliss and Emerson, 1990; Hermelin and Shimmield, 1990; Herguera and Berger, 1991; Schmiedl et al., 2000; Fontanier et al., 2002). The vertical distribution of living benthic foraminifera within the sediment is controlled mainly by the combination of organic matter flux and the oxygen concentration in bottom and pore waters (e.g. Corliss and Emerson, 1990; Jorissen et al., 1995). Species also react with a microhabitat change in response to variations in these conditions (Jorissen et al., 1995). The importance of infaunal species increases significantly in C_{org} enriched sediments (Sen Gupta and Machain-Castillo, 1993) and in areas with high organic matter fluxes (De Rijk et al., 2000; Gooday, 2003). In oligotrophic settings, where the labile fraction of the organic matter is consumed almost at the sediment-water interface, the fauna is characterized by epifaunal taxa (Linke and Lutze, 1993; Jorissen et al., 1995).

Various factors, including transport, dissolution and population dynamics, can influence the dead fauna (Murray, 1991; Loubere et al., 1993; Mackensen et al., 1995; Jorissen and Wittling, 1999), creating fundamental differences between the dead and live fauna at the same site. The live fauna represents a snapshot of actual environmental conditions, while the dead fauna represents a longer averaged time period. Therefore, knowledge about the differences between live and dead fauna is important to reconstruct paleoenvironmental conditions from the fossil fauna.

The stable carbon isotopic composition of benthic foraminiferal tests provides information about the carbon cycling in the world ocean and is widely used to reconstruct past deep-water circulation changes (Curry et al., 1988; Duplessy et al., 1988; Boyle, 1992; Sarnthein et al., 1994; Mackensen et al., 2001) as well as organic matter flux variations (e.g. Zahn et al., 1986; Loubere, 1987; Bickert and Wefer, 1999). The $\delta^{13}C$ distribution of dissolved inorganic carbon (DIC) in the oceans is dependent on the interaction of biological uptake at the sea surface, air-sea gas exchange and organic matter degradation. The benthic foraminiferal species *Cibicidoides wuellerstorfi* usually calcifies in 1:1 relationship with the ambient bottom water DIC (Belanger et al., 1981; Duplessy et al., 1984; Duplessy et al., 1988; McCorkle and Keigwin, 1994). However, in areas with pulsed organic matter inputs even $\delta^{13}C$ signals of *C. wuellerstorfi* are depleted (Mackensen et al., 1993b). Infaunal species are considered to record the pore-water $\delta^{13}C$ gradient (McCorkle et al., 1997; Mackensen and Licari, 2004).

In eutrophic regions, the benthic foraminiferal community is characterized by significant numbers of specimens living deeper within the sediment (Jorissen et al., 1995). Under these conditions the number of deeply infaunal specimens may be strongly underestimated when only the uppermost centimetre is investigated. Licari and Mackensen (2005) showed that in eutrophic settings the overall environmental signal, as deduced from the benthic foraminiferal community in the uppermost surface sediment (0 -1 cm), does not significantly differ from the information gained from the benthic foraminiferal fauna of the upper 10 cm. In very eutrophic regions, benthic foraminifera are concentrated at the sediment surface and, therefore, the investigation of the uppermost centimetre gives an accurate picture of the total fauna. Eutrophic conditions are predominant off Cape Ghir and Cape Yubi. Here, faunal differences within the sediment, different standing stocks, and variations in the average living depth of species were observed (Eberwein, unpubl. data). Still, the general conclusion drawn from the surface fauna (0 - 1 cm) is meaningful in terms of differences in overlying productivity regimes, which is the main purpose of this study.

In this study we describe the community pattern of live and dead benthic foraminifera from 30 surface sediment samples (0 - 1 cm) as well as the stable isotopic composition of the most common species in the upwelling region off Morocco. The high spatial resolution allows a better understanding of the relation between faunal changes, standing stocks and primary productivity. In addition, we examined the effect of productivity on benthic $\delta^{13}C$ values. This study aims to provide a modern analogue for the reconstruction of Late Pleistocene productivity changes in the investigation area.

2. Oceanographic setting

The area under investigation (Fig. 1) is located in the eastern part of the subtropical North Atlantic gyre off Morocco (NW Africa) at the continental margin between 27°N and 31°N. This gyre represents the connection of the Gulf Stream via the Azores Current (AC) and the Canary Current (CC) with the North Equatorial Current. The study area is part of the Eastern Boundary Current (EBC) regime, which belongs to one of the major eastern boundary upwelling systems of the world (Hagen, 2001; Carr, 2002). In general, the EBC regions are characterized by high primary productivity (Fig. 1). Thus, they play an important role in biogeochemical cycles, especially with respect to the carbon export to the sea floor. Off Morocco, upwelling of North Atlantic Central Water (NACW) (Mittelstaedt, 1991) occurs over the shelf and shelf break (Hagen, 2001) (Fig. 1). The upwelled water masses have a maximum extent of 70 km (Mittelstaedt, 1991; Hernández-Guerra and Nykjaer, 1997; Hagen, 2001). The intensity and occurence of upwelling depends on the position of the Azores High, which is located in its northernmost position during the boreal summer. During summer the trade wind belt affects the African coast between 32°N and 20°N. North of 25°N upwelling is predominant in summer and early fall (Wooster et al., 1976; Mittelstaedt, 1991; Van Camp et al., 1991; Nykjaer and van Camp, 1994). This is supported by a recent study of fluxes of upwelling-related microorganisms between Lanzarote Island and the African coast (Abrantes et al., 2002).

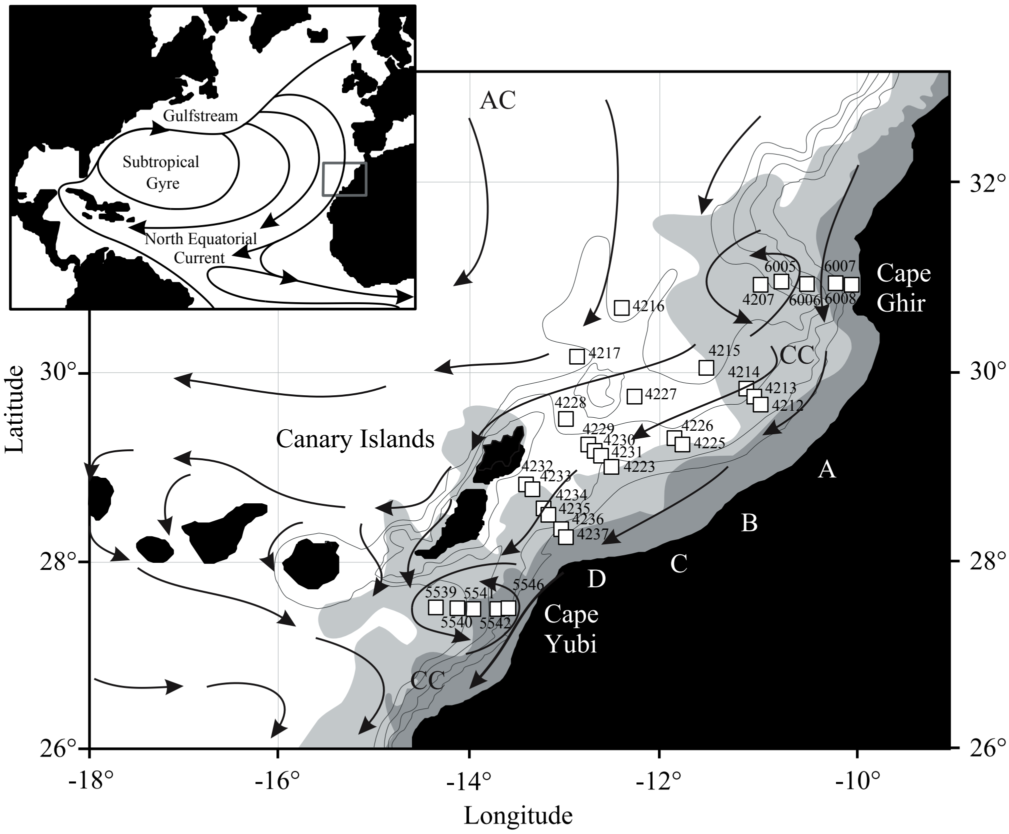

Fig.1: Study area, chlorophyll-*a* concentration in surface waters, bathymetry and location of the 30 sediment surface samples (0 - 1 cm). SeaWifs derived chlorophyll-*a* concentrations (mean March 1998; Helmke, pers. comm) that represent > 1 mg m^{-3} are shaded dark grey, 0.4 – 1 mg m^{-3} light grey and < 0.4 mg m^{-3} not shaded. Surface currents (AC: Azore Current, CC: Canary Current) are indicated by arrows after Mittelsteadt (1991). Isobaths indicate 500, 1000, 1500 and 2000 m water depths. Investigated sediment surface samples are marked by squares. Numbers represent stations, and transects are labled Cape Ghir, A, B, C, D and Cape Yubi.

Striking features of the area are filaments, which are situated off Cape Ghir and Cape Yubi (Fig. 1), where the upwelled waters are transported several hundred kilometers offshore (Van Camp et al., 1991; Nykjaer and van Camp, 1994; Hernández-Guerra and Nykjaer, 1997; Hagen, 2001). The filaments off Cape Ghir and Cape Yubi exist throughout the year, with a strong upwelling signal in summer and fall (Hernández-Guerra and Nykjaer, 1997). They are generated by the interaction of the current system and the coastal cape morphology (Hagen et al., 1996; Stevens and Johnson, 2003), and they play an important role in transport of nutrients from the shelf to the deep sea.

The water column is characterized by the southward flowing CC down to 100 m depth (Knoll et al., 2002; Llinás et al., 2002). Below the CC the southward flowing NACW occurs down to a depth of 600 m, with increasing portions of the northwards directed South Atlantic Central Water (SACW) to the south (Knoll et al., 2002; Llinás et al., 2002). The southward directed Mediterranean Outflow Water (MOW) underlies the NACW down to a depth of 1700 m (Knoll et al., 2002; Llinás et al., 2002). The impact of the northwards flowing Antarctic Intermediate Water (AAIW) on the MOW characteristics increases to the south. The deepest watermass is the southward flowing North Atlantic Deep Water (NADW) (Knoll et al., 2002; Llinás et al., 2002).

The investigated sites are positioned in the transition zone between upwelled eutrophic waters and the oligotrophic waters of the subtropical North Atlantic gyre in order to detect the influence of trophic differences on the benthic foraminiferal community.

3. Material and methods

A total of 30 sediment surface samples was collected with a multiple corer and a giant box corer in the upwelling region off Morocco (NW-Africa) from water depths ranging between 355 m and 2504 m. The investigated sediment surface samples are distributed along six transects, which are located between 31°N and 27°N. In the following the transects will be labelled Cape Ghir, A, B, C, D, and Cape Yubi transect from north to south (Fig. 1). The sediment surface samples were recovered during cruises in 1996, 1998 and 1999 with RV *Meteor* (Table 1).

The sediment samples (0 – 1 cm) were stored in a Rose Bengal / 95 % ethanol mixture (1 g / 1 L) and kept at 4 °C. They were washed over 125-µm and 63-µm sieves and dried. The procedure of staining with Rose Bengal has limitations (e.g. Douglas et al., 1980; Bernhard, 1988; Corliss and Emerson, 1990). However, it is still the most common and practical method to quantify living foraminiferal faunas (Murray and Bowser, 2000). Benthic foraminifera were analyzed from the fraction > 125 µm and determined to species level. Samples were split into aliquots of at least 300 individuals (Phleger, 1960; Fatela and Taborda, 2002) for both the living and dead faunas. We counted proloculi seperately for branch-like agglutinated foraminifera and assumed three fragments to represent one individual in samples without proloculi. The standing stocks of living specimens and the foraminiferal numbers of dead specimens are expressed in numbers of individuals per 50 cm^3 and were calculated for the fauna in the 0 – 1 cm interval and for the most abundant species.

A factor analysis with varimax rotation was applied in order to detect the composition of distinct assemblages and to reveal the important species of these assemblages, using the software SYSTAT™ 5.2.1. Species that occured at least at two stations with a minimum abundance of 1 % were included in the analysis. Some commonly used statistical methods in micropaleontological studies are based on the assumption that the abundances of species show a linear response to environmental parameters. This assumption does not hold in many cases, because of the fact that species show a Gaussian (unimodal) distribution with respect to environmental parameters. Therefore, we used the two-step approach of a detrended correspondence analysis (DCA) and a canonical correspondence analysis (CCA) (Ter Braak, 1986) of the CANOCO™ software (Version 4.0).

Table 1: List of surface samples investigated in this study with sampling date, position, water depth, and coring device (MUC: Multiple Corer, GBC: Giant Box Corer).

Core GeoB	Cruise	Date	Device	Latitude (°N)	Longitude (°W)	Water depth (m)
Transect Cape Ghir						
6008-2	M45/5	Oct / Nov 1999	MUC	30°50,7	10°05,9	355
6007-1	M45/5	Oct / Nov 1999	MUC	30°51,1	10°16,0	899
6006-2	M45/5	Oct / Nov 1999	MUC	30°52,1	10°37,8	1275
6005-1	M45/5	Oct / Nov 1999	MUC	30°52,8	10°53,8	1781
4207-1	M37/1	Dec 1996	GBC	30°51,8	11°04,3	2123
Transect A						
4212-3	M37/1	Dec 1996	MUC	29°36,2	10°57,0	1256
4213-1	M37/1	Dec 1996	MUC	29°41,8	11°04,7	1547
4214-3	M37/1	Dec 1996	MUC	29°46,9	11°11,8	1788
4215-1	M37/1	Dec 1996	MUC	30°02,2	11°33,2	2106
4216-2	M37/1	Dec 1996	MUC	30°37,9	12°23,8	2325
Transect B						
4225-3	M37/1	Dec 1996	MUC	29°16,5	11°46,9	1281
4226-1	M37/1	Dec 1996	MUC	29°19,2	11°50,0	1400
4227-1	M37/1	Dec 1996	MUC	29°46,1	12°20,2	1826
4217-1	M37/1	Dec 1996	MUC	30°26,1	12°53,7	2504
Transect C						
4223-1	M37/1	Dec 1996	MUC	29°01,1	12°28,0	777
4231-2	M37/1	Dec 1996	MUC	29°05,2	12°33,1	1197
4230-1	M37/1	Dec 1996	MUC	29°07,7	12°35,8	1316
4229-2	M37/1	Dec 1996	MUC	29°10,9	12°38,3	1422
4228-1	M37/1	Dec 1996	MUC	29°28,2	12°59,4	1633
Transect D						
4237-1	M37/1	Dec 1996	MUC	28°43,7	13°01,0	800
4236-2	M37/1	Dec 1996	MUC	28°47,0	13°05,7	1030
4235-1	M37/1	Dec 1996	MUC	28°51,4	13°11,4	1247
4234-1	M37/1	Dec 1996	MUC	28°53,4	13°13,6	1360
4233-2	M37/1	Dec 1996	MUC	28°58,5	13°19,8	1303
4232-1	M37/1	Dec 1996	MUC	29°01,3	13°23,2	1161
Transect Cape Yubi						
5546-3	M42/4	Oct 1998	MUC	27°32,2	13°44,2	1071
5542-3	M42/4	Oct 1998	MUC	27°32,2	13°50,8	1431
5541-2	M42/4	Oct 1998	MUC	27°32,2	13°59,7	1748
5540-3	M42/4	Oct 1998	MUC	27°32,1	14°10,5	2035
5539-2	M42/4	Oct 1998	MUC	27°32,2	14°21,3	2202

Table 2: Live and dead assemblages revealed by factor analysis with their dominant (score > 3) and associated (score > 1) species. Variance of each assemblage and total variance are given in percentages for both live and dead fauna.

	Variance (%)	Dominant species	Score	Associated species	Score
Live fauna	21.18	*Trifarina bradyi*	7.68	*Uvigerina mediterranea*	2.96
				Cibicidoides bradyi	2.47
Total variance 67.69%				*Reophax scorpiurus*	1.35
				Epistominella rugosa	1.29
				Gavelinopsis translucens	1.21
				Cribrostomoides subglobosus	1.20
				Melonis barleeanum	1.19
	15.73	*Hoeglundina elegans*	9.09	*Cribrostomoides subglobosus*	1.43
				Cibicidoides kullenbergi	1.43
				Karrerulina conversa	1.03
				Bulimina rostrata	1.02
	11.85	*Bulimina aculeata*	7.03	*Hyalinea baltica*	2.46
		Uvigerina mediterranea	5.09	*Gavelinopsis translucens*	1.70
	11.39	*Gavelinopsis translucens*	7.38	*Cibicidoides kullenbergi*	2.81
		Sphaeroidina bulloides	3.63	*Bulimina mexicana*	1.74
				Cibicidoides bradyi	1.04
	7.54	*Cribrostomoides jeffreysii*	5.18	*Reophax scorpiurus*	2.89
		Cibicidoides kullenbergi	4.77	*Reophax bilocularis*	2.53
				Cribrostomoides subglobosus	1.65
				Eponides pusillus	1.59
				Eggerella bradyi	1.32
				Uvigerina mediterranea	1.24
Dead fauna	21.41	*Epistominella rugosa*	4.69	*Cassidulina obtusa*	2.84
		Pyrgoella irregularis	4.45	*Globocassidulina subglobosa*	2.16
Total variance 68.53%				*Uvigerina proboscidea*	1.94
				Trifarina bradyi	1.74
				Miliolinella subrotunda	1.20
				Gavelinopsis translucens	1.19
				Lobatula lobatulus	1.15
				Cibicidoides bradyi	1.11
				Lagenammina difflugiformis	1.08
				Karreriella bradyi	1.06
	9.88	*Bulimina aculeata*	-6.77	*Epistominella rugosa*	-2.72
		Uvigerina mediterranea	-4.65	*Hyalinea baltica*	-1.86
				Melonis barleeanum	-1.30
				Uvigerina peregrina	-1.16
	10.40	*Hoeglundina elegans*	7.71	*Cibicidoides kullenbergi*	2.78
				Bulimina mexicana	2.41
				Bulimina rostrata	1.92
				Cibicidoides wuellerstorfi	1.57
	17.14	*Gavelinopsis translucens*	8.53	*Bulimina mexicana*	2.33
				Cassidulina laevigata	1.41
	9.70	*Pyrgoella irregularis*	4.54	*Cribrostomoides jeffreysi*	2.68
				Cibicidoides wuellerstorfi	2.24
				Eponides pusillus	2.10
				Epistominella exigua	1.87
				Cibicidoides kullenbergi	1.85
				Cribrostomoides wiesneri	1.47
				Ammodiscus incertus	1.38
				Paratrochammina challengeri	1.18
				Cribrostomoides subglobosus	1.17
				Reophax scorpiurus	1.02

The basic assumption of DCA is that the main species and site variations are caused by one environmental variable or a combination of environmental parameters. The direction of the main variation of species and sites is represented by the first DCA axis, whereas higher axes are related to other environmental parameters, which show decreasing importance for the variation. A species rises to its mode and disappears again within four standard deviations (SD). Consequently, samples that plot more than four SD's apart have no species in common (Hill and Gauch, 1980). If the length of the first axis is greater than 2 SD, unimodal response model can be assumed. In CCA, the species abundances are directly related to the environmental variables. The species data were transformed to approximately normal distributions, which is a prerequisite for CCA, by taking the logarithms. The environmental data set was standardized to have a mean equal to zero and a standard deviation equal to one. The Monte Carlo method with 200 permutations was used to test the significance of single environmental variables. The graphical representation of species and sites is given by points, whereas environmental variables are represented by arrows. The perpendicular projection of a species on the environmental parameter indicates the importance of this variable for the variation within this species. We included the relative abundance of the most important species revealed by factor analysis (Table 2) in the DCA / CCA analysis.

The environmental parameter data set (Table 3) for the CCA was taken from various published sources. Surface-water chlorophyll-α concentrations, sedimentary TOC contents, number of fragmented planktic foraminifera and carbonate contents are from Meggers et al. (2002). Silt and sand proportions are from Holz et al. (2004). Data from Meggers et al. (2002) and Holz et al. (2004) are available at www.pangaea.de. Salinity, bottom-water velocities and O_2 concentrations are from Knoll et al. (2002), Llinás et al. (2002), Hernández-Guerra et al. (2003), Sarnthein et al. (1982), and Wefer et al. (1999). All environmental parameters were obtained from the same stations as the foraminiferal samples.

Bottom water samples were taken from directly above the sediment-water interface for the determination of the stable carbon isotopic composition of bottom water dissolved inorganic carbon (DIC). Samples were poisoned with $HgCl_2$, sealed with wax, and kept at 4°C. The DIC of bottom water was extracted with a Finnigan Gas Bench using gas chromatography to purify CO_2. The stable carbon isotopic composition of the resulting CO_2 was determined with a Finnigan MAT 252 isotope ratio gas mass spectrometer and calibrated to VPDB (Vienna Pee Dee Belemnite). All water samples were run in duplicate. The overall precision is better than ± 0.1 ‰. The stable carbon isotopic composition of live and dead individuals of *Bulimina aculeata* (3-13 / 6-13, i.e. 3 to 13 live specimens and 6 to 13 dead specimens were measured), *Bulimina mexicana* (3-12 / 2-18), *Cibicidoides kullenbergi* (2-4 / 2-6), *Cibicidoides wuellerstorfi* (1-4 / 1-6), *Hoeglundina elegans* (2-4 / 1-4), *Uvigerina mediterranea* (1-11 / 2-9), and *Uvigerina peregrina* (3-9 / 3-8) was determined with a Finnigan MAT 251 isotope ratio gas mass spectrometer. The foraminiferal isotopic values are reported in δ–notation relative to the VPDB-scale with a precision better than ± 0.06 ‰ for $\delta^{13}C$.

Table 3: The environmental data used in the statistical analysis is listed. Surface water chlorophyll-*a* concentrations, sedimentary TOC contents, number of fragmented planktic foraminifera and carbonate contents are from Meggers et al. (2002). Salinity, bottom water velocities and O_2 concentrations are from Knoll et al. (2002), Llinás et al. (2002), Hernández-Guerra et al. (2003), Sarnthein et al. (1982), and Wefer et al. (1999). Silt and sand proportions are from Holz et al. (2004). Addtionally, water depth, water mass and the dominant species of the live and dead assemblages are given. Data from Meggers et al. (2002) and Holz et al. (2004) are available at www.pangaea.de.

GeoB station	Waterdepth (m)	Watermass	Dominant species of live fauna	Dominant species of dead fauna	Distance from African coast (km)	TOC (%)	Chlorophyll Ann. mean (1998) (mg/cm3)	Silt (wt-%)	Sand (wt-%)	Carbonate (%)	Fragmented plank.foram. (%)	O2 ml/l	Salinity	V (Sv)
Transect Cape Ghir														
6008	355	NACW	B. marginata	B. spathulata	22	1.65	2.27	42.36	0.46	24.91	24.68	4.52	35.75	0.80
6007	899	MOW	B. aculeata / U. mediterranea	B. aculeata / U. mediterranea	42	1.87	1.41	62.53	1.58	25.35	30.83	6.24	35.60	0.10
6006	1275	MOW	B. aculeata / U. mediterranea	G. translucens	76	1.12	0.81	49.40	9.90	30.76	32.33	6.89	35.60	0.05
6005	1781	NADW	G. translucens / S. bulloides	G. translucens	102	1.06	0.38	44.34	5.94	33.37	23.46	7.85	34.90	0.90
4207	2123	NADW	H. elegans	H. elegans	117	1.04	0.37			35.47	20.54	5.30	34.90	0.90
Transect A														
4212	1256	MOW	T. bradyi	E. rugosa	89	0.73	0.28	55.88	22.56	54.45	13.70	3.90	35.60	0.05
4213	1547	NADW	H. elegans	E. rugosa	110	0.74	0.28	31.63	37.07	61.07	7.80	5.30	34.90	0.05
4214	1788	NADW	G. translucens / S. bulloides	P. irregularis	127	0.80	0.27			66.87	16.10	5.30	34.90	0.90
4215	2106	NADW	C. jeffreysi / C. kullenbergi	P. irregularis	175	0.78	0.24	25.04	51.26	67.65	12.60	5.30	34.90	0.90
4216	2325	NADW	C. jeffreysi / C. kullenbergi	P. irregularis	270	0.59	0.20	31.09	57.29	71.69	8.48	5.30	34.90	0.90
Transect B														
4225	1281	MOW	T. bradyi	G. translucens	147	0.73	0.25	37.77	27.59	55.50	10.14	3.90	35.60	0.05
4226	1400	MOW	T. bradyi	E. rugosa	159	0.74	0.19	34.08	32.71	59.75	9.62	3.90	35.60	0.05
4227	1826	NADW	C. jeffreysi / C. kullenbergi	P. irregularis	234	0.80	0.19			64.13	4.35	5.30	34.90	0.90
4217	2504	NADW	H. elegans	P. irregularis	316	0.54	0.20			69.15	4.00	5.30	34.90	0.90
Transect C														
4223	777	MOW	T. bradyi	B. aculeata / U. mediterranea	186	0.74	0.24	51.38	12.59	52.69	13.87	3.90	35.60	0.10
4231	1197	MOW	T. bradyi	P. irregularis	203	0.85	0.21	44.03	23.45	55.68	10.28	3.90	35.60	0.05
4230	1316	MOW	T. bradyi	P. irregularis	208	0.77	0.21	41.18	20.58	55.98	5.69	3.90	35.60	0.05
4229	1422	MOW	T. bradyi	G. translucens	217	0.82	0.20	47.36	26.47	57.66	10.74	3.90	35.60	0.05
4228	1633	NADW	T. bradyi	P. irregularis	277	0.69	0.19	38.71	38.08	62.63	6.28	5.30	34.90	0.90
Transect D														
4237	800	MOW	B. aculeata / U. mediterranea	B. aculeata / U. mediterranea	183	0.93	0.27	56.39	15.16	48.60	19.62	3.90	35.60	0.10
4236	1030	MOW	T. bradyi	G. translucens	195	0.79	0.27	44.32	19.25	48.39	18.09	3.90	35.60	0.05
4235	1247	MOW	T. bradyi	G. translucens	222	0.91	0.25	44.48	17.27	49.41	13.21	3.90	35.60	0.05
4234	1360	MOW	T. bradyi	E. rugosa	234	0.81	0.26			48.49	6.35	3.90	35.60	0.05
4233	1303	MOW	T. bradyi	G. translucens	257	0.81	0.25	46.13	25.30	47.87	9.73	3.90	35.60	0.05
4232	1161	MOW	T. bradyi	P. irregularis	269	0.78	0.25	40.15	35.51	49.84	13.53	3.90	35.60	0.05
Transect Cape Yubi														
5546	1071	AAIW	B. aculeata / U. mediterranea	B. aculeata / U. mediterranea	49	1.55	0.50	63.02	6.24	35.60	32.01	3.80	35.31	0.05
5542	1431	AAIW	G. translucens / S. bulloides	G. translucens	57	1.25	0.50	45.50	8.19	35.12	29.08	4.70	35.30	0.05
5541	1748	NADW	G. translucens / S. bulloides	G. translucens	73	1.22	0.40	49.13	6.96	36.86	25.00	5.10	35.18	0.90
5540	2035	NADW	H. elegans	H. elegans	90	1.14	0.30	44.33	7.85	36.74	28.39	5.20	35.10	0.90
5539	2202	NADW	H. elegans	H. elegans	107	1.03	0.28	44.41	11.44	38.61	15.99	5.40	34.90	0.90

4. Results

4.1 Live and dead faunas

A total of 243 live and 281 dead species was identified. The foraminiferal standing stocks of surface samples (0 – 1 cm) vary between 24 and 3311 individuals per 50 cm^3 (Table 4). Generally, standing stocks are higher in the cape regions than in the area between the capes. Highest standing stocks are found at stations GeoB 6008-2 and GeoB 6007-1 off Cape Ghir. Furthermore, standing stocks decrease with increasing water depth on each transect (Table 4). Foraminiferal numbers vary between 267 and 18960 individuals per 50 cm^3 (Table 5). They do not show a decrease with increasing water depth as observed for standing stock values.

The factor analysis revealed five factors consisting of 21 important species for the living fauna (Table 2), and five factors consisting of 31 important species for the dead fauna (Table 2). The surface fauna at station GeoB 6008-2 shows a unique faunal composition in comparison to all other faunal assemblages (Figs. 2, 3). It is a striking observation that live and dead assemblages in the sediment surface show an almost identical faunal composition and succession on the Cape Ghir and Cape Yubi transect, while they differ in their composition and distribution in the area between the capes (Figs. 2, 3).

In DCA of the live and dead fauna, the lengths of the first and second axes exceed two standard deviations (Table 6), indicating that the species show a unimodal distribution in response to environmental parameters. The grouping of assemblages obtained from factor analysis is confirmed by DCA analysis (Figs. 4, 5). For the live fauna the first axis most likely represents a combination of water depth, chlorophyll-α concentration in surface waters and the sand content of the sediment. The second axis represents a combination of salinity, fragmented planktic foraminiferal content in the sediment and chlorophyll-α concentration in surface waters (Fig. 6, Table 6). For the dead fauna the significant parameters differ slightly. The first axis most likely represents a combination of water depth, carbonate content in the sediment, chlorophyll-α concentration in surface waters and distance from the African coast. The second axis represents a combination of salinity and chlorophyll-α concentration in surface waters (Fig. 7, Table 6).

A unique live fauna at the shallowest station GeoB 6008-2 (355 m) is characterized by *Bulimina marginata*, *Brizalina spathulata*, *Bigeneria cylindrica*, and *Uvigerina elongatastriata* (Fig. 2, Table 4). The dead fauna is characterized by *Brizalina spathulata*, *Gyroidina umbonata*, *B. marginata*, *Chilostomella oolina*, *Cassidulina laevigata*, and *Bulimina striata* (Fig. 3, Table 5). At station GeoB 6008-2 live and dead faunas show affinities to the highest chlorophyll-α concentration (2.3 mg / m^3) and salinity (35.75) (Figs. 6, 7, Table 3). The live fauna can also be attributed to an intermediate fragmented planktic foraminiferal content (25 %) and a very low sand content (0.5 %) (Fig. 6, Table 3). The dead fauna occurs at this station with intermediate carbonate content (25 %) and proximity to the African coast (22 km) (Fig. 7, Table 3).

Table 4: Standing stock values in individuals per 50 cm³ of surface fauna (0 – 1 cm) of dominant, associated, and remaining species as well as water depths.

Core GeoB	Water depths (m)	Total standing stock	*B. cylindrica*	*B. spathulata*	*B.aculeata*	*B.marginata*	*B. mexicana*	*B. rostrata*	*C. bradyi*	*C.kullenbergi*	*C.jeffreysi*	*C. subglobosus*	*E. bradyi*	*E. rugosa*	*E. pusillus*	*G.translucens*	*H.elegans*	*H. balthica*	*K. conversa*	*M. barleeanum*	*R. bilocularis*	*R. scorpiurus*	*S.bulloides*	*T.bradyi*	*U. elongatastriata*	*U.mediterranea*	Other species
Transect Cape Ghir																											
6008-2	355	3311	459	285	346	1101												31		10	10				183	102	784
6007-1	899	1966		31	780	97	20	10					5	5				499					10		5	173	330
6006-2	1275	268			82	9	10	3	4	2		3	1	10	14	27	3	7		3	1		7	3		21	59
6005-1	1781	164					6	2	9	17		2	1		6	29	6	1	1		1		21			2	64
4207-1	2123	116					3	13	11	5	1					9	25		3								47
Transect A																											
4212-3	1256	84			3		1	1	5			1		3		3	1			1		1		16		12	36
4213-1	1547	86					7	1	2	4		9		2		4	17		1		2	3	3	4		1	27
4214-3	1788	30					1			3	2	1				3	2				1						16
4215-1	2106	46						1	1	2	7	2	1		4	1	1		1		1	1					23
4216-2	2325	60						2	3	2	1	1	3		2	1	3		1		1	7					33
Transect B																											
4225-3	1281	84						1	4	1	1		4	6		1	1				1	1		3		3	57
4226-1	1400	42					1		1	1		1	2	3		2	4		5			3	1	2		1	16
4227-1	1826	67							1	10	8	2	3			2	1				7	4		1			28
4217-1	2504	39					1	3	1	6		4					5		3			1					15
Transect C																											
4223-1	777	171			9			1				5		10			1	3		18		2		24		46	53
4231-2	1197	71					2		1			3	2			4	2			1		3		6		4	42
4230-1	1316	124					3		2	1	1	11	3	3	1	9	16		1	5	1	3	3	18		3	42
4229-2	1422	81					3	1	2	1	1	1	1	1		4	2		3	4	2	3	11	10			31
4228-1	1633	64					1		2	4		1			1	3	3		4		1	2		5			37
Transect D																											
4237-1	800	107			6		1	1			1		1	3		1		2		7	2	8		8		23	42
4236-2	1030	140			6		8	6	5				2	8		13	1			2	8	1		20		17	43
4235-1	1247	79					4	1	9	1	1	1		3		7	1			1	1	1	1	12		1	35
4234-1	1360	24					1		5								1			1				1			15
4233-2	1303	51					1	1	4			3		1		2	1			2		1		8			28
4232-1	1161	57		1			1		2	2		3		1		2	2				2	3	1	11		3	22
Transect Cape Yubi																											
5546-3	1071	163			26			4		1		1		13		14	4	15		1		1		15		15	53
5542-3	1431	236			28		22	7	1	1	4	1	1	2		64					1		10	1		22	70
5541-2	1748	67					1	1		11	1					13	4		1			1	7				26
5540-3	2035	187					1	3		20					1	11	68		1		3	16	1			5	57
5539-2	2202	109						1		6		2				1	56		2			3	1				37

Table 5: Foraminiferal numbers of empty tests in individuals per 50 cm^3 of surface fauna (0 – 1 cm) of dominant, associated, and remaining species as well as water

Core GeoB	Water depths (m)	Foraminiferal number	A. incertus	*B. spathulata*	*B. aculeata*	*B. mexicana*	*B. rostrata*	*C. laevigata*	*C. obtusa*	*C. bradyi*	*C. kullenbergi*	*C. wuellerstorfi*	*C. jeffreysii*	*C. subglobosus*	*C. wiesneri*	*E. exigua*	*E. rugosa*	*E. pusillus*	*G. translucens*	*G. subglobosa*	*H. elegans*	*H. baltica*	*K. bradyi*	*L. diflugiformis*	*L. lobatula*	*M. barleeanum*	*M. subrotunda*	*P. challengeri*	*P. irregularis*	*R. scorpiurus*	*T. bradyi*	*U. mediterranea*	*U. peregrina*	*U. proboscidea*	Other species
Transect Cape Ghir																																			
6008-2	355	3535		510	82			234							10				10	10		71			31	31						173			2373
6007-1	899	800	3	38	214	8	10	5		3		3	3						5		3	324				18						38	13		112
6006-2	1275	3137			428	112	71			132	10						306	10	754	20		20		41	10	92				20	10	153	61	20	867
6005-1	1781	2674				397	87	326		82	189	5				5	15	5	647	15	107				5		15						5		769
4207-1	2123	677				96	55	15		38	56	17	1						33		91				4		1								270
Transect A																																			
4212-3	1256	6173	20		122	224	61	61	285	265				82			754	41	265	408	143		102	82	102	143	82		387		143	122		102	2177
4213-1	1547	4414	82			217	95	122	82	27	82	14		41	14		109	14	380	285	245			82	95				380	14	109			27	1898
4214-3	1788	1060	19			37	22	4	7	22	37	22	26	7	4			7	30	37				15	37		41	26	93	15	4				548
4215-1	2106	334	20				1	1		6	3	6	21	16	6	1		22		7			1	5	1		3	2	14	1					197
4216-2	2325	451	14				3			4	11	13	29	8	22	15		18	3	5	3			13			1	12	32	21					224
Transect B																																			
4225-3	1281	727	7			7	18	7	43	6	2	2	7	2	2	7	48	7	109		2		23		41	2	7	5	23	2	14		5	34	295
4226-1	1400	2009	3		3	76	43	122	117	59	25			18	8	18	158	28	97	46	8		41	23	25	13	18		135			3		79	843
4227-1	1826	1983	20					61		7	75	143	82	48	41	41		20	88	7	14		20	20	20		27	61	95	20					1073
4217-1	2504	3127					102			51	132	102		51	132	336		102		31	31		10				20	102	234	41					1650
Transect C																																			
4223-1	777	7538		20	775	20	122		204	20	82			82	41	41	1060	20	20	183	163	20	20		20	591	20		61	41	367	978	183	387	1997
4231-2	1197	2764	22		7	37	75	7	194	52	7	15	7	7			172	15	172	90	52		75	82	45	15	67		224	15	75	45	75	135	980
4230-1	1316	5476	16		16	114	98	33	228	114	130	16		147	16	49	424	49	179	245	65		228	245	49	65	16		408		212	49	16	277	1972
4229-2	1422	3912				132	71	143	82	82	41	10		71	20	20	245	143	377	31	51		102	61	71	10	61		224	20	143			71	1630
4228-1	1633	3919	24			48	48		24	48	96				24	24	96	72	239	108	132		24	144	24	12	120		299	96	96			12	2109
Transect D																																			
4237-1	800	1295			158	5	1		3	11		18		3	2		68				51	6	16		43	56		2		4	43	213	149	2	441
4236-2	1030	6468	51		357	1529	968			102		61	31	20	10	10	520		245		51		71	20	71	173					408	122	132	102	1414
4235-1	1247	1818	10			41	15	41	71	36				10	15		112	5	219	15			15	76	46	36		5	117		87		46	66	734
4234-1	1360	267	1		1	2				16			1		2		1				6		14		11	7		1	4		5	1	7	1	186
4233-2	1303	1711				36	36		31	36		5		15	20		127		173	15			10	56	31	61	41		41	5	71		20	20	861
4232-1	1161	18960	163	109	54		217	109	761	109	217	54		109			544		109	598	54		54	109	598	272	1087		544		272	272		435	12110
Transect Cape Yubi																																			
5546-3	1071	4044		5	1085	76	122	25		46	31	31					535	5	418		15	5	5		56	102	5	5	10		36	413	20	5	988
5542-3	1431	1747		5	102	214	71	56		31	15					5	31	15	443	5	5		5	20	20	51						97	15		541
5541-2	1748	858	5			20	28	18		5	87	64	3	3	3			3	158	10	46			3	8								28		366
5540-3	2035	2811				82	153	102		10	173	204	10						122	20	601				41								20		1273
5539-2	2202	391				6	12	4		1	37	20			1			2	16	1	139			2			1						2		147

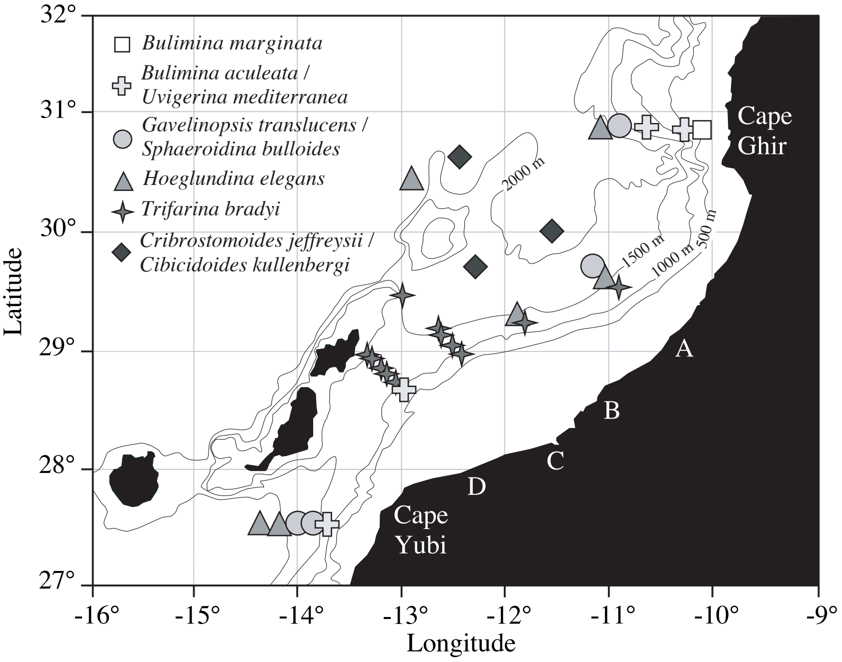

Fig. 2: Spatial composition and distribution of the five live assemblages in sediment surface samples and their dominant species revealed by factor analysis. Station GeoB 6008-2 (square) does not fit in any assemblage because of its unique faunal composition. Cape Ghir, A, B, C, D and Cape Yubi represent transects.

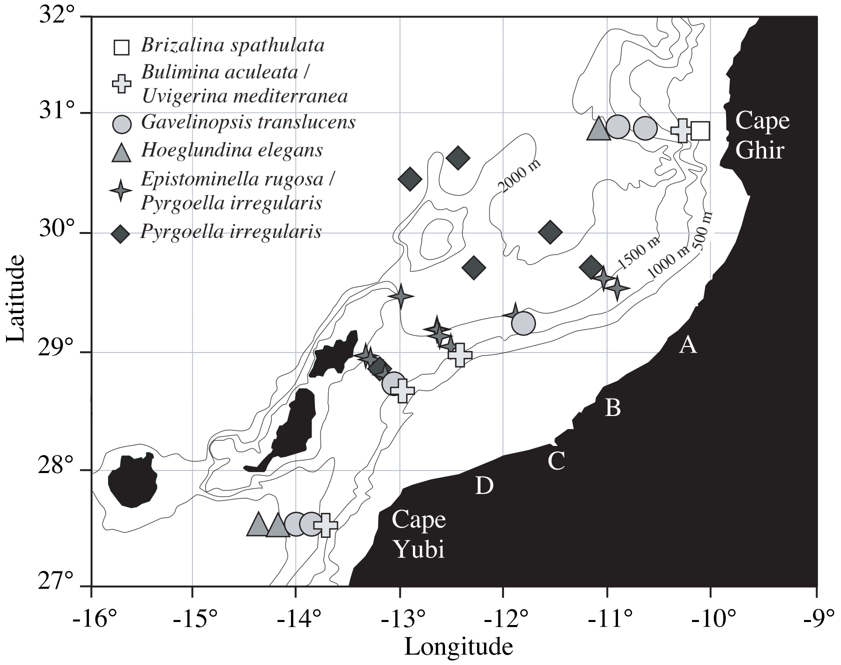

Fig. 3: Spatial composition and distribution of the five dead assemblages in sediment surface samples and their dominant species revealed by factor analysis. Station GeoB 6008-2 (square) does not fit in any assemblage because of its unique faunal composition. Cape Ghir, A, B, C; D and Cape Yubi represent transects.

Table 6: Results of the detrended correspondence analysis (DCA), and the canonical correspondence analysis (CCA) of the live and dead faunal data set. The length of the first and second axis in standard deviations (SD) and the variance (in %) explained by the axis of the DCA are listed. The significant environmental variables (95%, p value < 0.05, bold letters) are listed with their correlation coefficient for the first and second axis. Lambda (multiplied by 100) indicates the significance of the environmental parameter in percent.

	DCA axis 1		DCA axis 2		CCA				
	SD	Variance [%]	SD	Variance [%]	Variable	lambda	p value	Axis1	Axis2
Live	4.04	58.9	2.04	21.2	**Water depth**	0.22	**0.01**	**-0.83**	0.42
					Chlorophyll	0.11	**0.01**	**0.64**	**0.55**
					Fragmented PF	0.04	**0.01**	0.50	**0.58**
					Salinity	0.03	**0.03**	0.48	**-0.62**
					Sand	0.02	**0.03**	**-0.52**	-0.24
					Silt	0.03	0.08	0.67	0.08
					Velocity	0.03	0.14	-0.60	0.60
					O2	0.02	0.27	-0.55	0.63
					Carbonate	0.01	0.60	-0.52	-0.38
					TOC	0.01	0.44	0.57	0.57
					Distance f. African coast	0.01	1.00	-0.39	-0.50
Dead	4.16	61.3	2.75	25.3	**Water depth**	0.21	**0.01**	**-0.82**	0.43
					Carbonate	0.14	**0.01**	**-0.76**	-0.42
					Chlorophyll	0.10	**0.01**	**0.67**	**0.51**
					Salinity	0.04	**0.01**	0.53	**-0.71**
					Distance f. African coast	0.02	**0.03**	**-0.52**	-0.48
					Fragmented PF	0.02	0.10	0.64	0.53
					Velocity	0.02	0.17	-0.57	0.67
					Silt	0.01	0.38	0.64	0.11
					O2	0.02	0.57	-0.54	0.68
					TOC	0.01	0.65	0.69	0.59
					Sand	0.01	0.65	-0.64	-0.34

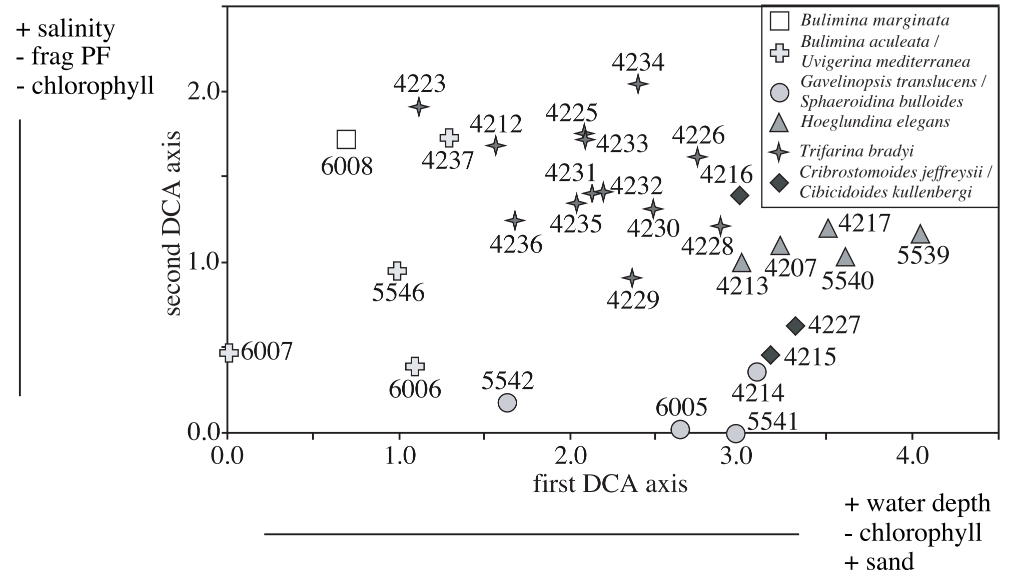

Fig. 4: Graph of the detrended correspondence analysis (DCA) of 30 sediment surface samples, based on the relative abundances of the 21 most important live species. DCA confirms the grouping of five assemblages by factor analysis. The first DCA axis most likely represents variation in species distribution caused by the chlorophyll-*a* concentrations, water depths and sand contents. The second DCA axis most likely represents variation in species distribution caused by salinity and chlorophyll-*a* concentrations.

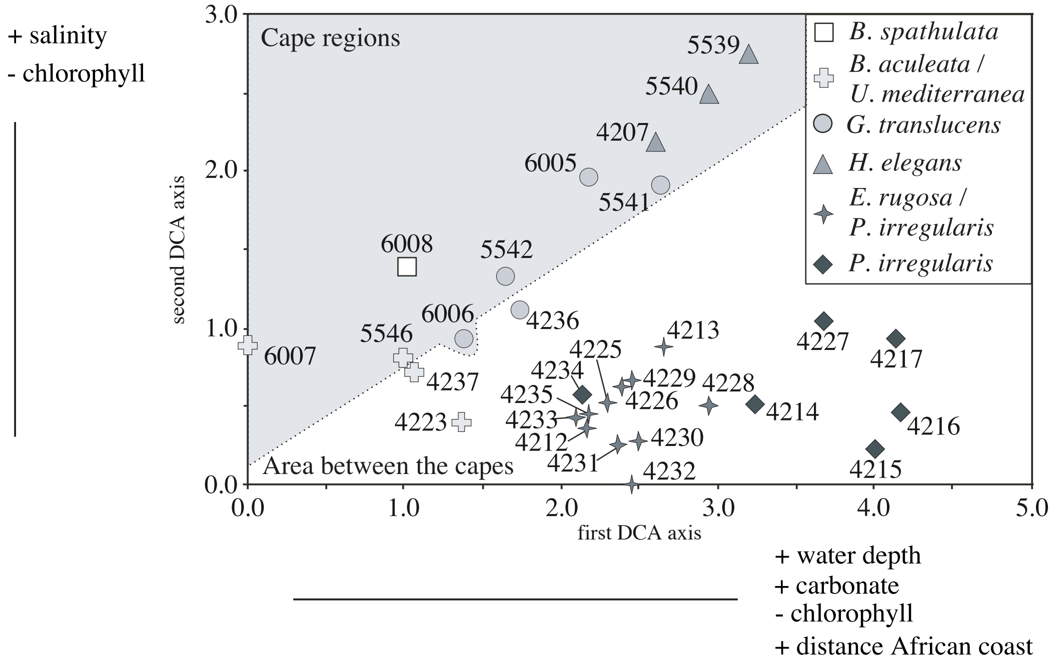

Fig. 5: Graph of the detrended correspondence analysis (DCA) of the 30 sediment surface samples, based on the relative abundances of the 31 most important dead species. DCA confirms the grouping of five assemblages by factor analysis. The first DCA axis most likely represents variation in species distribution caused by the water depths, carbonate contents, chlorophyll-*a* concentrations, and distance from the African coast. The second DCA axis most likely represents variation in species distribution caused by salinity, fragmented planktic foraminiferal contents, and chlorophyll-*a* concentrations. Stations positioned in the cape regions are shaded grey; stations in the area between the capes are not shaded.

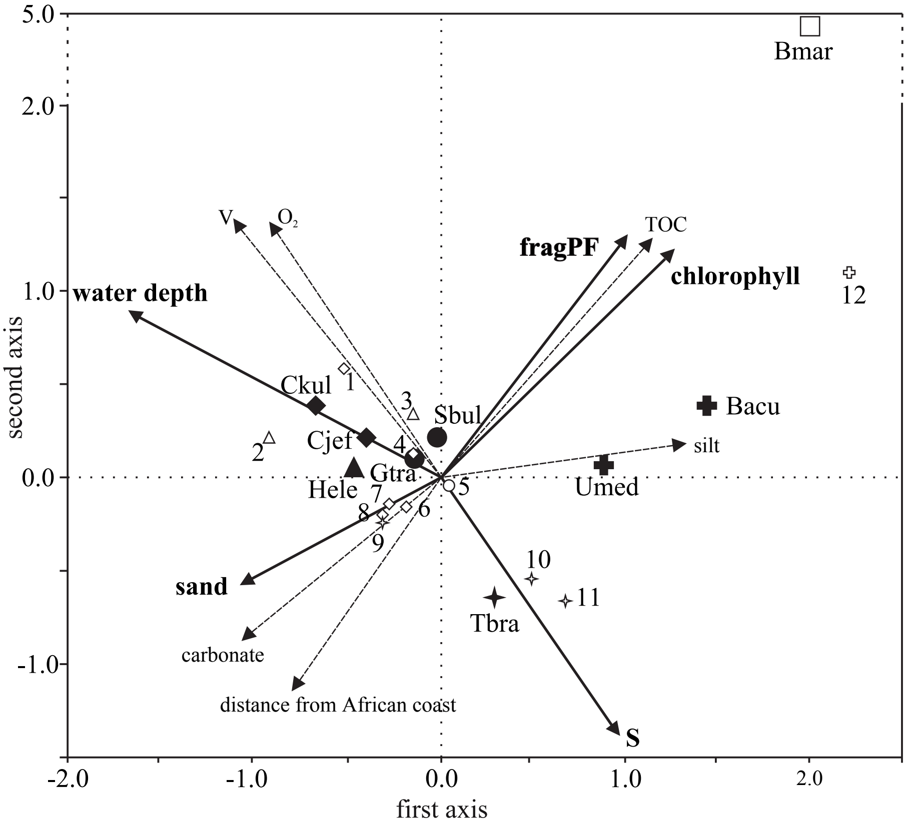

Fig. 6: Graph of the canonical correspondence analysis (CCA) represents the 21 most important live species and their correlation with environmental parameters. Dominant species are given by filled symbols with the following abbreviations: Bmar: *Bulimina marginata*, Bacu: *Bulimina aculeata*, Umed: *Uvigerina mediterranea*, Gtra: *Gavelinopsis translucens*, Sbul: *Sphaeroidina bulloides*, Hele: *Hoeglundina elegans*, Tbrad: *Trifarina bradyi*, Cjef: *Cribrostomoides jeffreysii*, Ckul: *Cibicidoides kullenbergi*. Associated species are given with numbers and open symbols as follows: 1: *Eponides pusillus*, 2: *Karrerulina conversa*, 3: *Bulimina rostrata*, 4: *Reophax bilocularis*, 5: *Bulimina mexicana*, 6: *Eggerella bradyi*, 7: *Cribrostomoides subglobosus*, 8: *Reophax scorpiurus*, 9: *Cibicidoides bradyi*, 10: *Epistominella rugosa*, 11: *Melonis barleeanum*, 12: *Hyalinea balthica*. Arrows represent environmental parameters. Abbreviation 'FragPF': fragmented planktic foraminifera. Significant (95 %) parameters are marked by solid arrow line and bold letters. The perpendicular projection of the species on the environmental parameter indicates the importance of this variable for the variation within this species, which increases with increasing length of the arrow.

The live and dead *Bulimina aculeata* / *Uvigerina mediterranea* assemblages dominate with high standing stocks (Tables 4, 5) at stations in shallow water depths between 777 and 1275 m on the Cape Ghir, C, D, and Cape Yubi transects (Figs. 2, 3, Table 3). At the same stations foraminiferal numbers of these species are considerably higher compared to standing stocks (Tables 4, 5). Both, live and dead assemblages show affinities to enhanced chlorophyll-α concentrations (0.3 to 1.4 mg / m^3) and intermediate to high salinities (35.31 to 35.60). Furthermore, the live assemblage occurs where high fragmented planktic foraminiferal contents (20 to 32 %) and low sand contents (2 to 15 %) are recorded (Fig. 6, Table 3). The dead assemblage correlates with low to intermediate carbonate contents (25 to 53 %) and short to middle distances from the African coast (42 to 186 km) (Fig. 7, Table 3).

The live *Gavelinopsis translucens / Sphaeroidina bulloides* assemblage shows high standing stocks mainly on the Cape Ghir, A, and Cape Yubi transects (Table 4) in intermediate water depths (1431 to 1788 m). The dead *G. translucens* assemblage occurs on transects Cape Ghir, B, D, and Cape Yubi (Figs. 2, 3) in intermediate water depths (1275 to 1788 m) (Figs. 2, 3, Table 3). Generally, at the same station foraminiferal numbers of *G. translucens* are considerably higher compared to standing stocks (Tables 4, 5). The live *G. translucens* / *S. bulloides* assemblage shows affinities to intermediate to high chlorophyll-α concentrations (0.8 to 1.3 mg / m^3), high fragmented planktic foraminiferal contents (16 to 29 %), low sand contents (6 to 8 %), and low to intermediate salinities (34.90 to 35.30) (Fig. 6, Table 3). The dead *G. translucens* assemblage additionally correlates with low to intermediate carbonate contents (10 to 32 %) and short to middle distances from the African coast (57 to 222 km) (Fig. 7).

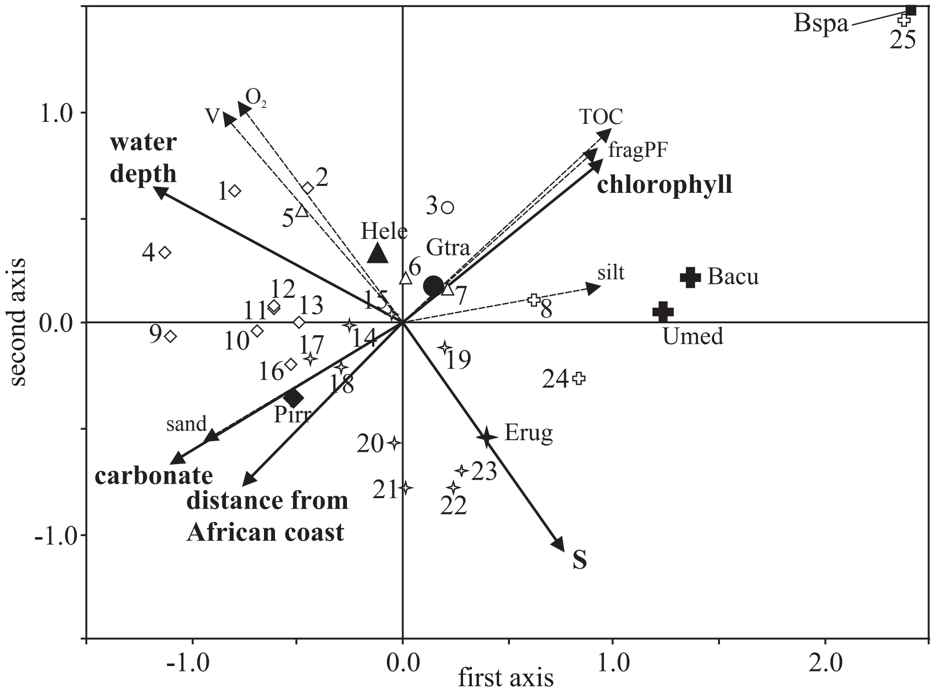

Fig. 7: Graph of the canonical correspondence analysis (CCA) represents the 31 most important dead species and their correlation with environmental parameters. Dominant species are given by filled symbols with the following abbreviations: Bspa: *Brizalina spathulata*, Bacu: *Bulimina aculeata*, Umed: *Uvigerina mediterranea*, Gtra: *Gavelinopsis translucens*, Hele: *Hoeglundina elegans*, Erug: *Epistominella rugosa*, Pirr: *Pyrgoella irregularis*. Associated species are given with numbers and open symbols as follows: 1: *Cribrostomoides jeffreysii*, 2: *Cibicidoides wuellerstorfi*, 3: *Cassidulina laevigata*, 4: *Paratrochammina challengeri*, 5: *Cibicidoides kullenbergi*, 6: *Bulimina rostrata*, 7: *Bulimina mexicana*, 8: *Uvigerina peregrina*, 9: *Epistominella exigua*, 10: *Reophax scorpiurus*, 11: *Cribrostomoides wiesneri*, 12: *Eponides pusillus*, 13: *Ammodiscus incertus*, 14: *Globocassidulina subglobosa*, 15: *Cibicidoides bradyi*, 16: *Cribrostomoides subglobosus*, 17: *Miliolinella subrotunda*, 18: *Lagenammina difflugiformis*, 19: *Lobatula lobatula*, 20: *Karreriella bradyi*, 21: *Cassidulina obtusa*, 22: *Uvigerina proboscidea*, 23: *Trifarina bradyi*, 24: *Melonis barleeanum*, 25: *Hyalinea balthica*. Arrows represent environmental parameters. Abbreviation 'FragPF': fragmented planktic foraminifera. Significant (95 %) parameters are marked by solid arrow line and bold letters. The perpendicular projection of the species on the environmental parameter indicates the importance of this variable for the variation within this species, which increases with increasing length of the arrow.

Hoeglundina elegans shows high standing stocks on the Cape Ghir, B, and Cape Yubi transects (Table 4) in intermediate to great water depths (1547 to 2504 m), whereas the dead assemblage occurs in greater water depths (2035 to 2504 m) only off the capes (Figs. 2, 3, 7, Table 3). At the same station, foraminiferal numbers of *H. elegans* are considerably higher compared to standing stocks (Tables 4, 5). The live and dead *H. elegans* assemblages show affinities to low to intermediate chlorophyll-α concentrations (0.2 to 0.4 mg / m^3) and salinities (34.90 to 35.30) (Figs. 6, 7, Table 3). Additionally, the live assemblage occurs at stations with intermediate to high sand contents (8 to 37 %) and low to high fragmented planktic foraminiferal contents (8 to 28 %) (Fig. 6, Table 3), whereas the dead assemblage occurs at stations with intermediate carbonate contents (35 to 39 %) (Figs. 3, 7, Table 3).

The live *Trifarina bradyi* assemblage dominates exclusively at stations in the area between the capes (Table 4) in shallow to intermediate water depths (777 to 1633 m) (Fig. 2, Table 3). The associated dead *Epistominella rugosa* / *Pyrgoella irregularis* assemblage (Table 5) dominates at stations in intermediate water depths (1161 to 1633 m) (Fig. 3, Table 3). Both assemblages depend on high salinity (35.60) and low chlorophyll-α concentrations (0.2 to 0.3 mg / m^3) (Figs. 6, 7, Table 3). The live *T. bradyi* assemblage occurs at stations with low to intermediate fragmented planktic foraminiferal contents (6 to 18 %), and intermediate to high sand contents (13 to 38 %) (Fig. 6, Table 3). The dead *E. rugosa* / *P. irregularis* assemblage correlates with high carbonate contents (48 to 63 %) (Fig. 7, Table 3).

The live *Cribrostomoides jeffreysii* / *Cibicidoides kullenbergi* assemblage (1826 to 2325 m) and the associated dead *P. irregularis* assemblage (1788 to 2504 m) occur at stations in great water depths further offshore in the area between the capes (Figs. 2, 3, Tables 4, 5). *Cibicidoides kullenbergi* shows also elevated standing stocks and foraminiferal numbers in the cape regions (Tables 4, 5). The live *C. jeffreysii* / *C. kullenbergi* assemblage and dead *P. irregularis* assemblage can be attributed to low chlorophyll-α concentrations (around 0.2 mg / m^3). The live *C. jeffreysi* / *C. kullenbergi* assemblage additionally correlates with low salinities (34.90), low fragmented planktic foraminiferal contents (4 to 13 %), and high sand contents (51 to 57 %) (Fig. 6, Table 3), whereas the dead *P. irregularis* assemblage correlates with high carbonate contents (64 to 72 %) and middle to great distances from the African coast (127 to 316 km) (Fig. 7, Table 3).

4.2 $\delta^{13}C_{DIC}$

The $\delta^{13}C_{DIC}$ of bottom waters ranges from 0.43 to 0.86 ‰ (Table 7). The NACW exhibits a $\delta^{13}C_{DIC}$ value of 0.49 ‰. The $\delta^{13}C_{DIC}$ values of the MOW range between 0.65 and 0.83 ‰, with a mean of 0.72 ± 0.08. The $\delta^{13}C_{DIC}$ values of the NADW range between 0.43 and 0.86 ‰, with a mean of 0.63 ± 0.17. Stations bathed by the AAIW are represented by a mean of 0.66 ± 0.14. We had to omit some data from the final interpretation because of a sampling error. Therefore, we calculated the mean carbon and oxygen values for each watermass and inserted these values at stations with no isotope data (Table 7).

4.3 Isotopic composition of live and dead specimens

The stable oxygen and carbon isotopic composition of calcareous tests of live and dead specimens of *Bulimina aculeata*, *Bulimina mexicana*, *Cibicidoides kullenbergi*, *Cibicidoides wuellerstorfi*, *Hoeglundina elegans*, *Uvigerina mediterranea,* and *Uvigerina peregrina* was determined (Fig. 8). The total range of $\delta^{13}C$ values is –1.61 ‰ to 2.66 ‰ for live specimens and –1.06 ‰ to 2.60 ‰ for dead specimens. Both $\delta^{13}C$ ranges and mean $\delta^{13}C$ values are generally comparable for live and dead specimens (Table 8).

All specimens show lower mean $\Delta\delta^{13}C$ values ($\delta^{13}C_{foram} - \delta^{13}C_{DIC}$) in the cape regions and higher mean $\Delta\delta^{13}C$ values in the area between the capes compared with the mean $\Delta\delta^{13}C$ values (Figs. 9, 10, 11, Table 8). In the live fauna high species-specific offsets between the cape regions and the area between the capes are recorded in *U. peregrina* (1.02 ‰), *U. mediterranea* (0.82 ‰), *C. kullenbergi* (0.65 ‰), *B. mexicana* (0.54 ‰), and *H. elegans* (0.50 ‰) (Fig. 9, Table 8). Negligible species-specific offsets are recorded in live *C. wuellerstorfi* (0.08 ‰) and *B. aculeata* (0.23 ‰) (Fig. 9, Table 8). In the dead fauna the species-specific offsets are generally comparable with those of the corresponding live species, with the exception of *U.peregrina*. High species-specific offsets between the two regions are recorded in *U. mediterranea* (0.87 ‰), *B. mexicana* (0.68 ‰), *C. kullenbergi* (0.62 ‰), *U. peregrina* (0.51 ‰), *H. elegans* (0.48 ‰), and *B. aculeata* (0.48 ‰) (Fig. 10, Table 8). Only *C. wuellerstorfi* (0.22 ‰) shows a negligible species-specific offset.

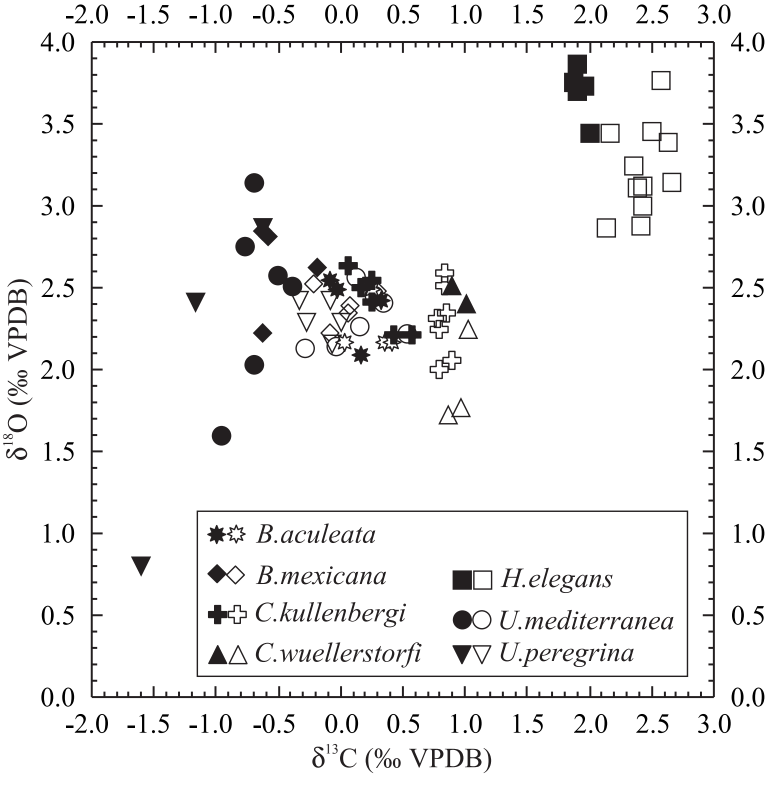

Fig. 8: Stable oxygen and carbon isotope signal of different live (Rose Bengal stained) benthic foraminifera from sites in the cape regions (filled symbols) and the area between the capes (open symbols).

Table 7: Isotope values of $\delta^{13}C_{DIC}$, water depth and water mass at each station. Italic letters represent means for a water mass. $\delta^{13}C$ value of 0.63 ‰ is characteristic for NADW, 0.72 ‰ for MOW and 0.66 ‰ for AAIW.

Core GeoB	Water depth (m)	Watermass	$\delta^{13}C_{DIC}$ (‰ VPDB)	Deviation $\delta^{13}C_{DIC}$ (‰ VPDB)
Transect Cape Ghir				
6008-2	355	NACW	0.49	0.02
6007-1	899	AAIW	*0.66*	*0.02*
6006-2	1275	MOW	*0.72*	*0.08*
6005-1	1781	NADW	*0.63*	*0.01*
4207-1	2123	NADW	*0.63*	*0.17*
Transect A				
4212-3	1256	MOW	*0.72*	*0.08*
4213-1	1547	MOW	*0.72*	*0.08*
4214-3	1788	NADW	*0.63*	*0.17*
4215-1	2106	NADW	*0.63*	*0.17*
4216-2	2325	NADW	0.61	0.02
Transect B				
4225-3	1281	MOW	*0.72*	*0.08*
4226-1	1400	MOW	0.65	0.02
4227-1	1826	NADW	0.62	0.02
4217-1	2504	NADW	0.43	0.09
Transect C				
4223-1	777	AAIW	*0.66*	*0.14*
4231-2	1197	MOW	*0.72*	*0.08*
4230-1	1316	MOW	*0.72*	*0.08*
4229-2	1422	MOW	0.72	0.06
4228-1	1633	NADW	*0.63*	*0.08*
Transect D				
4237-1	800	AAIW	*0.66*	*0.14*
4236-2	1030	MOW	*0.72*	*0.08*
4235-1	1247	MOW	0.69	0.01
4234-1	1360	MOW	*0.72*	*0.08*
4233-2	1303	MOW	*0.72*	*0.08*
4232-1	1161	MOW	0.72	0.03
Transect Cape Yubi				
5546-3	1071	MOW	0.79	0.02
5542-3	1431	MOW	0.83	0.01
5541-2	1748	NADW	*0.63*	0.00
5540-3	2035	NADW	*0.72*	*0.08*
5539-2	2202	NADW	0.86	0.01

Table 8: Mean values for the differences between test $\delta^{13}C$ and bottom water $\delta^{13}C_{DIC}$ for living and dead specimens from stations in the cape regions (CR) and the area between the capes (AbC). SD = Standard deviation, n = number of measured species. Sign in column in species-specific offset indicates lighter or heavier values in the cape regions.

	$\Delta\delta^{13}C$ Min	$\Delta\delta^{13}C$ Max	mean $\Delta\delta^{13}C$ CR	mean $\Delta\delta^{13}C$ Study area	mean $\Delta\delta^{13}C$ AbC	species specific offset between CR / AbC $\Delta\delta^{13}C$	n CR	n AbC	SD CR	SD AbC
Live Fauna										
C. wuellerstorfi	0.15	0.38	0.32	0.27	0.24	0.08	2	3	0.09	0.08
H. elegans	0.52	1.52	1.25	1.60	1.75	-0.50	5	11	0.13	0.21
C. kullenbergi	-1.23	-0.16	-0.44	-0.07	0.21	-0.65	6	8	0.19	0.12
B. aculeata	-0.91	-0.57	-0.65	-0.54	-0.42	-0.23	4	4	0.24	0.16
B. mexicana	-1.46	-0.94	-1.21	-0.92	-0.68	-0.54	4	5	0.23	0.20
U. mediterranea	-1.59	-0.93	-1.34	-0.9	-0.52	-0.82	6	7	0.16	0.26
U. peregrina	-2.33	-1.26	-1.87	-1.24	-0.86	-1.02	3	5	0.43	0.16
Dead Fauna										
C. wuellerstorfi	-0.08	0.30	0.19	0.30	0.41	-0.22	7	7	0.21	0.10
H. elegans	0.92	1.54	1.26	1.54	1.74	-0.48	7	10	0.25	0.11
C. kullenbergi	-0.56	0.01	-0.24	0.01	0.37	-0.62	7	5	0.19	0.13
B. aculeata	-0.80	-0.36	-0.58	-0.36	-0.09	-0.48	5	4	0.17	0.21
B. mexicana	-1.54	-0.60	-1.08	-0.60	-0.40	-0.68	5	12	0.39	0.30
U. mediterranea	-1.27	-0.71	-1.06	-0.71	-0.19	-0.87	6	4	0.16	0.12
U. peregrina	-1.72	-0.04	-1.21	-0.94	-0.70	-0.51	7	8	0.26	0.07

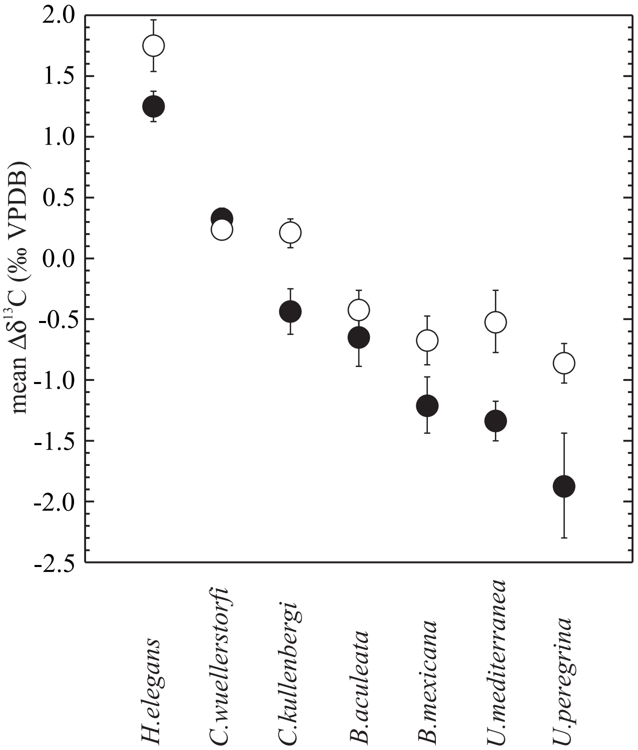

Fig. 9: Mean $\Delta\delta^{13}C$ values ($\delta^{13}C_{foram} - \delta^{13}C_{DIC}$) for different live species in the cape regions (filled symbols) and the area between the capes (open symbols). Vertical bars indicate standard deviation.

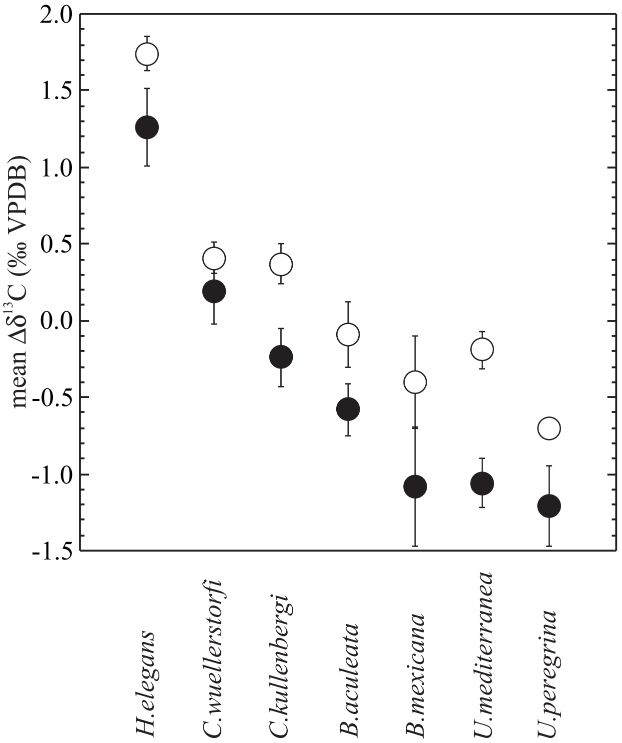

Fig. 10: Mean $\Delta\delta^{13}C$ values ($\delta^{13}C_{foram} - \delta^{13}C_{DIC}$) for different dead species in the cape regions (filled symbols) and the area between the capes (open symbols). Vertical bars indicate standard deviation.

5. Discussion

5.1 Faunal distribution

We found faunal differences in live and dead assemblages in the area between the capes in contrast to the area off the capes (Figs. 2, 3, Table 2). Generally, compared to the live fauna, the dead fauna represents a longer time period and is influenced by various chemical and physical processes, including productivity differences, interspecific differences in turnover rates, degradation due to bioerosion or dissolution, bioturbation, and transport (Mackensen et al., 1995; Jorissen and Wittling, 1999). So which of the significant environmental parameters (Table 6) influence the faunal composition and distribution, and what factors are responsible for the observed differences? The parameters chlorophyll concentration, water depth, and fragmented planktic foraminiferal content reflect similar environmental conditions. The chlorophyll concentration controls the quantity of exported organic matter to the sea floor, which in turn is a function of water depth. Furthermore, a higher content of fragmented planktic foraminifera indicate increased carbonate dissolution as a result of enhanced organic matter fluxes. Therefore, our discussion will focus mainly on chlorophyll concentrations, sand and carbonate contents and salinity.

We observed a good correlation between chlorophyll-α concentrations in surface waters and standing stocks. Increasing standing stocks parallel high chlorophyll-α concentrations (Fig. 11).

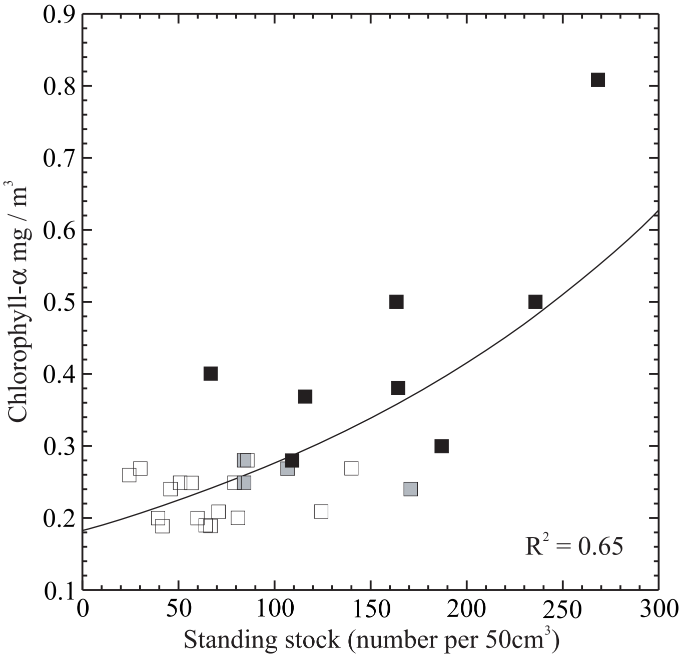

Fig. 11: Correlation between standing stock (28 stations) in individuals per 50 cm³ (0 – 1 cm) and chlorophyll-*a* concentration in surface waters. Black symbols: standing stock at stations in the cape regions, light grey symbols: standing stock at stations in shallowest water depths on transects A to D, open symbols: standing stock at stations in the area betwen the capes. Stations GeoB 6006-2 and GeoB 6008-2 are statistically outliers and are excluded from correlation. Standing stock values are listed in Table 4.

Furthermore, the live and dead assemblages are identical off the capes (Figs. 2, 3), but with considerably higher densities in the dead fauna (Tables 4, 5). In particular, *Bulimina aculeata, Bulimina marginata*, *Gavelinopsis translucens*, *Hoeglundina elgans, Sphaeroidina bulloides,* and *Uvigerina mediterranea* show enhanced standing stocks at stations underlying high chlorophyll-α concentrations with 0.7 mg/cm^{-3} on average in the cape regions and considerably lower standing stocks in the area between the capes with 0.2 mg/cm^{-3} on average (Fig. 11, Tables 3, 4). The dependence of standing stocks on organic matter fluxes has been reported from various areas (Lutze and Coulbourn, 1984; Schmiedl et al., 2000; Fontanier et al., 2002). The relationship between different species and chlorophyll-α concentrations is expressed in the CCA graph (Fig. 6). The positions of *Bulimina marginata, Hyalinea balthica*, *B. aculeata*, and *U. mediterranea* along the arrow representing chlorophyll-α concentrations reflect the continuous decrease in values of this parameter (Fig. 6). Hence, *B. marginata*, in particular, tends to be associated with highest chlorophyll-α concentrations, which in turn means an elevated organic matter supply. This is indicated by a high standing stock of *B. marginata* only at station GeoB 6008-2 off Cape Ghir (Table 4). *Hyalinea balthica*, *B. aculeata*, and *U. mediterranea* show highest standing stocks at stations off Cape Ghir and Cape Yubi. High standing stocks are also found at stations in shallowest water depths on transects C and D (Table 4), which are regularly influenced by the Cape Yubi filament (Davenport et al., 2002). *Bulimina marginata* is found in high, year-round productive areas (e.g. Lutze and Coulbourn, 1984; Jorissen et al., 1998; Fontanier et al., 2002). *Hyalinea balthica* often occurs in association with *B. marginata* (Morigi et al., 2001; Fontanier et al., 2002). *Bulimina aculeata* and *U. mediterranea* are commonly found in eutrophic areas with enhanced C_{org} contents in the sediment (e.g. Lutze and Coulbourn, 1984; Schmiedl et al., 2000). *Bulimina marginata* and *Bulimina aculeata* are described as opportunistic species with high standing stocks due to the response to fresh organic matter inputs (De Rijk et al., 2000). *Gavelinopsis translucens* and *S. bulloides* are observed in high primary productivity areas with a more seasonal variation in food supply (Jorissen et al., 1998; Loubere and Fariduddin, 1999; Licari and Mackensen, 2005). *Hoeglundina elegans* is described from mesotrophic to eutrophic environments with low organic carbon contents (Lutze and Coulbourn, 1984; Jorissen and Wittling, 1999), and under oxic conditions (Schönfeld, 2001). Kaiho (1994) considered *H. elegans* to be typical for suboxic conditions.

Live specimens of *B. aculeata*, *B. marginata*, *H. balthica*, and *U. mediterranea* are adapted to sediments with sand contents of less than 15 % (Fig. 6, Table 3). *Bulimina aculeata* has been reported in fine-grained sediments before (Mackensen et al., 1995). Generally, the cape regions are characterized by either fine-grained aeolian dust inputs or fluvially discharged mud, whereas the area between the capes is characterized by coarse-grained sediments (Holz et al., 2004). The dominant dead species in the cape regions are linked to lower carbonate contents with an average of 33 % compared to 57 % in the area between the capes (Figs. 4, 5, 6, 7, Table 3). These low carbonate contents may indicate higher carbonate dissolution rates in the cape regions (Meggers et al., 2002). In contrast, the dead fauna is enriched in numbers of *C. kullenbergi, C. wuellerstorfi,* and *H. elegans* (Tables 4, 5), which are known to dissolve easily (Corliss and Honjo, 1981). Furthermore, we did not observe any obvious signs of carbonate dissolution when counting dead specimens.

We suggest that the dominant species and their high standing stocks mirror the generally more eutrophic conditions in surface waters in the cape regions. Furthermore, the identical live and dead faunas indicate constant, high productivity conditions in these areas. Additionally, the succession of assemblages from the shelf to the deep sea most likely reflects the decreasing amount of organic matter reaching the sea floor. Carbonate dissolution did not alter benthic foraminiferal tests, and the sand content is of minor importance in determining benthic foraminiferal distribution.

In contrast to the cape regions, live and dead assemblages are different in the area between the capes (Figs. 2, 3). *Cibicidoides kullenbergi* occurs at stations with low chlorophyll-*a* concentrations (Tables 3, 4). Admittedly, this species also showed elevated standing stocks at stations off the capes where intermediate chlorophyll-*a* concentrations were observed (Fig. 6), thus indicating that *C. kullenbergi* is adapted to different productivity regimes. This is in agreement with Lutze and Coulbourn (1984), who reported this species in low organic carbon settings and Jorissen et al. (1998), who observed this species in areas continuously influenced by upwelling. Additionally, the relatively high abundances of agglutinated species, which are characteristic of oligotrophic settings (Jorissen et al., 1998), and low standing stocks indicate more oligotrophic conditions in the area between the capes (Tables 2, 4).

The *Trifarina bradyi* assemblage showed affinities to a high salinity of 35.6 (Fig. 6, Table 3) and occurred with highest densities at stations in water depths between 800 and 1300 m (Fig. 2, Table 4). These stations are bathed by the high-salinity Mediterranean Outflow Water (Knoll et al., 2002; Llinás et al., 2002). The *T. bradyi* assemblage plots in the center of all other significant parameters (Fig. 6), so either the assemblage is typical for intermediate values or it is adapted to a broad range of conditions. Therefore, we suggest that the salinity is an important parameter influencing the distribution of the *T. bradyi* assemblage.

Population dynamics are to a great extend controlled by food supply. We found high numbers of opportunistic species including *Epistominella exigua, Eponides pusillus*, and *Globocassidulina subglobosa* in the dead fauna (Tables 2, 5) in the area between the capes. These species show a rapid population increase in oligotrophic areas where seasonally pulsed phytodetritus inputs are predominant (Gooday, 1988; Gooday, 1993; Fariduddin and Loubere, 1997; Loubere, 1998; Gooday, 2001). Their population size strongly declines when the phytodetritus is consumed, and large numbers of dead tests are found in the sediment due to their high reproduction potential.

We suggest that the faunal composition and distribution as well as low standing stocks characterize more oligotrophic conditions in the area between the capes. The observed differences in live and dead assemblages are probably due to population dynamics, which are mainly a result of low and seasonally varying organic matter fluxes in the area between the capes. Summarizing, we conclude that primary productivity appears to have the largest influence on the composition and distribution of benthic foraminiferal faunas in the upwelling area off Morocco.

5.2 Foraminiferal stable carbon isotopic composition

The trophic differences as deduced from benthic foraminiferal faunas are also reflected by different $\delta^{13}C$ signals of infaunal living species. Our data show a strong depletion of mean $\delta^{13}C$ values of live and dead *Bulimina aculeata, Bulimina mexicana*, *Cibicidoides kullenbergi*, *Hoeglundina elegans, Uvigerina mediterranea*, and *Uvigerina peregrina* in the eutrophic cape regions compared to the oligotrophic area between the capes (Figs. 9, 10, 11, Table 8). The highest offset of 1.02 ‰ was recorded in live *U. peregrina*. Considerably lower $\delta^{13}C$ values are also seen in live *U. mediterranea* (0.82 ‰), *C. kullenbergi* (0.65 ‰), *B. mexicana* (0.54 ‰), and *H. elegans* (0.50 ‰). The $\delta^{13}C$ values of corresponding dead specimens exhibit similar ranges with the exception of *U. peregrina* (0.51 ‰) (Table 8). The impact of C_{org} fluxes on the $\delta^{13}C$ record was first shown for *U. peregrina* (Zahn et al., 1986). More recently McCorkle et al. (1997) reported a range of approximately 1.5 ‰ in $\delta^{13}C$ values of *U. peregrina*, depending on organic matter fluxes. Vergnaud Grazzini and Pierre (1991) demonstrated a depletion of - 0.9 ‰ for *U. peregrina* in eutrophic conditions, which is in good agreement with our observed depletion of - 1.02 ‰ for this species. In contrast to these findings Schmiedl et al. (2004) did not document lower $\delta^{13}C$ values of *U. peregrina* in eutrophic conditions.

The depletion of - 0.82 ‰ in live *U. mediterranea* exceeds the value of - 0.58 ‰ observed by Schmiedl et al. (2004), probably because of higher trophic differences in our study area. Here, to our knowledge for the first time, we report a strong lowering of $\delta^{13}C$ values of *C. kullenbergi* and *H.elegans* as a direct response to enhanced organic matter fluxes. We did not see a strong influence on the $\delta^{13}C$ values of *B. aculeata,* which is in contrast to findings of Mackensen et al. (2000), who reported a depletion by - 0.9 ‰ in this species. The measured individuals of *B. aculeata* in the area between the capes originate from stations in shallowest water depths on transect A, which is influenced by coastal upwelling, and from stations on transects C and D, which are regularly influenced by the Cape Yubi filament (Davenport et al., 2002). This points to the existence of trophic conditions at these stations comparable to those prevailing off the capes. Therefore, no high offset in $\delta^{13}C$ values of *B. aculeata* is to be expected.

Microhabitat differences cause most of the $\delta^{13}C$ signal variability of infaunal living benthic foraminifera (McCorkle et al., 1990; Rathburn et al., 1996; McCorkle et al., 1997). The $\delta^{13}C$ differences between infaunal species and bottom water DIC indicate the pore water $\delta^{13}C_{DIC}$ gradient (McCorkle et al., 1997). The pore water $\delta^{13}C$ gradient is a function of the degradation rate of organic matter. Therefore, the depletion of ^{13}C in pore water DIC is reflected by the decrease of $\delta^{13}C$ values with increasing living depths (e.g. Woodruff et al., 1980; McCorkle et al., 1990; Loubere et al., 1995; Mackensen et al., 2000; Holsten et al., 2004; Schmiedl et al., 2004). Obviously, the $\delta^{13}C$ values of all specimens of the same species vary little over the entire habitat depth in which they occur (e.g. Mackensen and Douglas, 1989; McCorkle et al., 1990; Rathburn et al., 1996; Mackensen et al., 2000; Mackensen and Licari, 2004). In our study mean $\delta^{13}C$ values of live and dead *B. aculeata*, *B. mexicana*, *C. kullenbergi, U. mediterranea* and *U. peregrina* exhibit negative deviations from the $\delta^{13}C_{DIC}$ of bottom water. The different $\delta^{13}C$ values seem to be in excellent agreement with their described microhabitat preferences (Fontanier et al., 2002; Licari et al., 2003). The isotopic composition of shallow-infaunal species shows higher $\delta^{13}C$ values than deep infaunal living species (McCorkle et al., 1990; Rathburn et al., 1996; Schmiedl et al., 2004). From our core-top data it is not possible to determine whether species indicate an average pore water $\delta^{13}C$ signal or a species-specific calcification depth.

It was shown that *Cibicidoides wuellerstorfi* secretes its test close to a 1:1 relationship with ambient bottom water DIC (Woodruff et al., 1980; Belanger et al., 1981; Graham et al., 1981; Zahn et al., 1986). Because of its preference for an elevated habitat above the sediment-water interface (Lutze and Thiel, 1989), *C. wuellerstorfi* reliably records the bottom water $\delta^{13}C_{DIC}$ (Duplessy et al., 1988; McCorkle and Keigwin, 1994; Mackensen and Licari, 2004), and is used to reconstruct deep-water circulation changes (Mackensen et al., 2001; Bickert and Mackensen, 2004; Curry and Oppo, 2005). Productivity-linked ^{13}C depletion in tests of *C. wuellerstorfi* has been reported from highly seasonal productivity areas with pulsed phytodetritus inputs (Mackensen et al., 1993b). In our study, mean $\delta^{13}C$ values of *C. wuellerstorfi* from the eutrophic cape regions and the oligotrophic area between the capes are almost identical (Figs. 9, 10, 11, Table 8).

Obviously, the $\delta^{13}C$ signal of *C. wuellerstorfi* tests is not influenced by sustained high organic matter fluxes in the cape regions, and our results indicate that *C. wuellerstorfi* is a faithful recorder of the bottom water $\delta^{13}C_{DIC}$ in the Canary Islands regions. In contrast, the lower $\delta^{13}C$ values of infaunal living species in the cape regions compared with the area between the capes reliably record the trophic differences. The observed differences in species-specific offsets in $\delta^{13}C$ signals of infaunal living species indicate infaunal microhabitat preferences. Thus, they either reflect the pore water $\delta^{13}C_{DIC}$ gradient or a species-specific calcification depth. The generally good agreement of $\delta^{13}C$ values in live and dead tests is a pre-condition for their application as a paleoproductivity proxy in this region.

6. Conclusion

The composition and distribution of live and dead benthic foraminiferal assemblages between Cape Ghir (31°N) and Cape Yubi (27°N) in the upwelling region off Morocco (NW-Africa) are mainly a response to primary productivity. The area of investigation can be divided into two trophic regions. The cape regions are characterized by eutrophic conditions, which are stable over time. The area between the capes is characterized by oligotrophic conditions with a more seasonal signal in primary productivity. These trophic differences are also reflected in the carbon isotopic signal of the most common species.

In the cape regions high standing stocks correlate with high chlorophyll-α concentrations, indicating enhanced organic matter fluxes. *Bulimina marginata*, the *B. aculeata* / *U. mediterranea* assemblage, the *S. bulloides* / *G. translucens* assemblage, and the *H. elegans* assemblage reflect generally more eutrophic conditions. Their faunal succession from the coast to the deep sea mirrors the decreasing amount of organic matter. The identical live and dead assemblages reflect constant, high productivity conditions in these areas. Additionally, these species occur in sediments with low sand contents. Carbonate dissolution is not a predominant influence as indicated by the high dominance of easy dissovable species including *C. kullenbergi, C. wuellerstorfi,* and *H. elegans* in the dead assemblages.

Between the capes oligotrophic conditions are accompanied by low standing stocks and the dominance of the *C. kullenbergi* / *C. jeffreysii* assemblage. *Cibicidoides kullenbergi* also showed considerably high standing stocks off the capes, indicating a tolerance for different trophic conditions. *Trifarina bradyi* occurs at stations that are mainly bathed by the saline Mediterranean Outflow Water. Low and seasonally varying organic matter fluxes most likely influence the population dynamics, which are responsible for observed differences in live and dead assemblage composition.

Enhanced organic matter fluxes in the cape regions are reflected by mean $\delta^{13}C$ values significantly lower in live *B. mexicana*, *C. kullenbergi*, *H. elegans*, *U. mediterranea,* and *U. peregrina* than $\delta^{13}C$ values of these species in the oligotrophic area between the capes. The highest species-specific offset between these two regions is recorded in live *U. mediterranea* and *U. peregrina*. The species-specific offsets for dead *B. mexicana*, *C. kullenbergi*, *H. elegans*, *U. mediterranea* are comparable to the mean $\delta^{13}C$ values of live specimens. This result is an important precondition for the reconstruction of paleoenvironmental conditions. Mean $\delta^{13}C$ values of *C. wuellerstorfi* are not influenced by sustained high organic matter fluxes, confirming that this species is a reliable recorder of bottom water $\delta^{13}C$ in the area of investigation.

Acknowledgements

We thank crews and scientific participants of *Meteor* cruises M 37/1, M42/4b and M45/4 for assistance during sampling, B. Hollmann and G. Meyer for running the mass spectrometer at the Alfred Wegener Institute, Bremerhaven, and M. Segl for running the mass spectrometer at the Departement of Geosciences, University of Bremen. We thank C. Holz for providing raw grain size data and P. Helmke for the chlorophyll map. We thank T. Freudenthal, H. Kuhlmann, and H. Meggers for providing the raw environmental data and for helpful discussions. We thank three anonymous reviewers for their constructive comments, which helped to improve an earlier version of this paper. We would also like to thank M.P. Bacon and A.J. Gooday for their thorough editorial suggestions. This work was funded by the Deutsche Forschungsgemeinschaft as part of the DFG-Research Center ‚Ocean Margins' at Bremen University.

Table A1: Stable carbon isotopic composition of live specimens and bottom water DIC. Italic letters represent mean δ^{13}C of bottom water mass (0.72 ‰: MOW, 0.78: NADW, 0.75 all water masses). n represents number of measured individuals. Region abbreviations: CR: Cape Regions, AbC: Area between capes

Live species	GeoB	Region	$\delta^{13}C_{DIC}$ (‰ VPDB)	$\delta^{13}C$ (‰ VPDB)	$\Delta\delta^{13}C$ (‰ VPDB)	n
B.aculeata	5542-3	CR	0.83	-0.08	-0.91	4
	5546-3	CR	0.79	-0.02	-0.80	13
	6006-2	CR	*0.72*	0.32	-0.40	7
	6007-1	CR	*0.66*	0.16	-0.50	6
	4212-3	AbC	*0.72*	0.36	-0.36	3
	4223-1	AbC	*0.66*	0.42	-0.24	7
	4236-2	AbC	*0.72*	0.25	-0.47	4
	4237-1	AbC	*0.66*	0.04	-0.62	4
B.mexicana	5542-3	CR	0.83	-0.63	-1.46	12
	6005-1	CR	*0.63*	-0.58	-1.21	12
	6006-2	CR	*0.72*	-0.18	-0.90	3
	6007-1	CR	*0.66*	-0.62	-1.28	5
	4213-1	AbC	*0.72*	-0.21	-0.93	12
	4226-1	AbC	0.65	0.07	-0.58	4
	4230-1	AbC	*0.72*	-0.08	-0.80	4
	4231-2	AbC	*0.72*	0.30	-0.42	4
	4236-2	AbC	*0.72*	0.06	-0.66	5
C.kullenbergi	4207-1	CR	*0.63*	0.22	-0.41	3
	5539-2	CR	0.86	0.23	-0.63	2
	5540-3	CR	*0.63*	0.04	-0.59	4
	5541-2	CR	*0.63*	0.14	-0.49	3
	5542-3	CR	0.83	0.40	-0.43	3
	6005-1	CR	*0.63*	0.54	-0.09	2
	4213-1	AbC	*0.72*	0.82	0.10	2
	4214-3	AbC	*0.72*	0.82	0.10	3
	4215-1	AbC	*0.72*	0.88	0.16	2
	4216-2	AbC	0.61	0.82	0.20	2
	4216-2	AbC	0.61	0.87	0.25	3
	4217-1	AbC	0.43	0.86	0.43	2
	4227-1	AbC	0.62	0.93	0.31	3
	4228-1	AbC	*0.72*	0.81	0.09	4
C.wuellerstorfi	4207-1	CR	*0.63*	1.01	0.38	4
	5540-3	CR	*0.63*	0.89	0.26	2
	4214-3	AbC	*0.72*	1.03	0.31	1
	4232-1	AbC	0.72	0.97	0.25	1
	4236-2	AbC	*0.72*	0.87	0.15	3
H.elegans	4207-1	CR	*0.63*	1.96	1.33	4
	5539-2	CR	0.86	1.90	1.04	3
	5540-3	CR	*0.63*	1.88	1.25	3
	5541-2	CR	*0.63*	1.90	1.27	2
	6005-1	CR	*0.63*	2.01	1.38	3
	4212-3	AbC	*0.72*	2.14	1.42	3
	4213-1	AbC	*0.72*	2.36	1.64	3
	4214-3	AbC	*0.72*	2.17	1.45	3
	4217-1	AbC	0.43	2.58	2.14	4
	4226-1	AbC	0.65	2.43	1.79	3
	4227-1	AbC	0.62	2.50	1.88	2
	4228-1	AbC	*0.72*	2.63	1.91	2
	4229-2	AbC	0.72	2.66	1.94	2
	4230-1	AbC	*0.72*	2.43	1.71	4
	4231-2	AbC	*0.72*	2.41	1.69	3
	4235-1	AbC	0.69	2.39	1.70	4
U.mediterranea	5540-3	CR	*0.63*	-0.68	-1.31	?
	5542-3	CR	0.83	-0.76	-1.59	11
	5546-3	CR	0.79	-0.49	-1.28	5
	6006-2	CR	*0.72*	-0.37	-1.09	2
	6007-1	CR	*0.66*	-0.69	-1.35	2
	6008-2	CR	0.49	-0.94	-1.42	7
	4212-3	AbC	*0.72*	0.17	-0.55	4
	4223-1	AbC	0.66	0.54	-0.21	3
	4231-2	AbC	*0.72*	0.36	-0.36	1
	4232-1	AbC	0.67	-0.27	-0.93	2
	4235-1	AbC	0.69	0.14	-0.55	3
	4236-2	AbC	*0.72*	0.28	-0.44	2
	4237-1	AbC	*0.66*	-0.03	-0.69	4
U.peregrina	5542-3	CR	0.83	-0.63	-1.46	5
	6006-2	CR	*0.72*	-1.61	-2.33	4
	6007-1	CR	*0.66*	-1.17	-1.83	9
	4212-3	AbC	*0.72*	-0.28	-1.00	4
	4223-1	AbC	*0.66*	-0.07	-0.73	7
	4230-1	AbC	*0.72*	-0.33	-1.05	3
	4231-2	AbC	*0.72*	0.00	-0.72	5
	4235-1	AbC	0.69	-0.09	-0.78	4

Table A2: Stable carbon isotopic composition of dead specimens and bottom water DIC. Italic letters represent mean δ^{13}C of bottom water mass (0.72 ‰: MOW, 0.78: NADW, 0.75 all water masses). n represents number of measured individuals. Region abbreviations: CR: Cape Regions, AbC: Area between capes

Dead species	Core GeoB	Region	δ^{13}C$_{DIC}$ (‰ VPDB)	δ^{13}C (‰ VPDB)	Δδ^{13}C (‰ VPDB)	n
B.aculeata	5542-3	CR	0.83	0.03	-0.80	13
	5546-3	CR	0.79	0.28	-0.51	9
	6005-1	CR	*0.63*	0.15	-0.48	9
	6006-2	CR	*0.72*	0.33	-0.39	10
	6007-1	CR	*0.66*	-0.05	-0.71	7
	4212-3	AbC	*0.72*	0.60	-0.12	6
	4223-1	AbC	*0.66*	0.69	0.03	10
	4236-2	AbC	*0.72*	0.34	-0.38	8
	4237-1	AbC	*0.66*	0.76	0.10	8
B.mexicana	4207-1	CR	*0.63*	0.06	-0.57	9
	5542-3	CR	0.83	-0.70	-1.54	11
	6005-1	CR	*0.63*	-0.49	-1.12	16
	6006-2	CR	*0.72*	-0.12	-0.84	7
	6007-1	CR	*0.66*	-0.68	-1.34	4
	4212-3	AbC	*0.72*	0.09	-0.63	8
	4213-1	AbC	*0.72*	0.56	-0.16	5
	4214-3	AbC	*0.72*	0.50	-0.22	4
	4226-1	AbC	0.65	0.61	-0.04	4
	4229-2	AbC	*0.72*	-0.12	-0.84	10
	4230-1	AbC	*0.72*	0.38	-0.34	6
	4231-2	AbC	*0.72*	0.39	-0.33	6
	4234-1	AbC	*0.72*	0.65	-0.07	3
	4235-1	AbC	0.69	0.21	-0.48	9
	4236-2	AbC	*0.72*	-0.28	-1.00	18
	4237-1	AbC	*0.66*	0.31	-0.35	2
	4237-1	AbC	*0.66*	0.37	-0.29	7
C.kullenbergi	4207-1	CR	*0.63*	0.69	0.06	5
	5539-2	CR	0.86	0.52	-0.34	4
	5540-3	CR	*0.63*	0.31	-0.32	4
	5541-2	CR	*0.63*	0.48	-0.15	4
	5542-3	CR	0.83	0.67	-0.17	3
	5546-3	CR	0.79	0.56	-0.23	2
	6005-1	CR	*0.63*	0.07	-0.56	2
	4213-1	AbC	*0.72*	1.12	0.40	2
	4214-3	AbC	*0.72*	1.07	0.35	2
	4217-1	AbC	0.43	0.99	0.56	6
	4227-1	AbC	*0.62*	0.99	0.37	3
	4228-1	AbC	*0.72*	0.91	0.19	4
C.wuellerstorfi	4207-1	CR	*0.63*	1.05	0.42	3
	5539-2	CR	0.86	0.93	0.07	5
	5540-3	CR	*0.63*	1.05	0.42	4
	5546-3	CR	0.79	0.80	0.01	3
	5546-3	CR	0.79	0.88	0.09	2
	6006-2	CR	*0.72*	1.09	0.37	4
	6007-1	CR	*0.66*	0.58	-0.08	3
	4214-3	AbC	*0.72*	1.07	0.35	4
	4217-1	AbC	0.43	1.02	0.59	1
	4227-1	AbC	*0.62*	1.03	0.41	4
	4232-1	AbC	*0.67*	1.14	0.47	3
	4236-2	AbC	*0.72*	1.08	0.36	4
	4236-2	AbC	*0.72*	1.11	0.39	6
	4237-1	AbC	*0.66*	0.95	0.29	4
H.elegans	4207-1	CR	*0.63*	2.27	1.64	4
	5539-2	CR	0.86	2.07	1.22	3
	5540-3	CR	*0.63*	1.71	1.08	2
	5541-2	CR	*0.63*	2.07	1.44	4
	5546-3	CR	0.79	1.92	1.13	3
	6005-1	CR	*0.63*	2.02	1.39	3
	6007-1	CR	*0.75*	1.67	0.92	1
	4212-3	AbC	*0.72*	2.48	1.76	2
	4213-1	AbC	*0.72*	2.50	1.78	3
	4223-1	AbC	*0.66*	2.31	1.65	3
	4228-1	AbC	*0.72*	2.29	1.57	3
	4229-2	AbC	*0.72*	2.51	1.79	3
	4230-1	AbC	*0.72*	2.60	1.88	?
	4232-1	AbC	0.67	2.49	1.82	4
	4234-1	AbC	*0.72*	2.56	1.84	4
	4236-2	AbC	*0.72*	2.40	1.68	4
	4237-1	AbC	*0.66*	2.25	1.59	4
U.mediterranea	5542-3	CR	0.83	-0.25	-1.08	2
	5546-3	CR	0.79	-0.48	-1.27	6
	6006-2	CR	*0.72*	-0.13	-0.85	9
	6007-1	CR	*0.66*	-0.57	-1.23	3
	6007-1	CR	*0.66*	-0.28	-0.94	2
	6008-2	CR	0.49	-0.50	-0.99	5
	4212-3	AbC	*0.72*	0.49	-0.23	3
	4223-1	AbC	*0.66*	0.62	-0.04	3
	4236-2	AbC	*0.72*	0.39	-0.33	2
	4237-1	AbC	*0.66*	0.50	-0.16	4
U.peregrina	5539-2	CR	0.86	-0.10	-0.96	7
	5540-3	CR	*0.63*	-0.63	-1.26	3
	5541-2	CR	*0.63*	-0.33	-0.96	5
	5542-3	CR	0.83	-0.50	-1.33	6
	5546-3	CR	0.79	-0.41	-1.20	4
	6006-2	CR	*0.72*	-0.36	-1.08	8
	6007-1	CR	*0.66*	-1.06	-1.72	8
	4223-1	AbC	*0.66*	-0.01	-0.67	8
	4231-2	AbC	*0.72*	-0.02	-0.74	6
	4232-1	AbC	0.67	0.09	-0.58	7
	4233-2	AbC	*0.72*	-0.08	-0.80	4
	4234-1	AbC	*0.72*	0.02	-0.70	7
	4235-1	AbC	0.69	0.04	-0.65	6
	4236-2	AbC	*0.72*	-0.06	-0.78	6
	4237-1	AbC	*0.66*	-0.04	-0.70	7

2.2 Manuscript 2

The influence of organic matter fluxes on the microhabitat distribution of live benthic foraminifera off Cape Ghir and Cape Yubi (NW-Africa)

Eberwein, A.[1] Mackensen, A.[1] and Davenport, R.[2]

1 Alfred Wegener Institute for Polar and Marine Research, Columbusstrasse, D-27568 Bremerhaven, Germany
2 University of Bremen – FB5 Geosciences, P.O.Box 330440, D-28334 Bremen, Germany

Keywords: Live Benthic Foraminifera, Microhabitat Distribution, Organic Matter Flux

Abstract

Live (Rose Bengal stained) benthic foraminifera were determined in the upper 10 cm from seven multiple corer samples to study the influence of exported organic matter on the benthic foraminifera microhabitat distribution. The stations are positioned on two transects off the high productive Cape Ghir (31°N) and Cape Yubi (27°N) in the upwelling region off Morocco. Primary productivity was computed from chlorophyll-*a* concentrations in surface waters at each station. Based on the primary productivity the export flux was determined. The calculated organic matter fluxes vary between 3 and 51 g C m^{-2} yr^{-1} off Cape Ghir and between 3 and 15 g C m^{-2} yr^{-1} off Cape Yubi. On both transects we observed an increase of total standing stocks with enhanced organic matter fluxes. The dependence between the average living depth (ALD) of the total live fauna and the organic matter flux shows an opposite trend comparing both capes with each other. Off Cape Ghir the ALD becomes shallower with increasing export flux, whereas it deepens off Cape Yubi. Here, the deepening of the ALD is explained by the strong dominance of the deep infaunal species *Globobulimina affinis*. The ALD of *G. affinis* becomes shallower with increasing export. Presumably, this indicates the compression of the redox zones in the sediment as a result of increasing export fluxes and decreasing dissolved oxygen concentrations. It seems that our data verify the conclusion that the ALD of *G. affinis* marks the oxygen penetration depth. Obviously, the higher permeability within the sediment off Cape Yubi compared to off Cape Ghir enables a deeper penetration of dissolved oxygen. As a result *G. affinis* escapes to greater depth within the sediment off Cape Yubi compared to off Cape Ghir. *Bulimina aculeata* and *Bulimina marginata* show high standing stocks off Cape Ghir most likely due to a quick response to the very high, and diatom rich organic matter fluxes. In contrast, off Cape Yubi, high organic matter amounts are incorporated into deeper sediment layers as indicated by highest standing stocks of *G. affinis.* These high standing stocks of *G. affinis* occur within a distinct range of export fluxes between 9 and 15 g C m^{-2} and oxygen concentration lower than 5 ml/l.

1. Introduction

The interpretation of live benthic foraminiferal distribution and their correlation with distinct productivity regimes is important for reconstructing past changes in ocean surface productivity. Exported organic carbon to the seabed has a large influence on the benthic foraminiferal assemblage composition (e.g. Corliss and Emerson, 1990; Loubere, 1991; de Rijk and others, 2000; Morigi and others, 2001), but also controls the density of benthic foraminifera (Altenbach, 1988; Gooday, 1994), which is confirmed by laboratory experiments (Ernst and others, 2002; Heinz and others, 2002). It has been known for two decades that benthic foraminifera show a vertical zonation within the sediment (Corliss, 1985), with a clear preference for discrete microhabitats (Lutze and Thiel, 1989; Mackensen and Douglas, 1989; Rathburn and Corliss, 1994; Mackensen and others, 2000; Schmiedl and others, 2000). It was shown that some species are closely related to distinct redox fronts within the sediment (Schönfeld, 2001; Fontanier and others, 2002; Licari and others, 2003). It is generally agreed that the quantity of organic matter and the availability of oxygen are the two main factors determining the benthic foraminiferal stratification within the sediment. The ongoing discussion is which factor is more important in determining benthic foraminiferal distribution. Some authors declare that the benthic foraminiferal distribution is controlled to a great extend by organic matter fluxes (Lutze and Coulbourn, 1984; Gooday, 1988; Corliss and Emerson, 1990; Rathburn and Corliss, 1994; Jannink and others, 1998; Schmiedl and others, 2000).

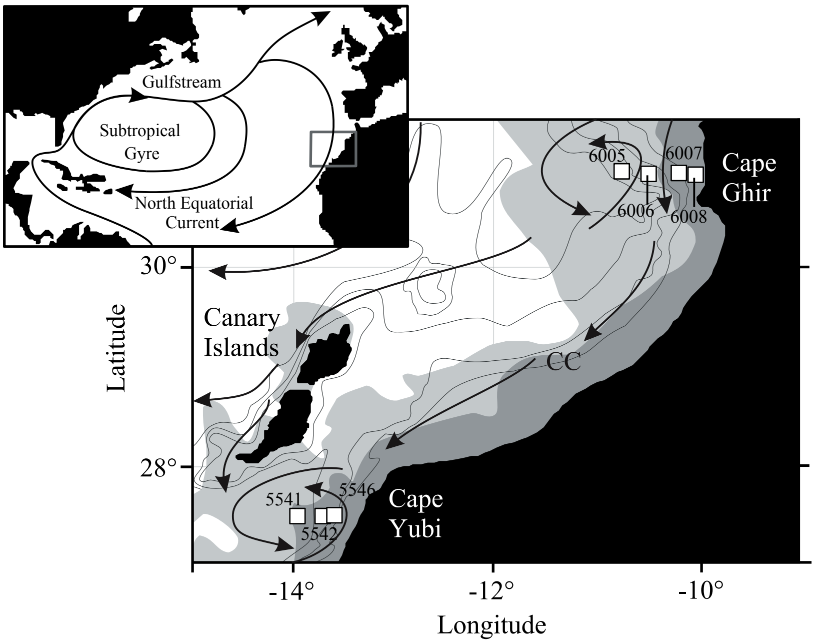

Fig. 1: Study area, chlorophyll-*a* concentration in surface waters, bathymetry and location of the seven investigated sediment surface samples (0 - 10 cm). SeaWifs derived chlorophyll-*a* concentrations, which represent > 1 mg m^{-3} are shaded dark grey, 0.4 – 1 mg m^{-3} light grey and < 0.4 mg m^{-3} are not shaded, (March 1998; Helmke, written communication). Surface currents (CC: Canary Current) are indicated by arrows after Mittelsteadt (1991). Isobaths indicate 500, 1000, 1500 and 2000 m water depths. Investigated sediment surface samples are marked by squares.

However, the oxygen concentration determines the distribution as well (Bernhard, 1992; Sen Gupta and Machain-Castillo, 1993; Kaiho, 1994; Loubere, 1994; Kaiho, 1999; Schönfeld, 2001; Geslin and others, 2004). Results of laboratory experiments demonstrated that changes in oxygen concentration cause benthic foraminifera to migrate to the depth of their preferred conditions (Geslin and others, 2004), and especially under a strong depletion or lack of oxygen species show a shallower living depth (Alve and Bernhard, 1995; Ernst and others, 2002; Duijnstee and others, 2003). It seems that varying oxygen concentrations influence the benthic foraminiferal assemblages on time scales up to a few weeks, whereas the organic flux is more important in benthic foraminiferal abundance on longer time scales (Ernst and van der Zwaan, 2004).

In this study we present a detailed description of live benthic foraminifera distribution and microhabitats from seven stations in the upwelling region off Morocco (NW-Africa). The investigated sites are positioned on two transects, underlying the high productivity Cape Ghir and Cape Yubi filaments. It is essential to gain a better understanding of the relationship between benthic foraminiferal distribution, primary productivity as well as early diagenetic processes in the sediment in order to use benthic foraminifera as a paleoenvironmetal proxy. Therefore, the main objective is to determine the imprint of calculated organic matter fluxes and oxygen concentration on the faunal composition and density as well as microhabitat preferences.

2. Area of investigation

The investigated stations (Fig. 1) are located at the NW African continental margin off Cape Ghir (31°N) and Cape Yubi (27°N) in the subtropical North Atlantic Ocean. This region belongs to one of the major eastern boundary upwelling systems of the world (Hagen, 2001; Carr, 2002). During boreal summer the trade winds affect the African coast between 32°N and 20°N. North of 25°N upwelling is predominant in summer and early fall (Wooster and others, 1976; Mittelstaedt, 1991; Van Camp and others, 1991; Nykjaer and van Camp, 1994). Trade wind driven upwelling, and therefore the highest concentration of biomass is generally restricted to a coastal band of 70 km (Mittelstaedt, 1991), where primary production reaches up to 5 g C m^{-2} day^{-1} (Parrilla and others, 1999). In filaments the upwelled water masses, of North Atlantic Central Water origin, are advected several hundred kilometers westwards into the open ocean off Cape Ghir and Cape Yubi (Van Camp and others, 1991; Nykjaer and van Camp, 1994; Hernández-Guerra and Nykjaer, 1997; Hagen, 2001) (Fig. 1). These filaments exist throughout the year with strong upwelling peaks in summer and fall (Hernández-Guerra and Nykjaer, 1997), and are generated by the interplay of the current system and the coastal morphology (Hagen and others, 1996; Stevens and Johnson, 2003). The Canary Current occurs down to 100 m water depth (Knoll and others, 2002; Llinás and others, 2002), and flows southwards along the African coast. The Cape Ghir filament usually extends to 200 km with its central part positioned at around 31°N and 10°W (Pelegrí and others, 2005).

Table 1: List of surface samples (0 – 10 cm) investigated in this study with sampling date, coring device (MUC: Multiple Corer), position, and water depth. Dissolved oxygen concentrations in bottom waters (ml/l), surface water chlorophyll concentrations (µg/l), primary productivity (g C m^{-2} day^{-1} and g C m^{-2} yr^{-1}), as well as calculated export fluxes (g C m^{-2} yr^{-1}) split into a fresh and refractory component after Berger and Wefer (1990) are given. Surface water chlorophyll-*a* concentration was sampled from the ship's seawater pump. Primary productivity (g C m^{-2} day^{-1}) was computed from these chlorophyll-*a* concentrations after Antoine and Morel (1996), and extrapolated to get the annual production (g C m^{-2} yr^{-1}). The oxygen concentrations (ml/l) at stations 60xx were taken from the NODC (Levitus) World Ocean Atlas 1998 data provided by the NOAA - CIRES ESRL/PSD Climate diagnostics branch, Boulder, Colorado, USA from their Web site at http://www.cdc.noaa.gov/, whereas the concentrations at stations 55xx were measured with a O_2 sensor attached to a CTD.

Core GeoB	Cruise	Sampling date	Device	Latitude (°N)	Longitude (°W)	Water depth (m)	O_2 (ml/l)	Chlorophyll (µg/l)	Primary productivity gC $m^{-2}day^{-1}$	Primary productivity gC $m^{-2}yr^{-1}$	Total export gC $m^{-2}yr^{-1}$	Fresh component gC $m^{-2}yr^{-1}$	Refractory component gC $m^{-2}yr^{-1}$
Transect Cape Ghir													
6008-2	M45/5	10/18/99	MUC	30°50,7	10°05,9	355	4.52	0.78	1.11	404	51.08	45.75	5.33
6007-1	M45/5	10/18/99	MUC	30°51,1	10°16,0	899	4.25	0.21	0.53	192	8.23	5.92	2.31
6006-2	M45/5	10/18/99	MUC	30°52,1	10°37,8	1275	3.90	0.10	0.34	123	3.69	2.14	1.55
6005-1	M45/5	10/18/99	MUC	30°52,8	10°53,8	1781	5.30	0.14	0.42	155	3.64	2.17	1.48
Transect Cape Yubi													
5546-3	M42/4	10/15/98	MUC	27°32,2	13°44,2	1071	3.75	0.58	0.98	357	15.48	12.60	2.89
5542-3	M42/4	10/14/98	MUC	27°32,2	13°50,8	1431	4.56	0.39	0.78	285	8.96	6.72	2.23
5541-2	M42/4	10/14/98	MUC	27°32,2	13°59,7	1748	5.12	0.11	0.36	130	3.06	1.70	1.36

The main core of the Cape Yubi filament is located at around 14°N and 27°W (Arístegui and others, 2004). The coast morphology is characterized by a continental shelf that extends about 25 km off Cape Ghir and up to 75 km off Cape Yubi (Summerhays and others, 1976). Therefore, the cape regions play an important role in nutrient supply to the deep-sea. High fluxes of phytoplankton (diatoms, coccolithophores) and zooplankton (planktic foraminifera) characterize the primary productivity signal in the Canary Islands region with peaks at times of strongest upwelling (Abrantes and others, 2002). Grain size analysis along the NW African coast revealed that the Cape Ghir region mainly is characterized by fluvial discharged mud, whereas the Cape Yubi region is dominated by fine-grained aeolian dust transported by the Saharan Air layer (Holz and others, 2004).

3. Material and methods

Sediment surface samples were retrieved with a multiple corer in the upwelling area between 31°N and 27°N off Morocco (NW-Africa) during cruises with RV *Meteor* in 1997, 1998 and 1999 (Table 1). We selected seven stations underlying high primary productivity to investigate the live benthic foraminiferal faunas. Four stations are located between 355 m and 1781 m water depth off Cape Ghir, and three stations are located between 1071 m and 1748 m water depth off Cape Yubi (Fig. 1).

For determination of the benthic foraminiferal fauna the uppermost ten centimeters were sliced horizontally into one centimeter intervals, preserved with Rose Bengal stained ethanol and kept at 4 °C. The samples were charged with water over 125 µm and 63 µm sieves and dried, and then the fraction > 125 µm was investigated for its benthic foraminiferal content. We counted prolocoli seperately for branch-like agglutinated foraminifera and assumed three fragments to represent one individual. Species with a relative abundance of more than 5 % of the total fauna were assumed to represent important species to determine the influence of organic matter fluxes. The standing stock was standardized for a surface volume of 50 cm^3. In the following the individuals per 50 cm^3 will be abbreviated as follows #/50 cm^3. The average living depth (ALD) was determined following Jorissen and others (1995):

$$ALD = \sum_{i = 1,x} (n_i * D_i) / N$$

where x is the lower boundary of the deepest sample included in the calculation, n_i the number of individuals in interval i, D_i is the midpoint of the sample interval i and N is the total number of individuals for all levels. Both, standing stocks and ALD of the upper 10 cm were determined for the total fauna as well as for the most abundant species.

Surface water was sampled for chlorophyll-*a* from the ship's seawater pump at each station (Table 1). Primary production estimates (g C m^{-2} day^{-1}) computed from these chlorophyll-*a* concentrations, which indicate a momentary situation at the time of sampling, were determined using the method of

Antoine and Morel (1996) as described and discussed in Davenport and others (2002). We extrapolated the daily primary productivity estimates to get the annual production (Table 1). It should be noted that in contrast to this method used here, the distribution of chlorophyll-*a* in surface waters (Fig. 1) is based on SeaWifs data, and gives an average signal over a month (March 1998). This map was selected to broadly clarify the upwelling event in the study area. Based on the annual primary productivity values we calculated the annual organic matter flux to the sea floor using the equation of Berger and Wefer (1990), which was extended by Herguera (1992). It calculates the total export (Jz) and distinguishes between a more fresh component (first term) and more refractory (second term) component:

$$Jz = (k * PP / z) + (r * PP / \sqrt{z})$$

Where $k = 2 * \sqrt{PP}$ and $r = 5 / \sqrt{PP}$, PP = primary productivity (g C m^{-2} day^{-1}), and Jz is the annual organic matter flux at the water depth z in meters (Table 1).

Bottom water oxygen concentrations were measured with an oxygen sensor attached to a CTD at stations GeoB 5546-3, GeoB 5542-3, and GeoB 5541-2 (Table 1). Whereas, the bottom water oxygen concentrations at stations GeoB 6008-2, GeoB 6007-1, GeoB 6006-2, and GeoB 6005-1 were taken from the NODC (Levitus) World Ocean Atlas 1998 data provided by the NOAA - CIRES ESRL/PSD Climate diagnostics branch, Boulder, Colorado, USA from their Web site at http://www.cdc.noaa.gov/.

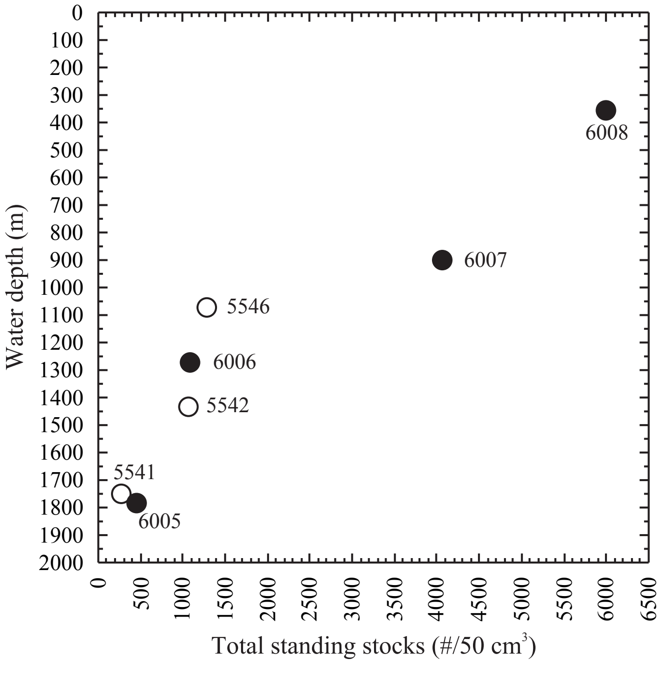

Fig. 2: Total standing stocks (#/50 cm^3) versus water depth in the upper 10 cm. Both transects are characterised by an increase in standing stocks with decreasing water depth. Filled circles mark stations off Cape Ghir, whereas open circles represent stations off Cape Yubi.

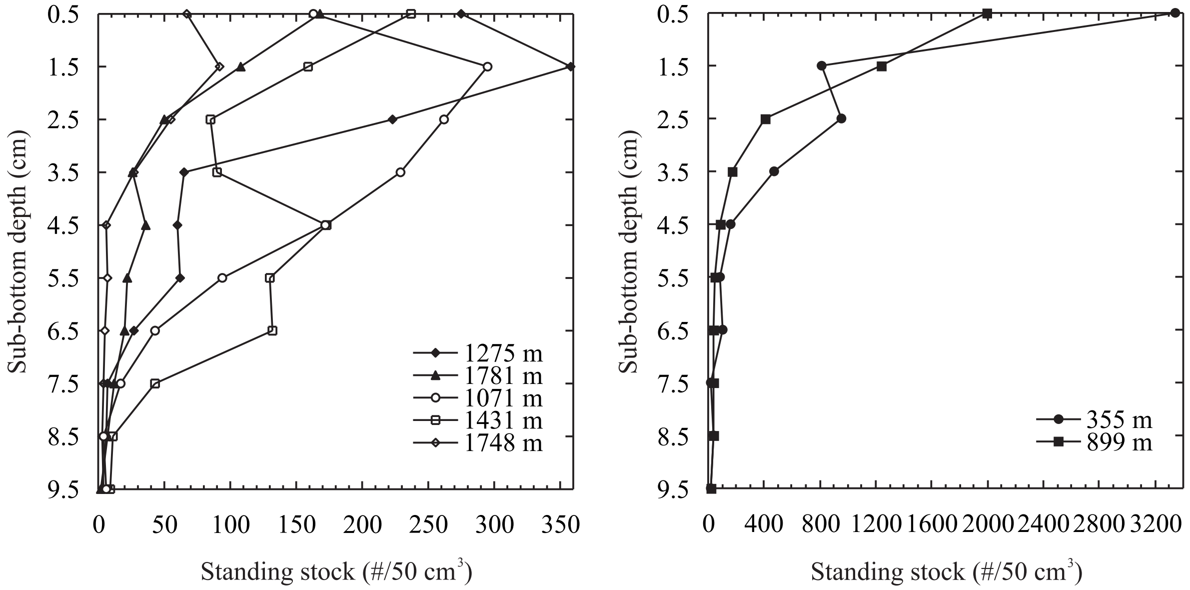

Fig. 3: Vertical distribution of foraminiferal standing stocks (#/50 cm^3) within the sediment. Stations in 355 m and 899 m water depth off Cape Ghir are plotted seperately due to their exceptionally high standing stocks. Filled symbols mark stations off Cape Ghir, whereas open symbols represent stations off Cape Yubi.

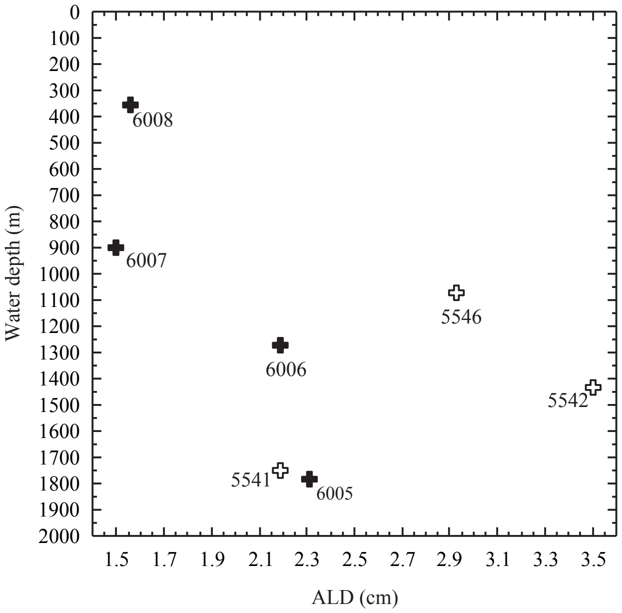

Fig. 4: Average living depth (ALD) versus water depth. An increase in ALD with increasing water depth is only observed at stations off Cape Ghir (marked by filled crosses). At stations off Cape Yubi (marked by open crosses) almost the reverse trend is pronounced. Deepest ALD are recorded at the two shallower stations GeoB 5546-3 and GeoB 5542-3.

4. Results

4.1 Export flux and dissolved oxygen concentrations in bottom water

The calculated total exported organic matter and the dissolved oxygen concentration in bottom water show a directly opposed trend off Cape Yubi. Here, the export flux decreases from 15.48 g C m^{-2} yr^{-1} in 1071 m water depth to 3.06 g C m^{-2} yr^{-1} in 1748 m water depth, and the dissolved oxygen concentration in bottom water increases from 3.80 ml/l to 5.10 ml/l (Table 1). Off Cape Ghir the export flux decreases from 51.08 g C m^{-2} yr^{-1} in 355 m water depth to 3.64 g C m^{-2} yr^{-1} in 1781 m water depth. The dissolved oxygen concentration in bottom water decreases from 4.52 ml/l to 3.90 ml/l, and than increases to 5.30 ml/l with increasing water depth (Table 1).

4.2 Standing stock and ALD of total live fauna

Total standing stocks vary between 269 and 5999 #/50 cm^3 (Fig. 2). They strongly decrease with increasing water depth on both, the Cape Ghir and Cape Yubi transect. Exceptionally high standing stocks with 5999 #/50 cm^3 in 355 m water depth and 4069 in 899 m are recorded off Cape Ghir. Comparable total standing stocks between 1068 and 1285 #/50 cm^3 are recorded at stations in similar water depths between 1071 m and 1431 m off both capes (Fig. 2). Lowest total standing stocks with 451 #/50 cm^3 occur in 1781 m water depth off Cape Ghir and with 269 #/50 cm^3 in 1748 m water depth off Cape Yubi.

Highest standing stocks in the top centimeter with a strong exponentially decrease within the sediment are recorded in 899 m and 1781 m water depth off Cape Ghir (Fig. 3). A clear subsurface maximum in 1.5 cm is recorded in 1275 m off Cape Ghir and in 1748 m water depth off Cape Yubi, as well as between 1.5 and 4.5 cm in 1071 m water depth off Cape Yubi. A peak in standing stocks is observed in 2.5 cm in 355 m water depth off Cape Ghir and between 4.5 and 6.5 cm in 1431 m water depth off Cape Yubi.

The ALD of the total live fauna varies between 1.5 and 3.5 cm (Fig. 4). The shallowest ALD with depths of 1.6 cm in 355 m and 1.5 cm in 899 m water depth is found off Cape Ghir. The deepest ALD with depths of 2.9 cm in 1071 m and 3.5 cm in 1431 m water depth cm are recorded off Cape Yubi. Almost identical ALD between 2.2 cm and 2.3 cm are recorded in 1275 m and 1781 m water depth, respectively, off Cape Ghir as well as in 1748 m water depth off Cape Yubi.

4.3 Standing stock and ALD of dominant species

A clear vertical stratification of species within the sediment is distinguishable (Figs. 5, 6, Table 2), and according to the calculated ALD the distribution within the sediment can be divided into four categories (Fig. 6, Table 3). These categories follow the classification of Schmiedl and others (2000). Remarkable is the absence of preferentially epifaunal species with mean ALD values < 0.7 cm.

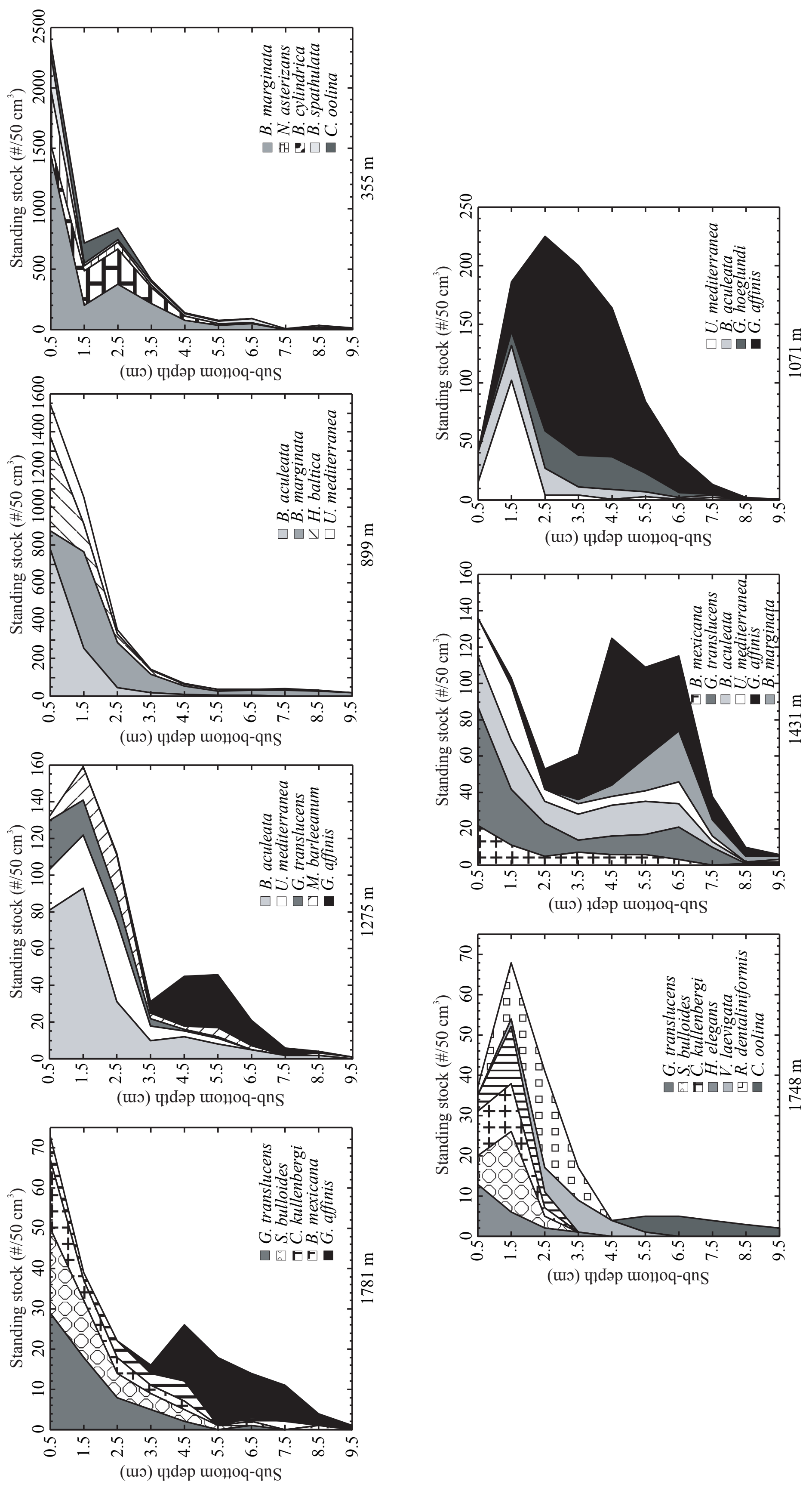

Fig. 5: Microhabitat distribution (standing stocks in #/50 cm^3) of main species off Cape Ghir and Cape Yubi.

Table 2: Dominant species (> 5 %) and associated species (> 1 %) with their standing stocks (St.S) in individuals per 50 cm³ (#/50cm³) as well as percentages at stations off Cape Ghir and Cape Yubi.

Cape Ghir	1781 m (GeoB 6005-1)	%	St.S	1275 m (GeoB 6006-2)	%	St.S	899 m (GeoB 6007-1)	%	St.S	355 m (GeoB 6008-2)	%	St.S
Dominant species (DS)	*Gavelinopsis translucens*	14.21	64	*Bulimina aculeata*	22.50	244	*Bulimina aculeata*	27.48	1118	*Bulimina marginata*	40.53	2432
	Globobulimina affinis	12.64	57	*Uvigerina mediterranea*	10.16	110	*Bulimina marginata*	27.12	1104	*Nonion asterizans*	14.17	850
	Sphaeroidina bulloides	10.68	48	*Globobulimina affinis*	7.53	82	*Hylinea baltica*	18.50	753	*Bigeneria cylindrica*	9.63	578
	Cibicidoides kullenbergi	6.91	31	*Gavelinopsis translucens*	6.05	66	*Uvigerina mediterranea*	8.49	345	*Brizalina spathulata*	7.54	453
	Bulimina mexicana	5.13	23	*Melonis barleeanum*	5.09	55				*Chilostomella oolina*	6.45	387
Associated species (AS)	*Eponides pusillus*	3.97	18	*Bulimina marginata*	3.24	35	*Brizalina spathulata*	1.94	79	*Uvigerina elongatastriata*	3.67	220
	Reophax dentaliniformis	3.74	17	*Lagenammina diflugiformis*	2.96	32	*Recurvoides contortus*	1.88	76	*Recurvoides contortus*	2.77	166
	Glomospira gordialis	3.67	17	*Eponides pusillus*	2.76	30	*Bulimina mexicana*	1.61	66	*Uvigerina mediterranea*	2.37	142
	Cibicidoides bradyi	3.40	15	*Epistominella rugosa*	2.67	29	*Globobulimina affinis*	1.28	52	*Uvigerina* cf. *mediterranea*	1.53	92
	Gyroidina lamarckhiana	3.23	15	*Uvigerina peregrina*	2.40	26	*Adercotryma glomerata*	1.04	42	*Hylinea baltica*	1.42	85
	Höglundina elegans	2.58	12	*Sphaeroidina bulloides*	2.37	26	*Discammina compressa*	1.00	41	*Bulimina striata*	1.36	81
	Chilostomella oolina	2.05	9	*Cyclammina trullissata*	1.89	20				*Globobulimina turgida*	1.04	62
	Recurvoides contortus	1.31	6	*Saccorhiza ramosa* (Frag.)	1.77	19						
	Usbekistania charoides	1.13	5	*Reophax bilocularis*	1.77	19						
	Cribrostomoides subglobosus	1.12	5	*Bulimina mexicana*	1.62	18						
	Cassidulina neoteretis	1.10	5	*Hylinea baltica*	1.58	17						
	Saccorhiza ramosa (Frag.)	1.06	5	*Cibicidoides bradyi*	1.24	13						
				Bulimina rostrata	1.21	13						
				Cribrostomoides wiesneri	1.12	12						
				Cassidulina neoteretis	1.08	12						

Cape Yubi	1748 m (GeoB 5541-2)	%	St.S	1431 m (GeoB 5542-3)	%	St.S	1071 m (GeoB 5546-3)	%	St.S
Dominant species (DS)	*Reophax dentaliniformis*	18.32	49	*Globobulimina affinis*	21.56	230	*Globobulimina affinis*	46.72	600
	Sphaeroidina bulloides	11.35	31	*Gavelinopsis translucens*	15.90	170	*Uvigerina mediterranea*	10.38	133
	Cibicidoides kullenbergi	9.10	25	*Bulimina aculeata*	12.53	134	*Globobulimina hoeglundi*	9.27	119
	Höglundina elegans	8.51	23	*Uvigerina mediterranea*	8.58	92	*Bulimina aculeata*	7.95	102
	Gavelinopsis translucens	8.04	22	*Bulimina marginata*	6.48	69			
	Valvulineria laevigata	7.45	20	*Bulimina mexicana*	5.69	61			
	Chilostomella oolina	6.26	17						
Associated species (AS)	*Uvigerina mediterranea*	4.85	13	*Globobulimina hoeglundi*	3.49	37	*Bulimina marginata*	4.75	61
	Marsipella cylindrica (Frag.)	2.13	6	*Chilostomella oolina*	2.46	26	*Chilostomella oolina*	3.01	39
	Brizalina earlandi	1.89	5	*Sphaeroidina bulloides*	2.33	25	*Melonis barleeanum*	1.81	23
	Cassidulina neoteretis	1.65	4	*Melonis barleeanum*	1.91	20	*Uvigerina peregrina*	1.65	21
	Bulimina mexicana	1.18	3	*Cibicidoides pachyderma*	1.76	19	*Epistominella rugosa*	1.62	21
	Pullenia subcarinata	1.18	3	*Bulimina rostrata*	1.31	14	*Gavelinopsis translucens*	1.61	21
				Lagenammina diflugiformis	1.26	13	*Trifarina bradyi*	1.32	17
							Hylinea baltica	1.14	15

Table 3: Vertical stratification of species within the upper 10 sediment centimeters according to the calculated average living depth (ALD) after Jorissen and others (1995). Shallow infauna occurs between 0.7 and 1.5 cm, intermediate infauna between 1.5 and 3.0 cm, and deep infauna > 3 cm. Listed are the minimum, maximum and mean ALD.

	Cape Ghir				Cape Yubi					
	1781 m	1275 m	899 m	355 m	1748 m	1431 m	1071 m	Min	Max	Mean
	GeoB 6005-1	GeoB 6006-2	GeoB 6007-1	GeoB 6008-2	GeoB 5541-2	GeoB 5542-3	GeoB 5546-3	ALD	ALD	ALD
Shallow infaunal										
Bigeneria cylindrica				0.90						0.90
Hoeglundina elegans	1.14	1.09			1.51	1.75	0.43	0.43	1.75	1.18
Hylinea balthica	0.50	1.42	1.17	2.11			0.50	0.50	2.11	1.14
Reophax dentaliniformis	1.42	0.5	0.5		2.33	1.86		0.50	2.33	1.32
Intermediate infaunal										
Brizalina spathulata		1.50	1.80	2.07				1.50	2.07	1.79
Bulimina aculeata		1.86	0.95			3.25	2.19	0.95	3.25	2.06
Bulimina mexicana	3.01	1.66	1.31		1.20	2.41	1.26	1.20	3.01	1.81
Cibicidoides kullenbergi	1.74	1.89			1.16	2.67	0.33	0.33	2.67	1.56
Gavelinopsis translucens	1.52	1.58	3.30		1.03	2.66	1.04	1.03	3.30	1.86
Melonis barleeanum	2.58	2.67	2.30	1.74		3.04	1.47	1.47	3.04	2.30
Nonion asterizans				2.27						2.27
Sphaeroidina bulloides	1.54	2.26	0.48	2.29	1.36	2.62	1.90	0.48	2.62	1.78
Uvigerina mediterranea	0.45	2.14	1.17	1.27	1.93	2.84	1.81	0.45	2.84	1.66
Uvigerina peregrina	1.00	2.16	0.50		1.79	2.19	1.56	0.50	2.19	1.53
Deep infaunal										
Bulimina marginata		1.67	2.56	1.58		6.27	3.31	1.58	6.27	3.08
Chilostomella oolina	5.88	5.70	2.53	1.69	7.16	4.68	3.65	1.69	7.16	4.47
Globobulimina affinis	5.91	5.26	3.26	1.18	5.75	5.10	3.72	1.18	5.91	4.31
Globobulimina hoeglundi	6.29	2.32	3.94		5.17	4.84	3.69	2.32	6.29	4.38
Valvulineria laevigata					3.45	3.01		3.01	3.45	3.23

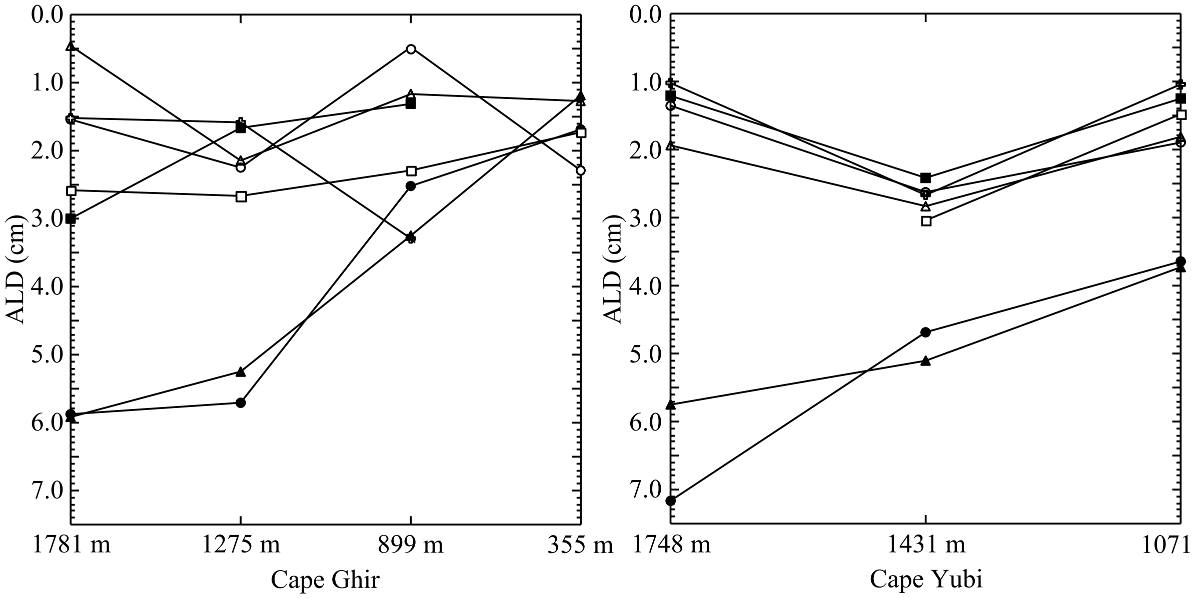

Fig. 6: Average living depth (ALD) of selected shallow, intermediate, and deep infaunal living species along the Cape Ghir and Cape Yubi transect. *Bulimina mexicana* (filled squares), *Chilostomella oolina* (filled circles), *Globobulimina affinis* (filled triangles), *Gavelinopsis translucens* (filled crosses), *Melonis barleeanum* (open squares), *Sphaeroidina bulloides* (open circles), and *Uvigerina mediterranea* (open triangles).

Preferentially shallow infaunal species with mean ALD values between 0.7 and 1.5 cm inlcude *Bigeneria cylindrica*, *Hoeglundina elegans*, *Hyalinea balthica*, and *Reophax dentaliniformis.* Preferentially intermediate infaunal species with mean ALD values between 1.5 and 3.0 cm include *Bulimina aculeata*, *Bulimina mexicana*, *Cibicidoides kullenbergi*, *Gavelinopsis translucens*, *Sphaeroidina bulloides*, and *Uvigerina mediterranea.* Preferentially deep infaunal species with mean ALD values > 3.0 cm inlcude *Brizalina spathulata, Bulimina marginata*, *Chilostomella oolina*, *Globobulimina affinis*, *Globobulimina hoeglundi*, *Melonis barleeanum*, *Nonion asterizans*, and *Valvulineria laevigata*.

The ALD of shallow and intermediate infaunal species displays irregular depth distributions along the Cape Ghir Transect (Fig. 6, Table 3). Off Cape Yubi a trend in the ALD of shallow and intermediate infaunal species is observed. The deepest ALD of these species are recorded in 1431 m water depth. In contrast to that, the ALD is characterized by a shallowing in 1071 m and 1748 m water depth (Fig. 6, Table 3). The ALD of *G. affinis* continuously and most strongly deepens from 1.18 cm in 355 m water depth to 5.91 cm in 1781 m water depth off Cape Ghir, and from 3.72 cm in 1071 m water depth to 5.75 cm in 1748 m waterdepth. The deep infaunal *C. oolina* shows a very similar trend of its ALD compared to the ALD of *G. affinis* off both capes (Fig. 6, Table 3).

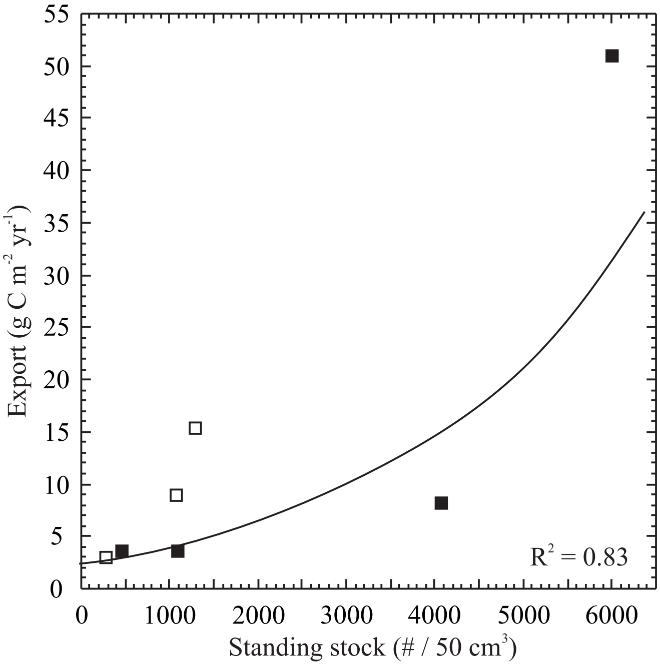

Fig. 7: Positive correlation between total exported organic matter and the total standing stocks (#/50 cm^3). Filled squares mark stations off Cape Ghir, whereas open squares represent stations off Cape Yubi.

Generally, *B. cylindrica*, *B. spathulata*, *B. aculeata*, *B. marginata, C. oolina, H. balthica, N. asterizans*, and *U. mediterranea* show highest standing stocks at stations off Cape Ghir (Fig. 5, Table 2), whereas, off Cape Yubi, highest standing stocks are recorded by *G. translucens*, *G. affinis*, *G. hoeglundi*, *H. elegans, R. dentaliniformis*, and *V. laevigata* (Fig. 5, Table 2). The standing stocks of *B. aculeata* are markedly higher with 244 #/50 cm^3 in 1275 m water depth off Cape Ghir compared to 102 #/50 cm^3 in 1071 m water depth and 134 #/50 cm^3 1431 m water depth off Cape Yubi. In contrast, the standing stocks of *G. affinis* are much higher with 600 #/50 cm^3 in 1071 m water depth and 230 #/50 cm^3 in 1071 m water depth compared to 82 #/50 cm^3 in 1275 m water depth off Cape Ghir.

5. Discussion

The stations off Cape Ghir and Cape Yubi are characterized by high organic matter fluxes between 3 g C m^{-2} yr^{-1} and 51 g C m^{-2} yr^{-1}. On both transects a strong increase of total standing stocks with increasing export fluxes is expressed (Fig. 7). Highest standing stocks of 5999 #/50 cm^3 in 355 m and 4069 #/50 cm^3 in 899 m water depth were observed off Cape Ghir. These stations are approximately located underneath the root of the Cape Ghir filament (31°N, 10.2°W) (Pelegrí and others, 2005), leading to high organic matter fluxes (Table 1).

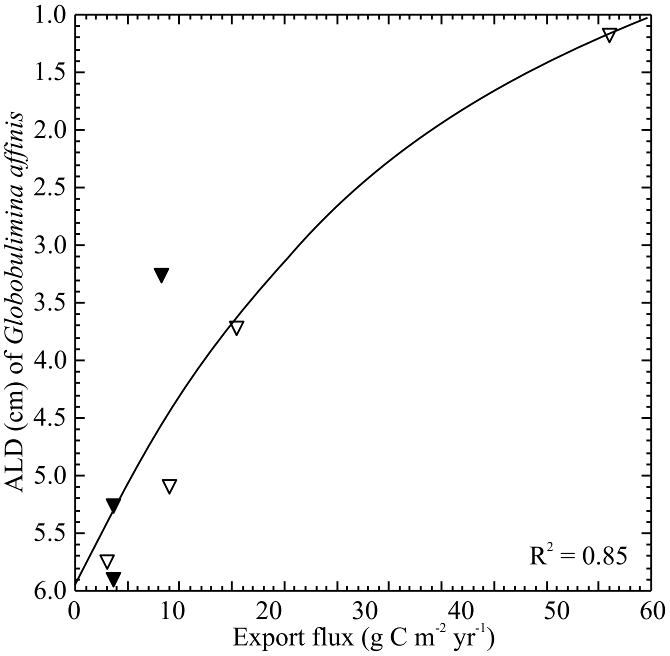

Fig. 8: Average living depth (ALD) of *Globobulimina affinis* versus export flux in g C m^{-2} yr^{-1}. Correlation between ALD of *G. affinis* and export flux is given. Filled symbols mark stations off Cape Ghir, whereas open symbols represent stations off Cape Yubi.

The increase in densities as a response to enhanced organic matter fluxes has been described before (e.g. Altenbach, 1988; Gooday, 1988; Herguera and Berger, 1991; Fontanier and others, 2002). The results of this study support the observation that the quantity of organic matter reaching the seafloor determines the total standing stocks of benthic foraminifera.

In contrast to the consistent trend of standing stocks on the export flux along both transects the reverse trend in ALD is noticeable along the Cape Ghir Transect compared to the Cape Yubi Transect (Fig. 4). Off Cape Ghir the ALD becomes shallower with increasing export, whereas off Cape Yubi high C_{org} fluxes are characterized by surprisingly deep ALD (Fig. 4). This deepening of the ALD is due to the strong dominance of the deep infaunal species *Globobulimina affinis* in 1071 m and 1431 m water depth off Cape Yubi (Fig. 5, Table 2). Here, this species accounts for approximately 22 % and 46 % of the total fauna (Table 2). Furthermore, the strong dominance of *G. affinis* explains the peak values of total live standing stocks within the sediment between 1.5 and 4.5 cm in 1071 m as well as between 4.5 and 6.5 cm in 1431 m water depth off Cape Yubi (Fig. 3). Presumably, the ALD of the total live fauna becomes shallower with increasing export as long as *G. affinis* does not dominate the fauna. Therefore, we suggest that the ALD is mainly controlled by the presence, or more precisely, the dominance of the deep infaunal species *G. affinis.*

A striking feature is the strong shallowing of *G. affinis* ALD with increasing organic matter fluxes, which is clearly expressed on both transects (Fig. 8, Table 1). In contrast to the findings of

Schönfeld (2001) we observed a correlation between the ALD of *G. affinis* and the exported organic matter (Fig. 8). As a result of the shallowing of *G. affinis* ALD a strong convergence with shallow infaunal living species is visible, particularly off Cape Yubi (Fig. 6). The degradation of organic matter depends on the amount and type of exported organic matter, the bottom water oxygen concentration, and the sediment type, which in turn determine the gradient of the pore water oxygen concentration. The stratification of benthic foraminifera within the sediment is closely linked to redox fronts in the pore water (Jannink and others, 1998; Jorissen and others, 1998; Fontanier and others, 2002; Licari and others, 2003). *Globobulimina affinis* is predominantly found in anoxic zones (Kitazato, 1994; de Stigter and others, 1998; Jorissen and Wittling, 1999; Schönfeld, 2001; Fontanier and others, 2002; Licari and others, 2003; Geslin and others, 2004; Fontanier and others, 2005). *Globobulimina affinis* is considered to be a facultative anaerobe species (Bernhard, 1993; 1996).

The export flux and the oxygen concentrations show a converse trend off Cape Yubi. The increasing export flux is accompanied by a decrease in oxygen concentrations (Table 1). This could mean that oxygen could be completely oxidized but C_{org} is still available in adequate amounts in shallowest water depth, whereas an excess of oxygen might be predominant in greater water depth. Obviously, the latter case is valid at the station in 1748 m water depth. Here, the relatively low C_{org} flux in combination with high oxygen concentration confines most of the shallow infaunal species closer to the sediment surface (Fig. 6) due to the scarcity of food, since it is degraded quickly in the upper sediment layers. In contrast, as a consequence of the excess oxygen, the deep infaunal species *G. affinis* is characterized by a deepening of its ALD (Fig. 6, Table 3). Off Cape Ghir the export flux and the oxygen concentration show a parallel trend, at least at the three shallower stations. The increasing export flux is accompanied by an increase in oxygen concentrations (Table 1). Apparently, an excess of organic matter is available at all stations since the shallow infaunal species show an irregular distribution in the top three centimeters along the transect. Furthermore, the oxygen is consumed more strongly by organic matter degradation as indicated by the shallowing of the ALD of *G. affinis* from greater to shallower water depth.

There are significant differences comparing the ALD in 899 m off Cape Ghir with the ALD 1431 m off Cape Yubi. Both stations are characterized by almost comparable export fluxes as well as dissolved oxygen concentrations in bottom waters (Table 1). Surprisingly, most species show a deeper ALD within the sediment off Cape Yubi compared to off Cape Ghir (Fig. 6, Table 3). Especially *G. affinis* is characterized by an ALD two centimeters deeper off Cape Yubi compared to off Cape Ghir (Fig. 6, Table 3). The deep infaunal *G. affinis* and *G. pacifica* start to occur where dissolved oxygen is completely consumed, show peaks in standing stocks where the nitrate concentration approaches zero (Fontanier and others, 2002; Licari and others, 2003) and dissolved Mn^{2+} and Fe^{2+} increase (Fontanier and others, 2005). Grain size analysis in surface sediments along the NW African coast revealed that the Cape Ghir region is mainly characterized by finer material compared to the Cape Yubi region, where coarser material is predominant (Holz and others, 2004). Presumably, oxygen diffuses more quickly into deeper parts in the coarser sediment off Cape Yubi than in the finer sediments off Cape Yubi.

We suggest that as a result of the deeper penetration of dissolved oxygen off Cape Yubi compared to off Cape Yubi *G. affinis* evades to greater depths within the sediment. Therefore, most likely the ALD of *G. affinis* approximately indicates the zero oxygen boundary along the Cape Ghir and Cape Yubi Transects (Fig. 6, Table 3). Furthermore, the higher permeability within the sediment off Cape Yubi compared to off Cape Ghir results in a deepening of all species ALD, since oxygen diffuses deeper into the sediment. The convergence of the ALD of *G. affinis* with the ALD of shallow infaunal species indicates the compression of the redox zones in the sediment along both, the Cape Ghir and Cape Yubi Transects. Additionally, the results indicate that the average living depths of species within the sediment are dynamic, and particularly, deep infaunal species compared to shallow and intermediate infaunal species cover a wide range (Fig. 6, Table 3).

It was believed for some time that foraminifera primarily feed on diatoms (Lee, 1980), and more recent culture experiments have shown that distinct species react with increased reproduction when feeding on diatoms. Particularly, *Bulimina marginata* and to a lesser extent *Bulimina aculeata* are considered to react quickly to diatom rich organic matter inputs (Heinz and others, 2002; Langezaal, 2003). The coastal upwelling between Cape Ghir and Cape Yubi is characterized by peaks of high diatom abundances during times of intensified upwelling (Abrantes and others, 2002). So far it has been only shown for the Cape Ghir region that the diatom genus *Chaetoceros* spp. is a main contributor of the bloom (Nave and others, 2001). In 355 m and 899 m water depth off Cape Ghir very high standing stocks of *B. aculeata*, *B. marginata*, and *Hylinea balthica* are present, whereas *G. affinis* is only of minor importance (Fig. 5, Table 2). Presumably, the opportunistic species *B. aculeata* and *B. marginata* react quickly due to the diatom-rich organic matter fluxes, and most of the organic matter is consumed in the upper sediment layers, as indicated by their high standing stocks (Fig. 5) at stations in 355m, 899 m, and 1275 m water depth off Cape Ghir. We suggest that *G. affinis* probably is out-competed by *B. marginata* and *B. aculeata*, which react fast to the organic matter inputs, and that the quantity of organic matter left to be incorporated into deeper sediment layers is below the threshold of optimum conditions of *G. affinis*.

Deep infaunal species react weeks to months after the deposit of the remains of a bloom, since the organic matter has to be incorporated into the sediment. Therefore, high organic matter fluxes are necessary for the occurrence or even dominance of *G. affinis*. According to Schönfeld (2001) an export of 3 g C m^{-2} yr^{-1} marks the lower limit of *G. affinis* occurrence. This limit is in good agreement with the result of this study, where *G. affinis* showed lowest abundances in 1748 m with an export flux of 3 g C m^{-2} yr^{-1} (Fig. 5, Table 2). It seems that *G. affinis* occurs with maximum densities in a strict interval of optimum conditions regarding both, the C_{org} flux and dissolved oxygen concentrations in bottom waters. Highest standing stocks of 239 #/50cm^3 in 1431 m and 600 #/50cm^3 in 1071 m water depth are reported predominantly off Cape Yubi (Figs. 5, 8, Table 2). At these stations intermediate to high C_{org} fluxes of 15 and 9 g C m^{-2} yr^{-1}, and bottom water oxygen concentrations are below 5 ml/l (Table 1). Obviously, the low standing stocks of *B. marginata* and *B. aculeata* indicate, that the quantity and quality of organic matter is not sufficient for these species. Therefore, adequate organic matter amounts are left to be incorporated into deeper sediment layers where *G. affinis* profits from these remains of organic matter. Either *G. affinis* feeds on particulate organic matter or, since it is tightly linked to the anoxic / dysoxic zone, on nitrate or sulphate reducing bacteria (Goldstein and Corliss, 1994; Jorissen and others, 1998; Fontanier and others, 2005). Summarizing we conclude that *G. affinis* is a delicate species concerning the availability of organic matter as well as the biogeochemical processes in the sediment.

6. Conclusion

Both, the Cape Ghir and the Cape Yubi region are characterized by high organic matter fluxes of at least 3 g C m^{-2} yr^{1}. The export flux varies between 3 g C m^{-2} yr^{1} and 51 g C m^{-2} yr^{1} off Cape Ghir and between 3 g C m^{-2} yr^{1} and 15 g C m^{-2} yr^{1} off Cape Yubi. The benthic foraminiferal community is mainly controlled by the exported organic matter, but also by bottom water oxygen concentration. The interplay between these two parameters is a critical process especially in determining the occurrence of deep infaunal living species.

- The total standing stocks of benthic foraminifera increase with enhanced export fluxes to the seafloor, which is pronounced off Cape Ghir as well as off Cape Yubi.
- The association between the ALD of the total live fauna and the organic matter flux shows a contrary trend comparing both capes with each other. The ALD becomes shallower with increasing C_{org} flux off Cape Ghir. In contrast, the ALD deepens with increasing organic matter flux off Cape Yubi, due to the strong dominance of the deep infaunal living species *Globobulimina affinis*.
- The ALD of *G. affinis* correlates with the exported organic matter. The ALD becomes shallower with increasing export along the Cape Ghir and Cape Yubi transects. This shallowing results in a convergence between the ALD of *G. affinis* and shallow infaunal living species, which most likely indicates the compression of the redox zones in the sediment. This strict behaviour of *G. affinis* suggests that this species is more tightly coupled to a distinct redox front than shallow infaunal species. Obviously, our data support the conclusion that the ALD of *G. affinis* approximately indicates the zero oxygen boundary. Furthermore, a higher permeability of the sediment, and hence a deeper oxygen penetration depth results in a deepening of *G. affinis* ALD off Cape Yubi.
- *Bulimina aculeata* and *Bulimina marginata* dominate the fauna off Cape Ghir probably due to a fast response to high as well as diatom rich organic matter fluxes, and therefore less organic matter is left to be incorporated into deeper sediment layers, as indicated by low standing stocks of *G. affinis* off Cape Ghir.
- *Globobulimina affinis* occurs with highest standing stocks, mainly off Cape Yubi, in a range of distinct organic matter fluxes and dissolved oxygen concentrations in bottom waters indicating

the optimum conditions for this species. Highest standing stocks are recorded for C_{org} fluxes between 9 and 15 g C m^{-2} yr^{-1}, and bottom water oxygen concentrations lower than 5 ml/l. The high standing stocks are a result of the interplay between the quantity of exported organic matter and the oxygen concentration.

Acknowledgements

We thank the crews and scientific participants of *Meteor* cruises M 37/1, M42/4b and M45/4 for assistance during sampling, A. Mascher and S. Wiebe for assistance in the lab. We thank P. Helmke for providing the chlorophyll-*a* map. This work was funded by the Deutsche Forschungsgemeinschaft as part of the DFG-Research Center ‚Ocean Margins' at Bremen University.

2.3 Manuscript 3

Last Glacial Maximum paleoproductivity and water masses off NW-Africa: evidence from benthic foraminifera and stable isotopes

Eberwein, A.* & Mackensen, A.

Alfred Wegener Institute for Polar and Marine Research, Am Alten Hafen 26, D-27568 Bremerhaven, Germany
* Corresponding author. eMail address: aeberwein@awi-bremerhaven.de

Abstract

Last Glacial Maximum (LGM) paleoproductivity and water mass stratification was reconstructed from benthic foraminiferal faunas and stable carbon and oxygen isotopes of foraminiferal calcite. Sediments of the LGM between 23000 to 19000 cal-yr BP of sixteen cores from the upwelling region off Morocco between Cape Ghir (31°N) and Cape Yubi (27.5°N) were investigated. Generally, in the area between capes, paleoproductivity during the LGM was higher than during the Holocene, whereas off Capes Ghir and Yubi it was comparably high. For the reconstruction of LGM water masses we used the $\delta^{13}C$ of *Cibicidoides wuellerstorfi* and equilibrium adjusted $\delta^{18}O$ of several species. The previously described glacial stratification of Mediterranean Outflow Water above North Atlantic Deep Water was corroborated by the identification of a water mass boundary at approximately 1900 m water depth. For paleoproductivity reconstruction we used characteristic faunal assemblages and indicator species as well as differences between $\delta^{13}C$ values of epifaunal *C. wuellerstorfi* and infaunal *Hoeglundina elegans* and *Melonis pompiloides* ($\Delta\delta^{13}C$). As a result we discriminate four major geographic regions by their characteristic paleoproductivity regime: (1) the Cape Yubi Upwelling Region with highest productivity as indicated by the *Bolivina albatrossi* / *Uvigerina mediterranea* Assemblage and lowest $\Delta\delta^{13}C$ values. In its northern part productivity was enhanced compared to the Holocene; (2) the Cape Ghir Upwelling Region with moderate to high, seasonally fluctuating paleoproductivity as indicated by the *Bulimina mexicana* / *Gavelinopsis translucens* Assemblage, and low $\Delta\delta^{13}C$ values. Within this region productivity was characterized by strong heterogeneity; (3) the Cape Yubi Filament Region, regularly influenced by the Cape Yubi filament southwest off Cape Yubi with moderate, highly seasonally varying paleoproductivity as indicated by the *Cassidulina laevigata* / *Nonionella iridea* Assemblage, and $\Delta\delta^{13}C$ values as low as those from the Cape Ghir Upwelling Region; and (4) the Cape Ghir Filament Region with highest seasonally varying productivity as indicated by the *Epistominella exigua* Assemblage, and highest $\Delta\delta^{13}C$ values. This region was effected by the oscillating Cape Ghir filament, which extended much further to the south and west than today.

Keywords: Last Glacial Maximum, Paleoproductivity, NW-Africa, Water Mass, Stable Carbon and Oxygen Isotopes, Benthic Foraminifera

1. Introduction

The reconstruction of past ocean productivity is a fundamental issue regarding global climate reconstructions. Variations in upwelling intensity and the resulting primary productivity changes are assumed to have a great influence on atmospheric CO_2 concentrations on glacial / interglacial time scales. Barnola et al. (1987) showed that atmospheric CO_2 concentrations were lower during the LGM. Generally, it was considered that increased marine productivity was one of the causes for lowered glacial CO_2 concentrations (e.g. Broecker, 1982; Broecker and Henderson, 1998). Coastal upwelling regions are characterized by enhanced productivity, thus they are important regions in terms of the marine biogeochemical cycle of organic carbon, acting as CO_2 sources and sinks. During the LGM, sealevel was lowered by about 120 m (Fairbanks, 1989). Large continental shelf areas were exposed and off NW-Africa the coastline was shifted westwards, which had a strong influence on transport and sedimentation mechanisms, especially close to the coast (Martinez et al., 1999; Bertrand et al., 2000). It has been suggested that the NE trade winds have been intensified during glacials (Hooghiemstra et al., 1987), even though no meridional shift was observed during the last glacial / interglacial transition (Sarnthein et al., 1981; Hooghiemstra et al., 1987; Hooghiemstra, 1989).

Two decades ago generally increased glacial productivity for the entire NW-African margin was proposed (e.g. Sarnthein et al., 1988). However, successively it became evident that this assumption has to be modified. In fact, enhanced glacial productivity was observed at 25°N (Bertrand et al., 1996; Abrantes, 2000; Sicre et al., 2000; Ternois et al., 2000). In contrast, glacial productivity was lower off Cape Blanc (21°N) (Martinez et al., 1999; Zhao et al., 2000; Sicre et al., 2001; Henderiks and Bollmann, 2004). This clarifies that explicit productivity differences could co-exist within a regionally small area (Bertrand et al., 1996). Even within the geographically limited region between 27.5°N and 31°N strong productivity variability has been reported for the LGM (Freudenthal et al., 2002; Henderiks and Bollmann, 2004). However, recent studies in the Canary Islands region revealed that enhanced productivity was prevailend during glacial time periods (Freudenthal et al., 2002; Henderiks et al., 2002; Henderiks and Bollmann, 2004; Kuhlmann et al., 2004).

Benthic foraminifera and their stable carbon isotopic compositions have been widely used for reconstructing paleoproductivity. Benthic foraminifera live epifaunal (Lutze and Thiel, 1989) or infaunal (Corliss, 1985) with a distinct microhabitat distribution within the sediment (e.g. Mackensen and Douglas, 1989; Rathburn and Corliss, 1994; Fontanier et al., 2002). The assemblage composition, distinct benthic foraminiferal species, and their stratification within the sediment are mainly linked to the quantity and mode of organic matter fluxes (e.g. Gooday, 1988; Corliss and Emerson, 1990; Rathburn and Corliss, 1994; Schmiedl et al., 2000; Fontanier et al., 2003). Therefore, benthic foraminiferal faunas can be used to reconstruct past productivity (Loubere, 1999). The $\delta^{13}C$ values of preferentially epifaunal *Cibicidoides wuellerstorfi* reflect the $\delta^{13}C$ dissolved inorganic carbon (DIC) of ambient water (Woodruff et al., 1980; Belanger et al., 1981; Graham et al., 1981). It was shown that the $\delta^{13}C$ values of this species reliably record the bottom water $\delta^{13}C_{DIC}$ (McCorkle and Keigwin, 1994; Mackensen and Licari, 2004; Eberwein and Mackensen, 2006) and are used to reconstruct past bottom and deep water circulation changes (e.g. Curry et al., 1988; Duplessy et al., 1988; Sarnthein et al., 1994; Mackensen et al., 2001). In contrast to *C. wuellerstorfi*, the $\delta^{13}C$ values of infaunal species mirror, in dependance of their microhabitat the $\delta^{13}C$ of the pore water in the sediment (e.g. McCorkle et al., 1990; Mackensen and Licari, 2004; Fontanier et al., 2006). The $\delta^{13}C$ pore water gradient is determined by organic matter degradation, which depends on the export flux and the availability of dissolved oxygen in bottom waters. Hence, $\delta^{13}C$ differences between epifaunal and infaunal species ($\Delta\delta^{13}C$ values) are considered to reflect productivity variations (Schmiedl et al., 2000; Fontanier et al., 2006; Eberwein and Mackensen, 2006) and are used for paleoproductivity reconstructions (e.g. Zahn et al., 1986).

In this paper we focus on the detailed paleoproductivity reconstruction during the LGM (23000 to 19000 cal-yr BP) between 31°N (Cape Ghir) and 27.5°N (Cape Yubi) off Morocco. In order to assess the regional paleoproductivity variability and to compare the LGM paleoproductivity pattern with the modern upwelling conditions we used benthic foraminiferal faunas and the stable carbon isotopic composition of three species with different microhabitat preferences. In particular, we used $\Delta\delta^{13}C$ values of *Hoeglundina elegans* and *Melonis pompiloides* to reconstruct spatial productivity variability. *Hoeglundina elegans* was described as having microhabitat preferences within the first two cm (Corliss, 1985; Licari et al., 2003; Eberwein et al., subm) and *M. pompiloides* within the first cm (Schumacher, 2001). The assumption that the $\delta^{13}C$ values of epifaunal *C. wuellerstorfi* indicate the LGM $\delta^{13}C$ of the bottom water dissolved inorganic carbon is discussed.

2. Present-day setting

Today, the area off Morocco is characterized by high primary productivity as it is part of one of the four major continental margin upwelling regions in the world oceans (Hagen, 2001; Carr, 2002). The duration and intensity of coastal upwelling is driven by NE trade winds, which in turn are coupled to the meridional shift of the Azores High in relation to the position of the Inter Tropical Convergence Zone. North of 25°N, strong upwelling events, which are restricted close to the coast were observed in boreal summer and early fall (Mittelstaedt, 1991; Van Camp et al., 1991; Hernández-Guerra and Nykjaer, 1997). However, within filaments nutrient-enriched upwelled waters, mainly comprised of the North Atlantic Central Water (NACW), are transported several hundred kilometers into the open ocean off Cape Ghir and Cape Yubi (Van Camp et al., 1991; Nykjaer and van Camp, 1994; Hernández-Guerra and Nykjaer, 1997; Hagen, 2001).

Both upwelling intensity as well as the duration and extension of the filaments depend on the coastal cape morphology, the NE trade wind intensity, and the surface Canary Current (Hagen et al., 1996; Stevens and Johnson, 2003). The sea floor morphology is characterized by a continental shelf that extends about 25 km off Cape Ghir and up to 75 km off Cape Yubi (Summerhayes et al., 1976). This is important in terms of the organic carbon accumulation in the deep-sea. The water mass stratification off Morocco is characterized by the NACW between 100 m – 600 m, the Mediterranean Outflow Water (MOW) between 600 m - 1700 m (Knoll et al., 2002; Llinás et al., 2002), the North Atlantic Deep Water (NADW) between 1700 m and 4000 m and the Antarctic Bottom Water (AABW) below 4000 m (Sarnthein et al., 1982). A northwards flowing undercurrent of Antarctic Intermediate Water (AAIW) between 600 m - 1000 m was observed (Knoll et al., 2002). Presently, the regions off Cape Ghir and Cape Yubi are characterized by high productivity, which is reflected by distinct species, identical live and dead benthic foraminiferal assemblages and low $\delta^{13}C$ values of infaunal species (Eberwein and Mackensen, 2006). By contrast, the area between these capes is characterized by lower and slightly seasonally varying productivity as indicated by different live and dead benthic foraminiferal assemblages and higher $\delta^{13}C$ values of infaunal species (Eberwein and Mackensen, 2006). In support with findings of these authors, the different productivity regimes are likewise reflected by geochemical proxies ($\delta^{15}N$, $\delta^{13}C_{org}$, C/N ratio, total organic carbon and carbonate contents) and the total numbers of microorganisms (diatoms, dinoflagellates, foraminifera and pteropods) (Meggers et al., 2002). The knowledge about the response of benthic foraminiferal to recent productivity conditions serves as the basis to reconstruct LGM paleoproductivity between Cape Ghir and Cape Yubi off Morocco.

3. Material & Methods

The 16 investigated sediment cores were collected between 31°N (Cape Ghir) and 27°N (Cape Yubi) in the upwelling region off Morocco (NW-Africa) in water depths ranging from 775 m to 2506 m (Fig. 1, Table 1). The sediment cores were recovered with the aid of a gravity and piston corer during cruises in 1996, 1998, and 1999 with RV *Meteor* (Table 1). We determined the benthic foraminiferal content and measured the stable carbon and oxygen isotopic composition of foraminiferal tests from the LGM time slice, which is dated to the time interval between 19000 to 23000 cal-yr BP with its center at 21000 cal-yr BP (Mix et al., 2001). For detailed information about the stratigraphic model of the Canary Islands sediment cores we refer to Kuhlmann et al. (2004).

Sediment samples were freeze-dried, wet-sieved over > 125 µm and > 63 µm sieves, and dried in an oven at < 60°C. Benthic foraminifera were analyzed from the fraction > 125 µm and determined to species level. The sampling interval was defined in dependance on the sedimentation rate of each core. The LGM time slice was covered with two or three samples around the centre of the LGM. Counts were adjusted for splits and at each station the counts of all samples were combined and are considered to represent the LGM (Table 2).

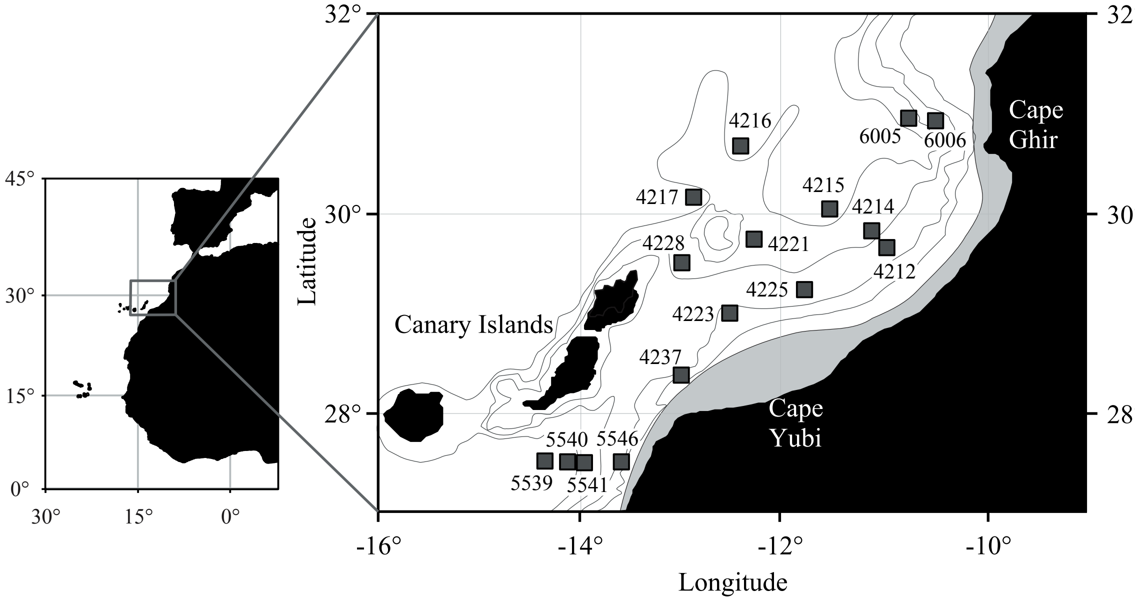

Fig. 1: Map showing study area, bathymetry, and location of the 16 investigated sediment cores of the Last Glacial Maximum time period (LGM). Sample locations are marked by squares and station numbers. Grey shaded area approximately indicates coastline during the LGM. Isobaths indicate 500, 1000, 1500 and 2000 m water depths.

To detect the composition of distinct benthic foraminiferal assemblages and to reveal the important species of these assemblages a factor analysis with varimax rotation was applied using the software SYSTAT™ 5.2.1. Species, which occurred at least at two stations with a minimum abundance of 1% were included into the analysis.

The stable carbon and oxygen isotopic composition of benthic foraminifera was determined with a Finnigan MAT 251 isotope ratio gas mass spectrometer. The foraminiferal isotopic values are reported in δ–notation relative to the Vienna Pee Dee Belemnite (VPDB)-scale. For calibration to the VPDB scale the international standard NBS19 was used. The reproducebility of the measurements as refered to a laboratory standard is better than ± 0.06 ‰ for $\delta^{13}C$ and ± 0.08 ‰ for $\delta^{18}O$, over a one-year period. The species analyzed were *Bulimina mexicana*, *Cibicidoides wuellerstorfi*, *Globobulimina affinis*, *Hoeglundina elegans*, *Melonis barleeanum*, *Melonis pompiloides,* and *Uvigerina mediterranea*. For interpretation we used stable carbon isotope ratios of *Cibicidoides wuellerstorfi*, *Hoeglundina elegans*, and *Melonis pompiloides* and stable oxygen isotope ratios of *Bulimina mexicana*, *C. wuellerstorfi*, *Globobulimina affinis*, *H. elegans*, *Melonis barleeanum* and *Uvigerina mediterranea*

We consider the $\delta^{13}C$ values of *C. wuellerstorfi* to be an indicator of glacial bottom water dissolved inorganic carbon (DIC), since we showed that $\delta^{13}C$ values of live *C. wuellerstorfi* reliably record the bottom water dissolved inorganic carbon (DIC) off Morocco (Eberwein and Mackensen, 2006). In the following the term $\delta^{13}C_{DIC}$ is used for LGM $\delta^{13}C$ values of *C. wuellerstorfi*.

Table 1: List of sediment samples with sampling date, position, water depth, glacial water mass, and the $\delta^{13}C_{DIC}$ of the bottom water. Italic letters represent mean $\delta^{13}C_{DIC}$ of glacial MOW or glacial NADW.

Core GeoB	Cruise	Date	Latitude (°N)	Longitude (°W)	Water depth (m)	Glacial Watermass	$\delta^{13}C_{DIC}$ (‰ VPDB)	mean $\delta^{13}C_{DIC}$ (‰ VPDB)	mean $\delta^{18}O_{EC}$ (‰ VPDB)
4212-2	M37/1	Dec 1996	29°36,3	10°57,0	1258	MOW	*1.16*	1.16 ± 0.17	4.42 ± 0.49
4214-1	M37/1	Dec 1996	29°46,9	11°11,9	1791	MOW	0.97	1.16 ± 0.17	4.42 ± 0.49
4215-2	M37/1	Dec 1996	30°02,2	11°33,1	2105	NADW	0.44	0.44 ± 0.10	5.10 ± 0.11
4216-1	M37/1	Dec 1996	30°37,8	12°23,8	2324	NADW	0.56	0.44 ± 0.10	5.10 ± 0.11
4217-5	M37/1	Dec 1996	30°25,2	12°54,7	2506	NADW	0.33	0.44 ± 0.10	5.10 ± 0.11
4221-1	M37/1	Dec 1996	29°46,5	12°20,1	1826	MOW	1.01	1.16 ± 0.17	4.42 ± 0.49
4223-2	M37/1	Dec 1996	29°01,0	12°28,0	775	MOW	*1.16*	1.16 ± 0.17	4.42 ± 0.49
4225-1	M37/1	Dec 1996	29°16,6	11°46,9	1281	MOW	1.32	1.16 ± 0.17	4.42 ± 0.49
4228-1	M37/1	Dec 1996	29°28,2	12°59,6	1632	MOW	1.15	1.16 ± 0.17	4.42 ± 0.49
4237-2	M37/1	Dec 1996	28°43,7	13°01,0	805	MOW	1.29	1.16 ± 0.17	4.42 ± 0.49
5539-3	M42/4	Oct 1998	27°32,2	14°21,3	2201	NADW	0.53	0.44 ± 0.10	5.10 ± 0.11
5540-2	M42/4	Oct 1998	27°32,1	14°10,5	2037	NADW	0.35	0.44 ± 0.10	5.10 ± 0.11
5541-4	M42/4	Oct 1998	27°32,2	13°59,8	1747	MOW	*1.16*	1.16 ± 0.17	4.42 ± 0.49
5546-2	M42/4	Oct 1998	27°32,2	13°44,2	1072	MOW	1.16	1.16 ± 0.17	4.42 ± 0.49
6005-2	M45/5	Oct / Nov 1999	30°52,8	10°53,9	1782	MOW	0.89	1.16 ± 0.17	4.42 ± 0.49
6006-1	M45/5	Oct / Nov 1999	30°52,1	10°37,7	1275	MOW	1.52	1.16 ± 0.17	4.42 ± 0.49

Table 2: This table represents the sum of total counts and the relative abundance of dominant (underlined) and associated species at each station. Abbreviations are as follows: CYUR = Cape Yubi Upwelling Region, CGUR = Cape Ghir upwelling Region, CYFR = Cape Yubi Filament Region and CGFR = Cape Ghir Filament Region. Numbers indicate stations.

Core	4223-2	4237-2	5546-2	4212-2	4214-1	4221-1	4225-1	4228-1	6005-2	6006-1	5539-3	5540-2	5541-4	4215-2	4216-1	4217-5
Region	CYUR	CYUR	CYUR	CGUR	CGUR	CGUR	CGUR	CGUR	CGUR	CGUR	CYFR	CYFR	CYFR	CGFR	CGFR	CGFR
Sum total counts	17375	9858	773	6840	6841	7049	9184	2248	3604	3016	4337	5071	6242	6558	6170	2739
B.dilatata	0.48		1.74	0.29	0.12	0.10				0.18	3.28	6.26	10.42			
B.albatrossi	8.57	16.91	5.48	1.89			1.93			4.34	0.47	0.16				0.07
B.mexicana	0.37		2.06	7.90	4.51	3.93	9.48	5.44	31.85	14.00	0.47	2.00	1.04	0.56	0.43	
C.laevigata	2.80	2.74	2.24	1.06	2.40	2.16	1.32	0.88	1.82	0.45	11.11	7.71	9.64	1.22	1.92	0.98
C.neoteretis	4.82	5.49	2.90	5.68	2.14	4.46	4.14	4.33	4.21	4.41	3.20	0.88		4.56	5.43	1.02
C.bradyi	1.12	0.40	3.11	11.50	3.01	2.16	11.39	0.72	2.08	8.86	2.45	0.80		5.26	3.16	4.99
E.exigua	0.28	0.09		0.12	0.86	2.45	0.17	0.18	0.30	0.07	0.75		0.26	25.72	42.79	31.72
G.translucens	2.05	1.63	13.13	9.02	3.02	3.76	10.57	7.06	4.50	11.53	0.28	0.96	2.08			0.07
L.lobatula	5.02	3.24	7.22	3.52	2.03	2.09	3.48	1.64	1.23	5.20	3.10	5.30	3.65	0.76	1.45	1.74
M.barleeanum	5.35	4.52	2.43	0.30	0.31	0.16	0.62	0.38	0.11	2.13	0.85	0.56	1.30	0.82	1.27	3.62
M.pompiloides		0.09			7.49	3.23		1.03	3.98		7.81	7.68	0.52	7.33	5.16	5.45
M.subrotunda	2.06	0.99	0.53	8.08	6.43	2.76	2.77	4.74	2.02	2.18	3.02	4.16		2.80	0.25	0.10
N.auberii	0.29	1.11	3.29		0.06		0.54	0.63			3.37	6.82	9.64	0.12	0.08	
N.iridea		0.13	0.17	0.23	8.38		0.09	0.19	4.92		6.40	12.50		3.68	2.69	0.86
P.irregularis	1.66	1.12	2.60	9.31	8.24	2.71	8.60	5.88	1.56	5.02	3.47	1.61	1.82	3.60	0.22	0.10
Q.waeveri	3.55	1.31	5.82	2.08	3.20	1.73	2.03	2.53	2.02	2.37	2.92	3.04	6.51	3.04	0.65	0.47
U.mediterranea	16.24	20.06	7.60	0.36		0.53	0.80	0.13	0.05	2.18	1.60	0.64	1.82			

In contrast, the $\delta^{13}C$ of infaunal species *H. elegans* and *M.pompiloides* reflect the pore water $\delta^{13}C$. The terms $\Delta\delta^{13}C_{H.elegans}$ and $\Delta\delta^{13}C_{M.pompiloides}$ indicate the differences between the bottom and pore water and are used to reconstruct past productivity variations (Zahn et al., 1986). The data used in this paper are not adjusted for a global shift in $\delta^{13}C$ (Curry et al., 1988; Duplessy et al., 1988).

The $\delta^{18}O$ of calcite precipitated in equilibrium with bottom water for a distinct temperature T (K) was calculated with the equation given in McCorkle et al. (1997). The conversion between SMOW and PDB values was calculated according to Friedman & O'Neil (1977). *Uvigerina peregrina* and *Uvigerina mediterranea* can be used for approximation of equlilibrium calcite as they calcify their tests close to equilibrium of the bottom water $\delta^{18}O$ (McCorkle et al., 1990; Eberwein, unpublished). In this study *U. peregrina* is almost absent, hence we used *U. mediterranea* to determine corrections factors of five species as follows: +0.01 ‰ for *Bulimina mexicana,* -0.78 ‰ for *C. wuellerstorfi*, -0.24 ‰ for *G. affinis*, -0.43 ‰ for *H. elegans*, and +0.57 ‰ for *M. barleeanum*.

4 Results

4.1 Benthic foraminiferal faunas

A total of 156 species were identified. Factor analysis revealed four assemblages, which explain 75 % of the total variance, consisting of 17 important (score > 3) and associated (score > 1) species (Table 3).

Table 3: Benthic foraminiferal faunas revealed by factor analysis with their dominant (score > 3) and associated species (score > 1). Variance of each fauna and total variance are given in percentages.

Variance [%] Total variance 75.01	Dominant species	Score	Associated species	Score
25.69	*Bulimina mexicana*	4.08	*Pyrgoella irregularis*	2.37
	Gavelinopsis translucens	3.26	*Cibicidoides bradyi*	2.30
			Miliolinella subrotunda	1.29
			Cassidulina neoteretis	1.18
18.54	*Epistominella exigua*	6.82	*Melonis pompiloides*	1.21
15.59	*Cassidulina laevigata*	3.72	*Melonis pompiloides*	2.52
	Nonionella iridea	3.05	*Neoeponides auberii*	1.98
			Bolivina dilatata	1.95
			Quinqueloculina waeveri	1.22
			Lobatula lobatula	1.08
15.19	*Uvigerina mediterranea*	4.92	*Gavelinopsis translucens*	1.55
	Bolivina albatrossi	3.35	*Lobatula lobatula*	1.49
			Melonis barleeanum	1.08

The *Uvigerina mediterranea* / *Bulimina albatrossi* Assemblage occurs between the African coast and the easternmost Canary Islands off Cape Yubi, where it dominates the benthic foraminiferal fauna at the shallowest stations (Fig. 2). The combined relative abundances of *U. mediterranea* and *B. albatrossi* vary between 13 and 37 % (Table 2). Main associated species are *Gavelinopsis translucens*, *Lobatula lobatula*, and *Melonis barleeanum* (Tables 2, 3). This region dominated by the *U. mediterranea* / *B. albatrossi* fauna we call Cape Yubi Upwelling region (CYUR).

The *Bulimina mexicana* / *Gavelinopsis translucens* Assemblage dominates the benthic foraminiferal fauna mainly in the northern part of the study area off Cape Ghir, and at shallower stations as far south as 29°N (Fig. 2). The combined relative abundances of *B. mexicana* and *G. translucens* vary between 8 and 36 % (Table 2). Main associated species are *Pyrgoella irregularis*, *Cibicidoides bradyi*, *Miliolinella subrotunda*, and *Cassidulina neoteretis* (Tables 2, 3). This region dominated by the *B. mexicana* / *G. translucens* fauna we call Cape Ghir Upwelling Region (CGUR).

The *Cassidulina laevigata* / *Nonionella iridea* Assemblage exclusively occurs on the southernmost transect (Fig. 2). The combined relative abundances of *C. laevigata* and *N. iridea* vary between 10 and 20 % (Table 2). Main associated species are *Melonis pompiloides*, *Neoeponides auberii*, *Bolivina dilatata*, *Quinqueloculina waeveri*, and *L. lobatula* (Tables 2, 3). This region dominated by the *Cassidulina laevigata* / *Nonionella iridea* fauna we call Cape Yubi Filament Region (CYFR).

The *Epistominella exigua* Assemblage occurs further away from the African coast at the deepest stations north and northeast of Lanzarote (Fig. 2). The relative abundances of *E. exigua* vary between 26 and 43 % (Table 2). Main associated species is *M. pompiloides* (Tables 2, 3). This region dominated by the *E. exigua* Assemblage we call Cape Ghir Filament Region (CGFR).

Fig. 2: Relative abundances of dominant benthic foraminiferal species (Table 2) were combined for each assemblage in sediment samples of the LGM. The Cape Yubi Upwelling Region is dominated by *Uvigerina mediterranea* and *Bulimina albatrossi*. The Cape Ghir Upwelling Region is dominated by *Bulimina mexicana* and *Gavelinopsis translucens*. The Cape Yubi Filament Region is dominated by *Cassidulina laevigata* and *Nonionella iridea*. The Cape Ghir Filament Region is dominated by *Epistominella exigua*. Line indicates the approximate African coast during the LGM.

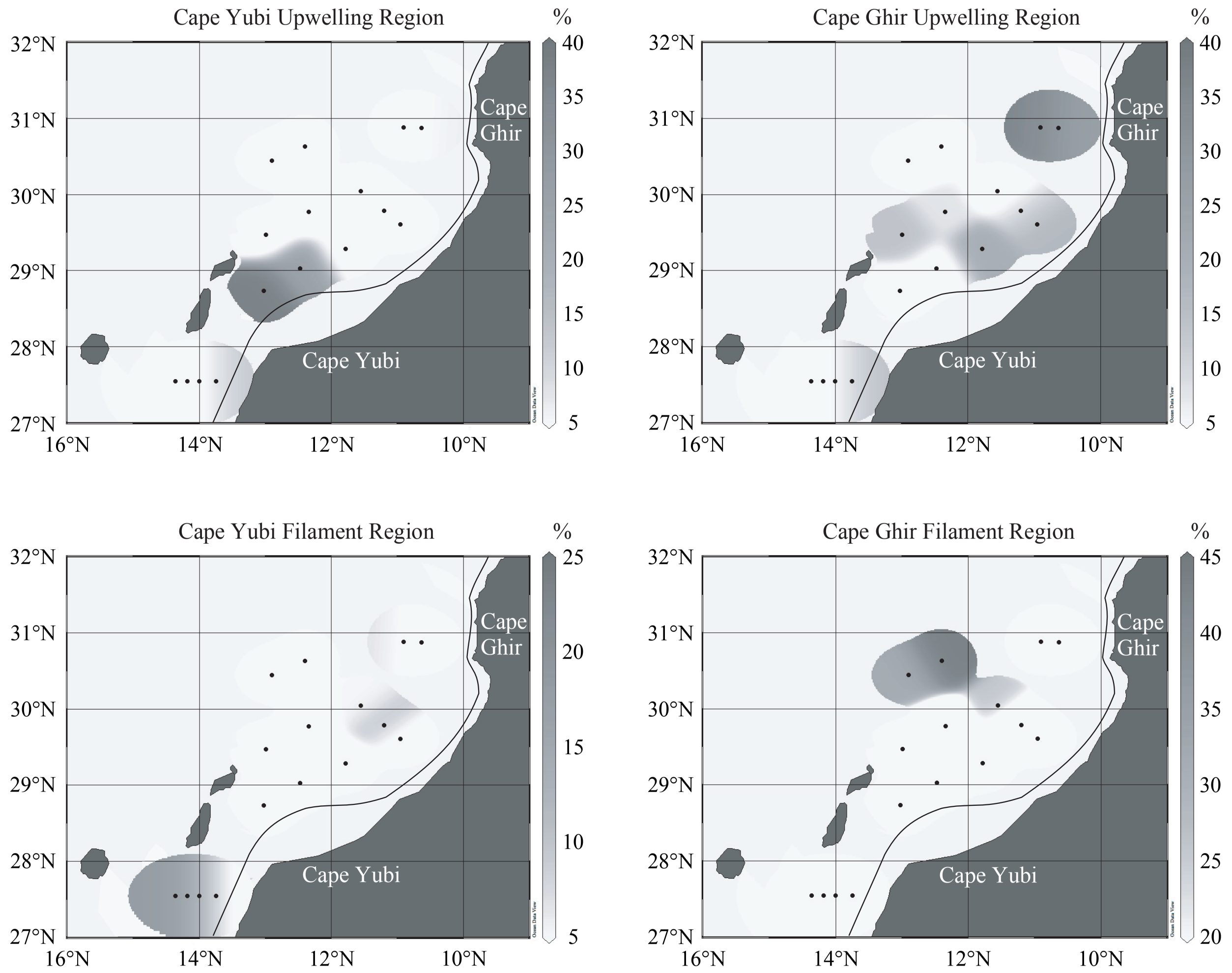

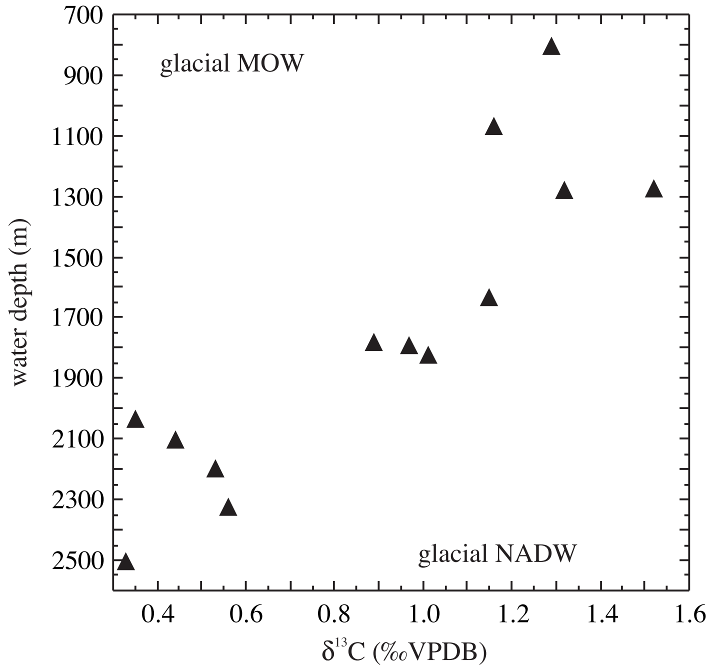

Fig. 3: The δ^{13}C values of *Cibicidoides wuellerstorfi* within the glacial MOW and the glacial NADW versus water depth are plotted.

4.2 Stable carbon and oxygen isotopes of species

The stable carbon isotopic compositions of *Cibicidoides wuellerstorfi*, *Hoeglundina elegans* and *Melonis pompiloides* tests have been measured. *Cibicidoides wuellerstorfi* exhibits δ^{13}C values between 0.33 ‰ and 1.52 ‰ VPDB with a gradual decrease with increasing water depth (Fig. 3). The δ^{13}C values of this species are greater than 0.90 ‰ from water depths shallower than approximately 1900 m, whereas δ^{13}C values lower than 0.6 ‰ are measured from below this depth (Fig. 3, Table 4). *Hoeglundina elegans* exhibits δ^{13}C values between 1.60 ‰ and 2.41 ‰, whereas *M. pompiloides* exhibits δ^{13}C values between –0.72 ‰ and 0.33 ‰ (Table 4).

The stable oxygen isotopic compositions of specimens of *Bulimina mexicana*, *C. wuellerstorfi*, *Globobulimina affinis*, *H. elegans*, *Melonis barleeanum*, and *Uvigerina mediterranea* were determined. The δ^{18}O values of *B. mexicana* vary between 3.93 ‰ and 4.91 ‰ VPDB, of *C. wuellerstorfi* between 3.37 ‰ and 4.63 ‰, of *G. affinis* between 3.57 ‰ and 5.40 ‰, of *H. elegans* between 3.63 ‰ and 5.80 ‰, of *M. barleeanum* between 2.51 ‰ and 4.56 ‰, and of *U. mediterranea* between 2.59 ‰ and 4.36 ‰ (Table 4).

Table 4: Stable carbon and oxygen isotope measurements of species discussed in the text. Italic $\delta^{13}C$ values represent mean of glacial MOW and glacial NADW (Table 1). Region abbreviations are as follows: CYUR = Cape Yubi Upwelling Region, CGUR = Cape Ghir Upwelling Region, CYFR = Cape Yubi Filament Region and CGFR = Cape Ghir Filament Region.

Species	Station	Region	$\delta^{13}C$ (‰ VPDB)	$\delta^{13}C_{DIC}$ (‰ VPDB)	$\Delta\delta^{13}C$ (‰ VPDB)	$\delta^{18}O$ (‰ VPDB)	$\delta^{18}O_{EC}$ (‰ VPDB)
B. mexicana	4212-2	CGUR				4.42	4.43
B. mexicana	4214-1	CGUR				4.64	4.65
B. mexicana	4221-1	CGUR				4.80	4.81
B. mexicana	4225-1	CGUR				4.11	4.12
B. mexicana	4228-1	CGUR				3.93	3.94
B. mexicana	5540-2	CYFR				4.91	4.92
B. mexicana	5541-4	CYFR				4.76	4.77
B. mexicana	6005-2	CGUR				4.79	4.80
B. mexicana	6006-1	CGUR				4.37	4.38
C. wuellerstorfi	4214-1	CGUR	0.97	0.97		4.21	4.99
C. wuellerstorfi	4215-2	CGFR	0.44	0.44		4.63	5.41
C. wuellerstorfi	4216-1	CGFR	0.56	0.56		4.35	5.13
C. wuellerstorfi	4217-5	CGFR	0.33	0.33		4.38	5.16
C. wuellerstorfi	4221-1	CGUR	1.01	1.01		3.64	4.42
C. wuellerstorfi	4225-1	CGUR	1.32	1.32		3.83	4.61
C. wuellerstorfi	4228-1	CGUR	1.15	1.15		4.18	4.96
C. wuellerstorfi	4237-2	CYUR	1.29	1.29		3.37	4.15
C. wuellerstorfi	5539-3	CYFR	0.53	0.53		4.26	5.04
C. wuellerstorfi	5540-2	CYFR	0.35	0.35		4.18	4.96
C. wuellerstorfi	5546-2	CYUR	1.16	1.16		3.75	4.53
C. wuellerstorfi	6005-2	CGUR	0.89	0.89		4.19	4.97
C. wuellerstorfi	6006-1	CGUR	1.52	1.52		3.94	4.72
G. affinis	4215-2	CGFR				5.40	5.16
G. affinis	4223-2	CYUR				3.57	3.33
G. affinis	4237-2	CYUR				4.18	3.94
G. affinis	6005-2	CGUR				5.39	5.15
G. affinis	6006-1	CGUR				4.87	4.63
H. elegans	4223-2	CYUR	2.04	*1.16*	*0.88*	3.63	3.08
H. elegans	4214-1	CGUR	2.34	0.97	1.37	5.53	4.98
H. elegans	4215-2	CGFR	2.23	0.44	1.79	5.80	5.25
H. elegans	4216-1	CGFR	2.13	0.56	1.57	5.62	5.07
H. elegans	4217-5	CGFR	2.22	0.33	1.89	5.59	5.04
H. elegans	4221-1	CGUR	2.41	1.01	1.40	5.38	4.83
H. elegans	4228-1	CGUR	2.35	1.15	1.20	5.38	4.83
H. elegans	4237-2	CYUR	2.16	1.29	0.87	4.56	4.01
H. elegans	5539-3	CYFR	1.67	0.53	1.14	5.76	5.21
H. elegans	5540-2	CYFR	1.60	0.35	1.25	5.62	5.07
H. elegans	5541-4	CYFR	1.87	*1.16*	*0.71*	5.00	4.45
H. elegans	6005-2	CGUR	2.01	0.89	1.12	5.65	5.10
M. barleeanum	4214-1	CGUR				4.49	5.06
M. barleeanum	4217-5	CGFR				4.56	5.13
M. barleeanum	4223-2	CYUR				2.51	3.08
M. barleeanum	4237-2	CYUR				3.43	4.00
M. barleeanum	6006-1	CGUR				4.06	4.63
M. pompiloides	4214-1	CGUR	0.33	0.97	-0.64		
M. pompiloides	4215-2	CGFR	0.09	0.44	-0.35		
M. pompiloides	4216-1	CGFR	-0.25	0.56	-0.81		
M. pompiloides	4217-5	CGFR	-0.09	0.33	-0.42		
M. pompiloides	4221-1	CGUR	0.24	1.01	-0.77		
M. pompiloides	4228-1	CGUR	0.32	1.15	-0.83		
M. pompiloides	5539-3	CYFR	-0.53	0.53	-1.06		
M. pompiloides	5540-2	CYFR	-0.72	0.35	-1.07		
M. pompiloides	5541-4	CYFR	-0.43	*1.16*	*-1.59*		
M. pompiloides	6005-2	CGUR	-0.21	0.89	-1.10		
M. pompiloides	6006-1	CGUR	-0.27	1.52	-1.79		
U. mediterranea	4212-2	CGUR				4.33	4.33
U. mediterranea	4223-2	CYUR				3.34	3.34
U. mediterranea	4237-2	CYUR				4.02	4.02
U. mediterranea	5539-3	CYFR				2.59	2.59
U. mediterranea	5546-2	CYUR				4.04	4.04
U. mediterranea	6006-1	CGUR				4.36	4.36

5 Discussion

This discussion focuses on the reconstruction of paleoproductivity patterns during the LGM off Morocco, based on the benthic foraminiferal faunal composition and distribution and the $\Delta\delta^{13}C$ of infaunal species *Hoeglundina elegans* and *Melonis pompiloides*. The reliability of *Cibicidoides wuellerstorfi* to record the bottom water DIC is the basic assumption for paleoproductivity reconstructions based on $\delta^{13}C$ differences between epifaunal and infaunal species. Therefore, we need to discuss the stratification of water masses and particularly, their stable carbon isotopic composition.

5.1 Water masses during the LGM

Generally, *Cibicidoides wuellerstorfi* calcifies its test close to a 1:1 relationship with the $\delta^{13}C$ of ambient DIC (Woodruff et al., 1980; Belanger et al., 1981; Graham et al., 1981; Zahn et al., 1986), and thus faithfully records bottom water $\delta^{13}C_{DIC}$ (Duplessy et al., 1988; McCorkle and Keigwin, 1994; Mackensen and Licari, 2004). Productivity-linked low $\delta^{13}C$ values in tests of live *C. wuellerstorfi* have been reported from oceanographic fronts with high seasonally varying productivity in the south Atlantic (Mackensen et al., 1993b). Similarly, lower $\delta^{13}C$ values were determined in fossil tests from high productive upwelling areas off NW- and SW-Africa (Sarnthein et al., 1988; Sarnthein et al., 1994; Bickert and Wefer, 1999). However, in the high productivity area off Morocco it was shown that $\delta^{13}C$ values of live *C. wuellerstorfi* are reliable proxies for DIC (Eberwein and Mackensen, 2006).

Based on $\delta^{13}C_{DIC}$ and $\delta^{18}O$ of foraminiferal calcite two water masses with disctinct isotopic compositions can be distinguished (Fig. 4).

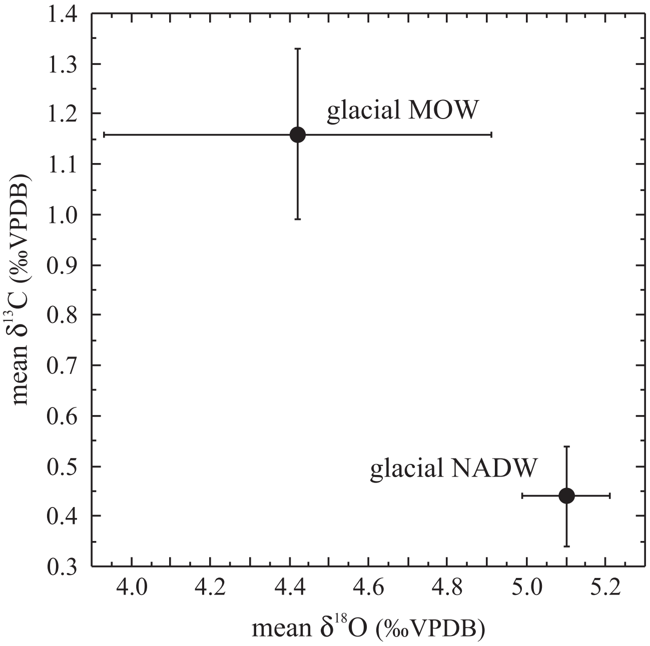

Fig. 4: Mean $\delta^{13}C$ and $\delta^{18}O$ isotopic composition of water masses during the LGM off Morocco. The $\delta^{13}C$ values of *Cibicidoides wuellerstorfi* ($\delta^{13}C_{DIC}$) versus the $\delta^{18}O$ of *Uvigerina mediterranea* ($\delta^{18}O_{EC}$) are plotted (Table 4). The $\delta^{18}O$ of calcite in equilibrium with the bottom water was calculated for five species (see Material & Methods) with the equation given by McCorkle et al. (1997).

Furthermore, the $\delta^{13}C_{DIC}$ values of this study perfectly match with published values (Fig. 5) that have been interpreted to reflect the approximate boundary between glacial MOW and glacial NADW (Sarnthein et al., 1994). In the present study glacial MOW is characterized by a mean $\delta^{13}C$ of 1.16 ± 0.17 ‰ VPDB and a mean $\delta^{18}O$ of 4.42 ± 0.49 ‰, whereas glacial NADW is described by a mean $\delta^{13}C$ of 0.44 ± 0.10 ‰ and a mean $\delta^{18}O$ of 5.10 ± 0.11 ‰ (Fig. 4, Table1). The $\delta^{13}C_{DIC}$ values of both water masses are in good agreement with Sarnthein et al. (1994), who reported a range of 0.70 to 1.20 ‰ for the glacial MOW and a range of 0.40 to 0.60 ‰ for the glacial NADW. The glacial MOW was traced to 20°N, i.e. as far south as today (Zahn et al., 1987). Even to 30°S glacial MOW was identified with $\delta^{13}C_{DIC}$ values greater than 1 ‰ (adjusted by 0.32 ‰ for global shift) (Bickert and Mackensen, 2004). The $\delta^{13}C$ values of around 0.8 ‰ were attributed to be characteristic of the so called Glacial North Atlantic Intermediate Waters (GNAIW), which was composed of glacial MOW amongst other intermediate water masses (Duplessy et al., 1988). The decrease of $\delta^{13}C_{DIC}$ values with increasing water depth within the glacial MOW (Fig. 3) suggests the mixing with the underlying ^{13}C depleted glacial NADW. Compared to the modern $\delta^{13}C_{DIC}$ value of 0.72 ‰ of MOW and 0.63 ‰ of NADW (Eberwein and Mackensen, 2006) the glacial MOW was enriched by 0.44 ‰, whereas the glacial NADW was depleted by 0.19 ‰. The enrichment of 0.44 ‰ of glacial MOW fits to 0.46 ‰ given by Sarnthein et al. (1994) and it suggests that glacial MOW was nutrient depleted compared to modern conditions. In the South Atlantic, glacial NADW with a $\delta^{13}C$ by 0.25 ‰ (global shift adjusted) lower than Holocene values was interpreted to reflect a reduction of the NADW formation (e.g. Bickert and Mackensen, 2004), whereas Zahn et al. (1987) did not consider ^{13}C enriched MOW to be indicative of an enhanced Mediterranean outflow. Our $\delta^{18}O$ values of glacial MOW and NADW are in good agreement with data from off NW-Africa (Zahn and Mix, 1991). These authors reported $\delta^{18}O$ values between 4.20 and 4.60 ‰ in water depths from 1000 to 1500 m and values between 4.99 and 5.20 ‰ in water depths from 2000 to 2500 m.

Summarizing we conclude that both, $\delta^{13}C$ and $\delta^{18}O$ of benthic foraminiferal calcite indicate a deep-water mass stratification during the LGM characterized by glacial MOW above approximately 1900 m and glacial NADW below this depth. This implies that $\delta^{13}C$ values of *Cibicidoides wuellerstorfi* were not influenced by any productivity introduced artifacts during the LGM.

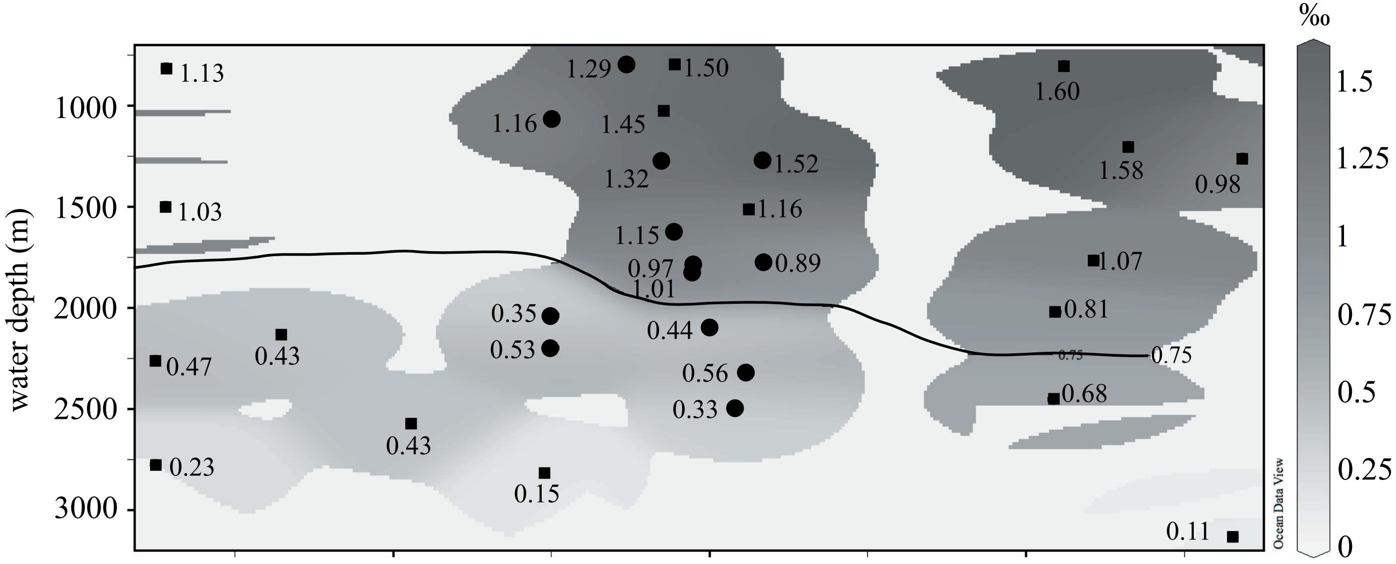

Fig. 5: Distribution of δ^{13}C (in ‰ VPDB) of *Cibicidoides wuellerstorfi* this study (circles) and of *C. wuellerstorfi* and *Cibicidoides ariminensis* published by Sarnthein et al. (1994) (squares) along the NW-African margin during the LGM.

5.2 Spatial reconstruction of paleoproductivity between Cape Ghir and Cape Yubi

In the Cape Yubi Upwelling Region *Uvigerina mediterranea* and *Bolivina albatrossi* show higher abundances in the north at stations GeoB 4237-2 and GeoB 4223-2, whereas only minor abundances were observed in the south at station GeoB 5546-2 (Fig. 2, Table 2). Today, *Uvigerina mediterranea* is a dominant species in high productive regions, such as the Mediterranean Sea (Schmiedl et al., 2000), the Bay of Biscay (Fontanier et al., 2002) and off NW-Africa (Lutze and Coulbourn, 1984; Jorissen et al., 1998; Eberwein and Mackensen, 2006). *Uvigerina mediterranea* is representative for enhanced annual organic matter fluxes varying between 4 and 20 g C m^{-2} yr^{-1} (Schmiedl et al., 2000; Fontanier et al., 2002; Eberwein et al., subm). *Bolivina albatrossi* occurs with high abundances in C_{org} enriched sediments containing up to 3 % TOC in the Gulf of Guinea (Schiebel, 1992; Timm, 1992), which suggests its adaptation to high primary productivity. Thus, we conclude that the *U. mediterranea* / *B. albatrossi* Assemblage reflects very high paleoproductivity off Cape Yubi during the LGM. Additionally, this imprint of high productivity is recorded by lowest $\Delta\delta^{13}C$ values of *Hoeglundina elegans* (Fig. 6). Productivity linked lowered $\delta^{13}C$ values in live and dead *H. elegans* have been reported from sediments underlying the high productive Cape Ghir and Cape Yubi filaments (Eberwein and Mackensen, 2006). At stations GeoB 4223 and GeoB 4237 the LGM $\Delta\delta^{13}C$ values compared to the Holocene values of *H. elegans* are lower by 0.77 and 0.72 ‰, respectively (Eberwein and Mackensen, in press). This indicates that paleoproductivity was enhanced at these stations during the LGM. In support of our results, two times higher total organic carbon accumulation rates (Henderiks et al., 2002) and low $\delta^{15}N$ values (Freudenthal et al., 2002) also indicated enhanced glacial productivity at station GeoB 4223-2. During the LGM the Cape Yubi coastline shifted northwards and the cape had a much geater extension (Figs. 1, 7), due to the lowered sea level. Sea level changes are considered to be responsible for the zonal shift of upwelling cells, which in turn controls the productivity signal (Bertrand et al., 1996; Martinez et al., 1999; Zhao et al., 2000). Power spectra of benthic foraminiferal $\delta^{18}O$, total organic carbon, $\delta^{15}N$ and $\delta13_{Corg}$ at station GeoB 4223-2 showed that sea level changes controlled by precessional forcing mechanism have been responsible for observed productivity variations (Freudenthal et al., 2002).

We conclude that the Cape Yubi Upwelling Region was characterized by very high paleoproductivity during the LGM. Most likely, the main core of the Cape Yubi upwelling cell was positioned above stations GeoB 4237-2 and GeoB 4223-2, whereas station GeoB 5546-2 was situated close to the edge of this cell. Obviously, the northern boundary of the Cape Yubi upwelling cell was positioned at approximately 29°N (Figs. 1, 7).

In the Cape Ghir Upwelling Region the two dominant species show highly variable relative abundances. *Bulimina mexicana* is more abundant off Cape Ghir, whereas *Gavelinopsis translucens* generally, is more abundant at stations southwest off this cape (Fig. 2, Table 2). *Bulimina mexicana* was described in areas of high productivity in the Mediterranean Sea (Schmiedl et al., 2000) and off SW-Africa (Licari et al., 2003) with low variations in the seasonality signal of primary productivity (Loubere and Fariduddin, 1999).

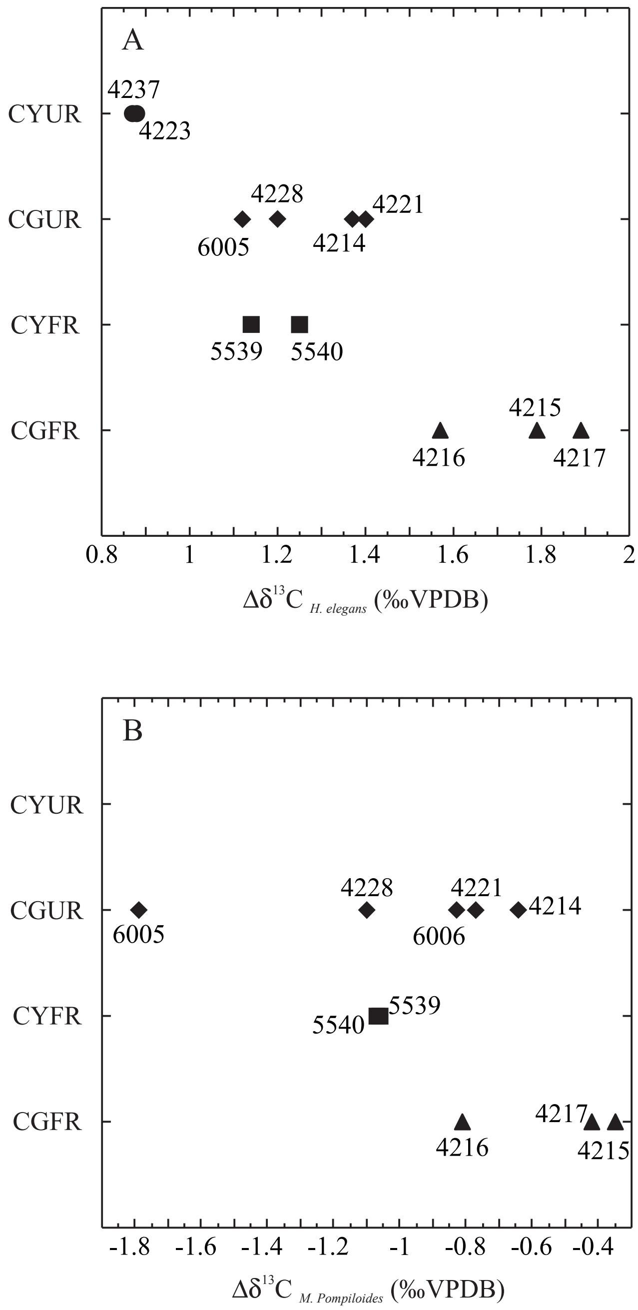

Fig. 6: Mean $\Delta\delta^{13}C$ values of *Hoeglundina elegans* (A), and *Melonis pompiloides* (B) within the four regions. Abbreviations are as follows: CYUR = Cape Yubi Upwelling Region, CGUR = Cape Ghir Upwelling Region, CYFR = Cape Yubi Filament Region and CGFR = Cape Ghir Filament Region. Numbers indicate stations.

Gavelinopsis translucens is recorded in higher productive regions (Jorissen et al., 1998; Eberwein and Mackensen, 2006) but, off Cape Blanc and SW-Africa it dominates outside the productivity maximum under the influence of seasonally varying primary productivity (Jorissen et al., 1998; Licari and Mackensen, 2005). *Gavelinopsis translucens* is adapted to an annual organic matter flux between 3 and 9 g C m^{-2} yr^{-1} (Jorissen et al., 1998; Eberwein et al., subm). Based on the preferences of *B. mexicana* and *G. translucens* regarding productivity we conclude that the Cape Ghir Upwelling Region was characterized by high paleoproductivity, but with a clear seasonal signal. In similarity to the varying abundances of the dominant species the $\Delta\delta^{13}C$ values of *M. pompiloides* strongly scatter by 1.2 ‰ and the $\Delta\delta^{13}C$ values of *H. elegans* by 0.4 ‰ (Fig. 6), which indicates that the Cape Ghir Upwelling Region was characterized by a locally strong varying paleoproductivity. Within this region the lowest $\Delta\delta^{13}C$ values of *H. elegans* and *M. pompiloides* were measured at station GeoB 6005-2 off Cape Ghir (Fig. 6), thus indicating the highest productivity of the Cape Ghir upwelling cell, which presumably was located directly west off Cape Ghir (Figs. 1, 7). At station GeoB 6005 almost identical Holocene and LGM faunas (cf. Eberwein and Mackensen (2006)) as well as a minor difference between Holocene and LGM $\Delta\delta^{13}C$ values (0.27 ‰) in *H. elegans* were observed. This suggests that the LGM Cape Ghir upwelling area and the Holocene Cape Ghir filament were characterized by comparably high productivity. At stations GeoB 4221-1 and GeoB 4228-1 LGM $\Delta\delta^{13}C$ values of *H. elegans* were by 0.48 ‰ and 0.54 ‰ lower, respectively, than Holocene values of this species at the same stations (Eberwein and Mackensen, 2006). Thus, we conclude that paleoproductivity was increased in this area during the LGM compared to the Holocene (Fig. 7). This is corroborated by distinct benthic foraminiferal assemblages, which reflect low productivity in the Holocene (Eberwein and Mackensen,2006). Most likely, these stations and, generally, stations located between 29°N and 30°N within the Cape Ghir Upwelling Region were predominantly influenced by the Cape Ghir upwelling filament. Furthermore, it is conceivable that the oscillating Cape Yubi filament influenced this area, since a regularly northwards expansion of the recent Cape Yubi filament was observed (Davenport et al., 2002).

The Cape Yubi Filament Region is characterized by highest abundance of *Nonionella iridea* at station GeoB 5540-2 (Fig. 2, Table 2). Gooday & Hughes (2002) associated *N. iridea* with seasonal primary productivity. *Cassidulina laevigata* is adapted to a wide productivity range. It occurs together with high productivity indicating species (either buliminids or uvigerinids) in the South Atlantic (Mackensen et al., 1995) and the Mediterranean Sea (de Rijk et al., 2000). However, *Cassidulina laevigata* was also found together with the seasonal primary productivity indicating species *Eponides pusillus* in the upwelling region off SW-Africa (Licari et al., 2003). In summary, we suggest that in the Cape Yubi Filament Region the benthic foraminiferal fauna reflects seasonal varying paleoproductivity. Noteworthy are the almost identical $\Delta\delta^{13}C$ values of both *H. elegans* and *M. pompiloides* in this region compared to their $\Delta\delta^{13}C$ values in the Cape Ghir Upwelling Region (Fig. 6).

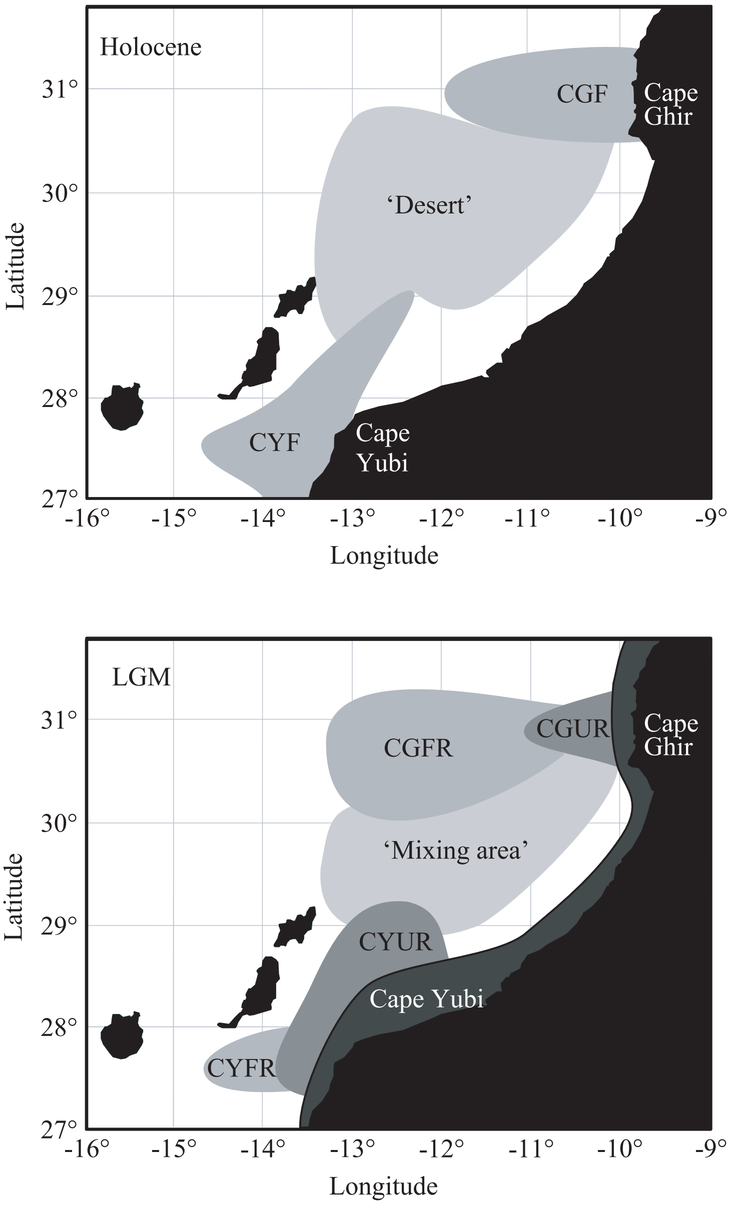

Fig. 7: Schematic presentation of the Holocene and LGM productivity patterns in the upwelling region off Morocco. Holocene productivity pattern is based on the study by Eberwein & Mackensen (2006). Abbreviations are as follows: CYUR = Cape Yubi Upwelling Region, CGUR = Cape Ghir Upwelling Region, CYFR = Cape Yubi Filament Region and CGFR = Cape Ghir Filament Region, 'Desert' indicates low productivity, and 'Mixing area' indicates the area influenced by both, upwelling cells and filaments during the LGM. The figure should give an overview rather than a true picture of the productivity patterns.

This indicates that, in fact the annual paleo-export flux was comparably high in both regions, even though the benthic foraminiferal assemblages seem to reflect different modes of productivity. In the Cape Yubi Filament Region seasonality was stronger pronounced than in the Cape Ghir Upwelling Region. The comparison of Holocene and LGM benthic foraminiferal assemblages reveals a productivity change from constant, high productivity in the Holocene (Eberwein and Mackensen, 2006) to seasonally varying paleoproductivity during the LGM. Obviously, the Cape Yubi Filament Region was regularly influenced by the oscillating Cape Yubi filament (Fig. 7).

Within the Cape Ghir Filament Region (Fig. 2) the highest abundance of 43 % of *E. exigua* and the lowest $\Delta\delta^{13}C$ values in *Hoeglundina elegans* and *Melonis pompiloides* were observed at station GeoB 4216-1 (Fig. 6, Tables 2, 3). In comparison, at the other two stations lower relative abundances of *E. exigua* (Table 2) and higher $\Delta\delta^{13}C$ values of *Hoeglundina elegans* and *Melonis pompiloides* were found (Fig. 6, Tables 2, 3). *Epistominella exigua* is considered to be a faithful proxy for seasonally varying productivity (Gooday, 1988; Gooday and Lambshead, 1989; Gooday, 1993; Smart et al., 1994; Mackensen et al., 1995; Thomas and Gooday, 1996; Smart and Gooday, 1997). Loubere (1999) linked this species to multiple pulsed phytodetritus flux events per year. Hence, this species is adapted to a wide range of organic matter fluxes up to 100 g C m^{-2} yr^{-1} (Gooday, 2003). We conclude that presumably, seasonality was strongest pronounced at station 4216-1 and less strong at stations GeoB 4215-2 and GeoB 4217-5. The comparison of Holocene low productivity indicating benthic foraminiferal assemblages at these stations (Eberwein and Mackensen, 2006) with the seasonally varying productivity reflecting *E. exigua* Assemblage indicates that paleoproductivity was enhanced during the LGM (Figs. 1, 7). Our results are supported by Henderiks et al. (2002), who reported five times enhanced total organic carbon accumulation during the LGM. Furthermore, geochemical as well as geophysical parameters also indicate higher paleoproductivity. Freudenthal et al. (2002) interpreted the enhanced glacial productivity as a result of the far-westwards reaching Cape Ghir filament, which was coupled to variations in trade wind intensity. Therefore, we conclude that the Cape Ghir Filament Region was highly dependend on the strongly oscillating Cape Ghir filament during the LGM. We suggest that the Cape Ghir filament extended much further westwards than presently (Fig. 7).

Finally, we summarize that paleoproductivity patterns between 31°N and 27.5°N were rather complex with a strong regional heterogeneity during the LGM. Our results indicate the importance of spatially highly resolved studies for reliable reconstructions of paleoproductivity.

6. Conclusion

Benthic foraminiferal faunas and the stable carbon isotopic composition of *Cibicidoides wuellerstorfi*, *Hoeglundina elegans* and *Melonis pompiloides* were used to reconstruct paleoproductivity during the LGM between Cape Ghir and Cape Yubi off Morocco. The interpretation of these proxies revealed four different paleoproductivity regimes.

- In the Cape Yubi Upwelling Region off Cape Yubi (27.5°N) the upwelling cell was characterized by highest paleoproductivity. The northern boundary of this cell was located at approximately 29°N hence, 2° latitude further north than present.
- The Cape Ghir Upwelling Region off Cape Ghir (31°N) was characterized by high paleoproductivity. Within this region the area between 29°N and 31°N could be assumed to be the ‘mixing area’, which was characterized by higher paleoproductivity than present. Obviously, the ‘mixing area’ was influenced by both, the Cape Ghir filament and the Cape Yubi upwelling cell.
- The Cape Yubi Filament Region was located southwest off Cape Yubi (27.5°N), and was characterized by moderate, seasonally varying paleoproductivity as a result of the oscillating Cape Yubi filament.
- The Cape Ghir Filament Region was located further offshore Cape Ghir (31°N) and was characterized by highest seasonally varying paleoproductivity. Presumably, this region was under the influence of the strongly oscillating and far reaching ‘giant’ Cape Ghir filament.

Furthermore, two main water masses could be distinguished. The glacial Mediterranean Outflow Water occured with a mean $\delta^{13}C$ of 1.16 ± 0.17 ‰ and a mean $\delta^{18}O$ of equilibrium calcite of 4.42 ± 0.49 ‰ above approximately 1900 m. The glacial North Atlantic Deep Water with a mean $\delta^{13}C$ of 0.44 ± 0.10 ‰ and a mean $\delta^{18}O$ of 5.10 ± 0.11 ‰ was predominant below this depth.

Acknowledgements

We thank crews and scientific participants of *Meteor* cruises M 37/1, M42/4b and M45/4 for assistance during sampling, B. Hollmann and G. Meyer for running the mass spectrometer at the Alfred Wegener Institute, Bremerhaven. We thank S. Brückner, H. Meggers and S. Schumacher for discussion. This work was funded by the Deutsche Forschungsgemeinschaft as part of the DFG-Research Center ‚Ocean Margins’ at Bremen University.

3. CONCLUSIONS AND FUTURE PERSPECTIVES

In the following, the key results of this PhD thesis entitled 'Holocene and Last Glacial Maximum (paleo-) productivity off Morocco: evidence from benthic foraminifera and stable carbon isotopes' are presented. The main results of each of the three manuscripts dealing with different issues are summarised. Concluding a brief outlook of existing problems, which remain open for future work is given.

3.1 Modern benthic foraminifera and their stable carbon isotopic composition reflect primary productivity

The investigation and interpretation of modern (live and dead) benthic foraminifera give evidence that their faunal composition, distribution and standing stocks were mainly dependent on chlorophyll-α concentrations in surface waters, and hence, primary productivity. The results revealed that the identical live and dead assemblages, high standing stocks as well as the significant ^{13}C depletion in species reflect constant, high productivity off Cape Ghir and Cape Yubi. Highest primary productivity is indicated by *Bulimina marginata*, which dominates closest to the coast off Cape Ghir. Generally, the faunal succession of the *Bulimina aculeata* / *Uvigerina mediterranea* assemblage, the *Sphaeroidina bulloides* / *Gavelinopsis translucens* assemblage, and the *Hoeglundina elegans* assemblage mirror the decreasing productivity gradient from the coast to the deep-sea off both capes. In these regions, the mean $\delta^{13}C$ of live and dead specimens are comparable and significantly lower in tests of *Bulimina mexicana*, *Cibicidoides kullenbergi*, *H. elegans, U. mediterranea* and *Uvigerina peregrina* than $\delta^{13}C$ values of these species in the area between the capes. High abundances of dead *C. kullenbergi, Cibicidoides wuellerstorfi,* and *H. elegans* off the capes indicate that carbonate dissolution is of minor importance.

In the area between the capes, different live and dead assemblages, low standing stocks and lower mean $\delta^{13}C$ indicate low primary productivity. High numbers of *Epistominella exigua, Eponides pusillus*, and *Globocassidulina subglobosa* in the dead fauna indicate slightly seasonally varying primary productivity. Most likely, this seasonal signal in productivity caused the differences in live and dead assemblages. *Cibicidoides kullenbergi* is adapted to different productivity conditions, since it shows considerably high standing stocks in the entire study area. *Trifarina bradyi* occurs at stations that are mainly bathed by saline Mediterranean Outflow Water. *Cibicidoides wuellerstorfi* is a faithful recorder of bottom water $\delta^{13}C$ in the Canary Islands regions.

3.2 Dependance of benthic foraminiferal microhabitats on organic matter fluxes

The impact of organic matter fluxes in interaction with the bottom water oxygen concentrations on the vertical zonation of live benthic foraminifera within the sediment was investigated at stations underneath the high productive Cape Ghir and Cape Yubi filaments. The amount of organic matter reaching the sea-floor is an important parameter in controlling the benthic foraminiferal densities.

Particularly stations, which are approximately located beneath the root of either the Cape Ghir or Cape Yubi filament are characterised by high standing stocks. The marginal dominance of the deep infaunal living species *Globobulimina affinis* off Cape Ghir and strong dominance off Cape Yubi explains the diverging behaviour of the average living depth (ALD) of the total live fauna, which becomes shallower with increasing export flux off Cape Ghir. A striking observation is the strong shallowing of the ALD of *G. affinis* with increasing organic matter fluxes, which results in a convergence with the ALD of shallow infaunal living species. Finally, almost identical ALD of all species were observed at the station with highest organic matter fluxes. Presumably, this indicates the compression of the redox zones in the sediment on both transects as a result of the oxygen consumption by organic matter degradation. Obviously, our data support the observation that the ALD of *G. affinis* approximately indicates the zero oxygen boundary. *Globobulimina affinis* occurs with highest standing stocks in a strict interval of organic matter fluxes between 9 and 15 g C m^{-2} yr^{-1} and bottom water oxygen concentrations lower than 5 ml/l. Highest standing stocks were recorded mainly off Cape Yubi, indicating that sufficient amounts of organic matter are incorporated into deeper sediment layers. By contrast, the quantity of organic matter left to be incorporated into the sediment is below *G. affinis* optimum conditions off Cape Ghir. Here, *G. affinis* is out-competed by the more opportunistic *Bulimina marginata* and *Bulimina aculeata*. We showed that particularly *G. affinis* is sensitive regarding biogeochemical processes within the sediment, which are controlled by organic matter fluxes and bottom water oxygen concentrations.

3.3 Reconstruction of paleoproductivity and water masses during the LGM

Last Glacial Maximum paleoproductivity and water mass stratification was reconstructed from sixteen sediment cores between Cape Ghir (31°N) and Cape Yubi (27.5°N) in the upwelling region off Morocco. An essential conclusion is that paleoproductivity conditions were rather complex with a strong regional heterogeneity. Based on $\delta^{13}C$ of *Cibicidoides wuellerstorfi* and equilibrium adjusted $\delta^{18}O$ of several species the reconstruction of LGM water masses showed that glacial Mediterranean Outflow Water (MOW) occured above approximately 1900 m depth and glacial North Atlantic Deep Water (NADW) below this depth. The investigations revealed that generally, paleoproductivity in the area between the capes was higher than in the Holocene, whereas it was comparably high off Capes Ghir and Yubi. The Cape Ghir filament extended much further south- and westwards than today. The benthic foraminiferal faunas and the stable carbon isotopic composition of *Hoeglundina elegans* and *Melonis pompiloides* reflect four different productivity regions. Highest paleoproductivity was identified off Cape Yubi. Moderate to high, seasonally varying paleoproductivity was predominant off Cape Ghir. Moderate, highly seasonally varying paleoproductivity occured in the area southwest off Cape Yubi. Highest seasonally varying paleoproductivity was determined in the region further offshore Cape Ghir.

3.4 Future perspectives

The investigations of live and dead benthic foraminifera, their distribution and densities as well as the stable carbon isotopic composition of distinct species in the variable upwelling region off Morocco revealed that benthic foraminifera are mainly influenced by primary productivity. The results of this study improved our understanding to what extent benthic foraminifera depend on productivity variations within a geographically restricted area. Consequently, this knowledge was the basis in using benthic foraminifera as a trustworthy proxy for reconstructing paleoproductivity during the Last Glacial Maximum within the same region. Paleoproductivity variations are of major interest concerning the global carbon cycle, and in this context benthic foraminifera can be used to gain a better understanding of earth's climate. However, in the future, longer-term activities and research should focus on the following aspects:

- Biogeochemical parameters (e.g. bacterial stock, element and isotopic composition of the pore water) should be measured at the same samples as the benthic foraminiferal samples are taken, to determine as accurately as possible the dependance of live benthic foraminifera on the processes in the porewater and sediment.
- To minimize or eliminate size dependent fractionation of ^{13}C, investigations should be accomplished within a very narrow and standardised size range.
- To detect seasonal variations in benthic foraminiferal communities and stable carbon isotopic composition, sampling should be accomplished several times a year, depending on the productivity signal. Furthermore, the particle flux through the water column should be determined to correlate it with benthic foraminiferal species and standing stocks.

4. REFERENCES

Abrantes, F., 2000. 200000 yr diatom records from Atlantic upwelling sites reveal maximum productivity during LGM and a shift in phytoplankton community structure at 185000 yr. Earth and Planetary Science Letters 176, 7-16.

Abrantes, F., Meggers, H., Nave, S., Bollmann, J., Palme, S., Sprengel, C., Henderiks, J., Spies, A., Salgueiro, E., Moita, T., Neuer, S., 2002. Fluxes of micro-organisms along a productivity gradient in the Canary Islands region (29 °N): implications for paleoreconstructions. Deep-Sea Research II 49, 3599-3629.

Altenbach, A.V., 1988. Deep-sea benthic foraminifera and flux rate of organic carbon. Revue de Paléobiologie 2, 719-720.

Altenbach, A.V., Sarnthein, M., 1989. Productivity record in benthic foraminifera. In: Berger, W.H., Smetacek, V.S., Wefer, G. (Eds.), Productivity of the ocean: present and past. Wiley, Chichester, 255-269.

Alve, E., Bernhard, J.M., 1995. Vertical migratory response of benthic foraminifera to controlled oxygen concentrations in an experimental mesocosm. Marine Ecology Progress Series 116, 137-151.

Antoine, D., Morel, A., 1996. Oceanic primary productivity production 1. adaptation of a spectral light-photosynthesis model in view of application to satellite chlorophyll observations. Global Biogeochemical Cycles 10 (1), 43-55.

Arístegui, J., Barton, E.D., Tett, P., Montero, M.F., García-Muñoz, M., Basterretxea, G., Cussatlegras, A.-S., Ojeda, A., de Armas, D., 2004. Variability in plankton community structure, metabolism, and vertical carbon fluxes along an upwelling filament (Cape Juby, NW Africa). Progress in Oceanography 62, 95-113.

Barker, R.W., 1960. Taxonomic notes on the species figures by H.B. Brady in his report on the forminifera dredged by H.M.S. *Challenger* during the years 1873-1876, Special publication No. 9, Tulsa, Oklahoma, 238 pp.

Barnola, J.-M., Raynaud, D., Neftel, Y.S., Korotchvich, Y.S., Lorius, C., 1987. Vostok ice core provides 160,000 years record of atmospheric CO_2. Nature 329, 408-414.

Belanger, P.E., Curry, W.B., Matthews, R.K., 1981. Core-top evaluation of benthic foraminiferal isotopic ratios for paleo-oceanographic interpretations. Palaeogeography, Palaeoclimatology, Palaeoecology 33, 205-220.

Bemis, B.E., Spero, H.J., Bijma, J., Lea, D.W., 1998. Reevaluation of the oxygen isotopic composition of planktic foraminifera: experimental results and revised paleotemperature equations. Paleoceanography 13, 150-160.

Berger, W.H., Smetacek, V.S., Wefer, G., 1989. Ocean productivity and paleoproductivity - An Overview. In: Berger, W.H., Smetacek, V.S., Wefer, G. (Eds.), Productivity of the ocean: Present and past. S. Bernhard, Dahlem Konferenzen, John Wiley & Sons Limited, 1-34.

Berger, W.H., Wefer, G., 1990. Export productivity: seasonality and intermittency, and paleoceanographic implications. Palaeogeography, Palaeoclimatology, Palaeoecology 9, 245-254.

Berger, W.H., Herguera, J.C., 1992. Reading the sedimentary record of the ocean‘s productivity. In: Falkowski, P.G., Woodhead, A.D. (Eds.), Primary productivity and biogeochemical cycles in the sea, New York, 455-486.

Bernhard, J.M., 1988. Postmortem vital staining in benthic foraminifera: duration and importance in population and distributional studies. Journal of Foraminiferal Research 18 (2), 143-146.

Bernhard, J.M., 1992. Benthic foraminiferal distribution and biomass related to porewater oxygen content: central California continental slope and rise. Deep-Sea Research 39 (3/4), 585-605.

Bernhard, J.M., Bowser, S.S., 1992. Bacterial biofilms as a trophic resource for certain benthic foraminifera. Marine Ecology Progress Series 83, 263-272.

Bernhard, J.M., 1993. Experimental and field evidence of Antarctic foraminiferal tolerance to anoxia and hydrogen sulfide. Marine Micropaleontology 20, 203-213.

Bernhard, J.M., 1996. Microaerophilic and facultative anaerobic benthic foraminifera: a review of experimental and ultrastructural evidence. Revue de Paléobiologie 15 (1), 261-275.

Bertrand, P., Shimmield, G.B., Martinez, P., Grousset, F., Jorissen, F.J., Paterne, M., Pujol, C., Bouloubassi, I., Buat Menard, P., Peypouquet, J.-P., Beaufort, L., Sicre, M.-A., Lallier-Verges, E., Foster, J.M., Ternois, Y., and other participants of the Sedorqua program, 1996. The glacial ocean productivity hypothesis: the importance of regional temporal and spatial studies. Marine Geology 130, 1-9.

Bertrand, P., Pedersen, T.F., Martinez, P., Calvert, S., Shimmield, G., 2000. Sea level impact on nutrient cycling in coastal upwelling areas during deglaciation: evidence from nitrogen isotopes. Global Biogeochemical Cycles 14 (1), 341-355.

Bickert, T., Wefer, G., 1996. Late Quaternary deep water circulation in the South Atlantic: reconstruction from carbonate dissolution and benthic stable isotopes. In: Wefer, G., Berger, W.H., Siedler, G., Webb, D. (Eds.), The South Atlantic: present and past circulation. Springer-Verlag, Berlin, Heidelberg, 599-620.

Bickert, T., Wefer, G., 1999. South Atlantic and benthic foraminifer $\delta^{13}C$ deviations: implications for reconstructing the Late Quaternary deep-water circulation. Deep-Sea Research II 46, 437-452.

Bickert, T., Mackensen, A., 2004. Last glacial Holocene changes in South Atlantic deep water circulation. In: Wefer, G., Mulitza, S., Ratmeyer, V. (Eds.), The South Atlantic in the Late Quaternary: Reconstruction of material budgets and current systems. Springer-Verlag, Berlin Heidelberg New York Tokyo, pp. 671-695.

Boyle, E.A., 1992. Cadmium and $\delta^{13}C$ paleochemical ocean distributions during the stage 2 glacial maximum. Annual Review of Earth and Planetary Sciences 20, 245-287.

Brady, H.B., 1879. Notes on some of the reticularian Rhizopoda of the *Challenger* expedition. Part I, Quart. J. Microsc. Sci. 19, 20-63.

Brady, H.B., 1881. Notes on some of the reticularian Rhizopoda of the *Challenger* expedition. Part III, Quart. J. Microsc. Sci. 21, 31-71.

Brady, H.B., 1884. Report on the foraminifera dredged by H.M.S. *Challenger*, during the years 1873-1876, IX. Rep. Sci. Results Explor. Voyage H.M.S. *Challenger* Zoology, Edinburgh, 1-814 pp.

Broecker, W.S., 1982. Ocean chemistry during glacial times. Geochimica et Cosmochimica Acta 46, 1689-1705.

Broecker, W.S., Henderson, G.M., 1998. The sequence events surrounding Termination II and their implications for the cause of glacial-interglacial CO_2 changes. Paleoceanography 13 (4), 252-364.

Caralp, M.-C., 1989a. Abundance of *Bulimina exilis* and *Melonis barleeanum*: Relationship to the quality of marine organic matter. Geo-Marine Letters 9, 37-43.

Caralp, M.H., 1989b. Size and morphology of the benthic foraminifer *Melonis barleeanum*: relationships with marine organic matter. Journal of Foraminiferal Research 19 (3), 235-245.

Carr, M.-E., 2002. Estimation of potential productivity in Eastern Boundary Currents using remote sensing. Deep-Sea Research II 49, 59-80.

Corliss, B.H., Honjo, S., 1981. Dissolution of deep-sea benthonic foraminifera. Micropaleontology 27 (4), 356-378.

Corliss, B.H., 1985. Microhabitats of benthic foraminifera within deep-sea sediments. Nature 314, 435-438.

Corliss, B.H., Emerson, S., 1990. Distribution of Rose Bengal stained deep-sea benthic foraminifera from the Nova Scotian continental margin and Gulf of Maine. Deep-Sea Research I 37 (3), 381-400.

Corliss, B.H., Sun, X., Brown, C.W., Showers, W., 2006. Influence of seasonal primary productivity on $\delta^{13}C$ of North Atlantic deep-sea benthic foraminifera. Deep-Sea Research I 53 (4), 740-746.

Curry, W.B., Duplessy, J.-C., Labeyrie, L., Shackleton, N.J., 1988. Changes in the distribution of $\delta^{13}C$ of deep water CO_2 between the last glaciation and the Holocene. Palaeogeography, Palaeoclimatology, Palaeoecology, 317-341.

Curry, W.B., Oppo, D.W., 2005. Glacial water mass geometry and the distribution of $\delta^{13}C$ of ΣCO_2 in the western Atlantic Ocean. Paleoceanography 20, doi:10.1029/2004PA001021.

Cushman, J.A., 1918-1931. The Foraminifera of the Atlantic Ocean. U.S. National Museum Bulletin, 104pp.

Cushman, J.A., 1948. Arctic foraminifera. Cushman Lab. Foram. Res., spec. publ. 23, 1-80.

d'Orbigny, A., 1826. Tableau methodique de la classe des Cephalopodes. Annales des Sciences Naturelles ser 1, 245-314.

Davenport, B., Neuer, S., Helmke, P., Perez-Marrero, J., Llinas, O., 2002. Primary productivity in the northern Canary Islands region as inferred from SeaWiFS imagery. Deep-Sea Research II 49, 3481-3496.

de Rijk, S., Jorissen, F.J., Rohling, E., Troelstra, S.R., 2000. Organic flux control on bathymetric zonation of Mediterranean benthic foraminifera. Marine Micropaleontology 40, 151-166.

de Stigter, H.C., Jorissen, F.J., van der Zwaan, G.J., 1998. Bathymetric distribution and microhabitat partitioning of live (Rose Bengal stained) benthic foraminifera along a shelf to bathyal transect in the southern Adriatic Sea. Journal of Foraminiferal Research 28 (1), 40-65.

Douglas, R.G., Liestman, J., Walch, C., Blake, G., Cotton, M.L., 1980. The transition from live to sediment assemblage in benthic foraminifera from the southern California borderland. In: Field, M.E., Bouma, A.H., Colburn, I.P., Douglas, R.G., Ingle, J.C. (Eds.), Quaternary Depositional Environments from the Pacific coast. Pacific coast Paleoceanogr. Symp. 4 Pac. Sect. SEPM, Los Angelos, 257-280.

Duijnstee, I.A.P., Ernst, S.R., van der Zwaan, G.J., 2003. Effect of anoxia on the vertical migration of benthic foraminifera. Marine Ecology Progress Series 246, 85-94.

Duplessy, J.-C., Shackleton, N.J., Matthews, R.K., Prell, W.L., Ruddiman, W.F., Caralp, M.-C., Hendy, C.H., 1984. 13C record of benthic foraminifera in the Last Interglacial Ocean: implications for the carbon cycle and the global deep water circulation. Quaternary Research 21, 225-243.

Duplessy, J.-C., Shackleton, N.J., Fairbanks, R.G., Labeyrie, L., Oppo, D.W., Kallel, N., 1988. Deepwater source variations during the last climatic cycle and their impact on the global deepwater circulation. Paleoceanography 3 (3), 343-360.

Eberwein, A., Mackensen, A., 2006. Live and dead benthic foraminifera and test $\delta^{13}C$ record primary productivity off Morocco (NW-Africa). Deep-Sea Research I, 53 (8), 1379-1405.

Eberwein, A., Mackensen, A., Davenport, B., subm. The influence of organic matter fluxes on the microhabitat distribution of live benthic foraminifera off Cape Ghir and Cape Yubi (NW-Africa). Journal of Foraminiferal Research.

Eichwald, C.E., 1830. Zoologia specialis, pars altera. Volume 2: Vilnea, D.E. Eichwaldus, 1-323 pp.

Ellis, B.F., Messina, A., 1940. Catalogue of Foraminifera, and supplements. American Museum of Natural History, New York, 74360 pp.

Ernst, S., Duijnstee, I., van der Zwaan, B., 2002. The dynamics of the benthic foraminiferal microhabitat: recovery after experimental disturbance. Marine Micropaleontology 46, 343-361.

Ernst, S., van der Zwaan, G.J., 2004. Effects of experimentally induced raised levels of organic flux and oxygen depletion on a continental slope benthic foraminiferal community. Deep-Sea Research I 51, 1709-1739.

Fairbanks, R.G., 1989. A 17,000 year glacio-eustatic sea level record: influence of glacial melting rate on the Younger Dryas event and deep-ocean circulation. Nature 342, 637-642.

Fariduddin, M., Loubere, P., 1997. The surface ocean productivity response of deeper water benthic foraminifera in the Atlantic Ocean. Marine Micropaleontology 32, 289-310.

Fatela, F., Taborda, R., 2002. Confidence limits of species proportions in microfossil assemblages. Marine Micropaleontology 45, 169-174.

Fontanier, C., Jorissen, F.J., Licari, L., Alexandre, A., Anschutz, P., Carbonel, P., 2002. Live benthic foraminiferal faunas from the Bay of Biscay: faunal density, composition and microhabitats. Deep-Sea Research I 49, 751-785.

Fontanier, C., Jorissen, F.J., Chaillou, G., David, C., Anschutz, P., Lafon, V., 2003. Seasonal and interannual variability of benthic foraminiferal faunas at 550 m depth in the Bay of Biscay. Deep-Sea Research II 50, 457-494.

Fontanier, C., Jorissen, F.J., Chaillou, G., Anschutz, P., Gremare, A., Griveaud, C., 2005. Live foraminiferal faunas from a 2800 m deep lower canyon station from the Bay of Biscay: faunal response to focusing of refractory organic matter. Deep-Sea Research I 52, 1189-1227.

Fontanier, C., Mackensen, A., Jorissen, F.J., Anschutz, P., Licari, L., Griveaud, C., 2006. Seasonal and trophic impacts on stable oxygen and carbon isotopes in live benthic foraminifera from the Bay of Biscay. Marine Micropaleontology 58, 159-183.

Freudenthal, T., Meggers, H., Henderiks, J., Kuhlmann, H., Moreno, A., Wefer, G., 2002. Upwelling intensity and filament activity off Morocco during the last 250000 years. Deep-Sea Research II 49, 3655-3674.

Friedman, I., O‘Neil, J.R., 1977. Compilation of stable isotope fractionations factors of geochemical interest. In: Fleischer, M. (Ed.), Data of geochemistry. U.S: Government Printing Office, Washington, DC, 1-12.

Geslin, E., Heinz, P., Jorissen, F.J., Hemleben, C., 2004. Migratory responses of deep-sea benthic foraminifera to variable oxygen conditions: laboratory investigations. Marine Micropaleontology 53, 227-243.

Goldstein, S.T., Corliss, B.H., 1994. Deposit feeding in selected deep-sea and shallow-water benthic foraminifera. Deep-Sea Research I 41 (2), 229-241.

Gooday, A.J., 1986. Meiofaunal foraminiferans from the bathyal Porcupine Seabight (north-east Atlantic): size structure, standing stock, taxonomic composition, species diversity and vertical distribution in the sediment. Deep-Sea Research 33 (10), 1345-1373.

Gooday, A.J., 1988. A response by benthic foraminifera to the deposition of phytodetritus in the deep sea. Nature 332, 70-73.

Gooday, A.J., Lambshead, P.J.D., 1989. Influence of seasonally deposited phytodetritus on benthic foraminiferal populations in the bathyal northeast Atlantic: the species response. Marine Ecology Progress Series 5, 53-67.

Gooday, A.J., Levin, L.A., Linke, P., Heeger, T., 1992. The role of benthic foraminifera in deep-sea food webs and carbon cycling. In: Rowe, G.T., Pariente, V. (Eds.), Deep-sea food chains and the global carbon cycle. Kluwer Academic Publishers, 63-91.

Gooday, A.J., 1993. Deep-sea benthic foraminiferal species which exploit phytodetritus: characteristic features and controls on distribution. Marine Micropaleontology 22, 187-205.

Gooday, A.J., 1994. The biology of deep-sea foraminifera: a review of some advances and their applications in paleoceanography. Advances in Deepsea Paleoecology, 14-31.

Gooday, A.J., 1996. Epifaunal and shallow infaunal foraminiferal communities at three abyssal NE Atlantic sites subject to differing phytodetritus input regimes. Deep-Sea Research 43 (9), 1395-1421.

Gooday, A.J., 2001. Benthic foraminifera. In: Steele, J., Thorpe, S., Turekian, K. (Eds.), Encyclopedia of Ocean Science, San Diego, 274-286.

Gooday, A.J., Hughes, J.A., 2002. Foraminifera associated with phytodetritus deposits at a bathyal site in the northern Rockall Trough (NE Atlantic): seasonal contrasts and a comparison of stained and dead assemblages. Marine Micropaleontology 46, 83-110.

Gooday, A.J., 2003. Benthic Foraminifera (Protista) as Tools in Deep-water Palaeoceanography: Environmental Influences on Faunal Characteristics. Advances in Marine Biology 46, 1-90.

Graham, D.W., Corliss, B.H., Bender, M.L., Keigwin Jr., L.D., 1981. Carbon and oxygen isotopic disequilibria of recent deep-sea benthic foraminifera. Marine Micropaleontology 6, 483-497.

Haake, F.-W., 1980. Benthische Foraminiferen in Oberflächen-Sedimenten und Kernen des Ostatlantiks vor Senegal/Gambia (Westafrika). Meteor Forschungsergebnisse Reihe C, (32), 1-29.

Hagen, E., Zülicke, C., Feistel, R., 1996. Near-surface structures in the Cape Ghir filament off Morocco. Oceanologica Acta 19 (6), 577-598.

Hagen, E., 2001. Northwest African upwelling scenario. Oceanologica Acta 24, 113-128.

Heinz, P., Hemleben, C., Kitazato, H., 2002. Time-response of cultured deep-sea benthic foraminifera to different algal diets. Deep-Sea Research I 49, 517-537.

Henderiks, J., Freudenthal, T., Meggers, H., Nave, S., Abrantes, F., Bollmann, J., Thierstein, H., 2002. Glacial-interglacial variability of particle accumulation in the Canary Basin: a time-slice approach. Deep-Sea Research II 49, 3675-3705.

Henderiks, J., Bollmann, J., 2004. The *Gephyrocapsa* sea surface palaeothermometer put to the test: comparison with alkenone and foraminifera proxies off NW Africa. Marine Micropaleontology 50, 161-184.

Herguera, J.C., Berger, W.H., 1991. Paleoproductivity from benthic foraminifera abundance: glacial to postglacial change in the west-equatorial Pacific. Geology 19, 1173-1176.

Herguera, J.C., 1992. Deep-sea benthic foraminifera and biogenic opal: glacial to postglacial productivity changes in the western equatorial Pacific. Marine Micropaleontology 19, 79-98.

Hermelin, J.O.R., Shimmield, G.B., 1990. The importance of the oxygen minimum zone and sediment geochemistry in the distribution of recent benthic foraminifera in the Northwest Indian Ocean. Marine Geology 91, 1-29.

Hernández-Guerra, A., Nykjaer, L., 1997. Sea surface temperature variability off Northwest Africa: 1981-1989. International Journal of Remote Sensing 18 (12), 2539-2558.

Hernández-Guerra, A., Fraile-Nuez, E., Borges, R., López Laatzen, F., Vélez-Belchí, P., Parrilla, G., Müller, T.J., 2003. Transport variability in the Lanzarote passage (eastern boundary current of the North Atlantic subtropical gyre). Deep-Sea Research I 50, 189-200.

Heron-Allen, E., Earland, A., 1922. Protozoa, Part II Foraminifera. British Antarctic („Terra Nova“) Expedition, 1910. Natural History Reports, Zoology 6, 25-268.

Hill, M.O., Gauch, H.G., 1980. Detrended correspondence analysis, an improved ordination technique. Vegetatio 42, 47-58.

Hill, T.M., Kennett, J.P., Spero, H.J., 2003. Foraminifera as indicators of methane-rich environments: a study of modern methane seeps in Santa Barbara Channel, California. Marine Micropaleontology 49, 123-138.

Hoeglund, 1947. Foraminifera in the Gullmar Fjord and the Skagerrak. Zoologiska bidrag fran Uppsala 26, 1-328.

Hogg, J., 1860. On the distinctions of a plant and an animal and on a fourth Kingdom of nature. Edinburg Natural Philosophy Journal (New Series) 12, 216-225.

Holsten, J., Stott, L., Berelson, W., 2004. Reconstructing benthic carbon oxidation rates using $\delta^{13}C$ of benthic foraminifers. Marine Micropaleontology 53, 117-132.

Holz, C., Stuut, J.-B.W., Henrich, R., 2004. Terrigenous sedimentation processes along the continental margin off NW Africa: implications from grain-size analysis of seabed sediments. Sedimentology 51, 1145-1154.

Hooghiemstra, H., Bechler, A., Beug, H.J., 1987. Isopollen maps for 18,000 years B.P. of the Atlantic offshore of northwest Africa: evidence for paleowind circulation. Paleoceanography 2 (6), 561-582.

Hooghiemstra, H., 1989. Variations of the NW African trade wind regime during the last 140000 years: changes in pollen flux evidenced by marine sediment records. In: Leinen, M., Sarnthein, M. (Eds.), Paleoclimatology and Paleometerology: modern and past patterns of global atmospheric transport. Kluwer Academic Publishers, 733-770.

Jannink, N.T., Zachariasse, W.J., van der Zwaan, G.J., 1998. Living (Rose Bengal stained) benthic foraminifera from the Pakistan continental margin (northern Arabian Sea). Deep-Sea Research I 45, 1483-1513.

Jones, R.W., 1994. The *Challenge*r foraminifera. Oxford University Press, New York, 150 pp.

Jorissen, F.J., Barmawidjaja, D.M., Puskaric, S., van der Zwaan, G.J., 1992. Vertical distribution of benthic foraminifera in the northern Adriatic Sea: the relation with the organic flux. Marine Micropaleontology 19, 131-146.

Jorissen, F.J., de Stitger, H.C., Widmark, J.G.V., 1995. A conceptual model explaining benthic foraminiferal microhabitats. Marine Micropaleontology 26, 3-15.

Jorissen, F.J., Wittling, I., Peypouquet, J.-P., Rabouille, C., Relexans, J.C., 1998. Live benthic foraminiferal faunas off Cape Blanc, NW-Africa: community structure and microhabitats. Deep-Sea Research I 45, 2157-2188.

Jorissen, F.J., Wittling, I., 1999. Ecological evidence from live-dead comparisons of benthic foraminiferal faunas off Cape Blanc (Northwest Africa). Palaeogeography, Paleoclimatology, Paleoecology 149, 151-170.

Kaiho, K., 1994. Benthic foraminiferal dissolved-oxygen index and dissolved-oxygen levels in the modern ocean. Geology 22, 719-722.

Kaiho, K., 1999. Effect of organic carbon flux and dissolved oxygen on the benthic foraminiferal oxygen index (BFOI). Marine Micropaleontology 37, 67-76.

Kennett, J.P., Cannariato, K.G., Hendy, C.H., Behl, R.J., 2003. Methane hydrates in quaternary climate change: the clathrate gun hypothesis. American Geophysical Union, Washington, DC, 216 pp.

Kitazato, H., 1994. Foraminiferal microhabitats in four marine environments around Japan. Marine Micropaleontology 24, 29-41.

Knoll, M., Hernández-Guerra, A., Lenz, B., López Laatzen, F., Machin, F., Müller, T.J., Siedler, G., 2002. The eastern boundary current system between the Canary Islands and the African coast. Deep-Sea Research II 49, 3427-3440.

Kuhlmann, H., Freudenthal, T., Helmke, P., Meggers, H., 2004. Reconstruction of paleoceanography off NW Africa during the last 40,000 years: influence of local and regional factors on sediment accumulation. Marine Geology 207, 209-224.

Langezaal, S., 2003. The foraminiferal - bacterial connection: an interdisciplinary study of meiofaunal behaviour in the deeper marine redox zone. PhD Thesis, Universiteit Utrecht, Utrecht, 239 pp.

Lee, J.J., 1980. Nutrition and physiology of the foraminifera. In: Levandowsky, M. (Ed.), Biochemistry and Physiology of Protozoa. Academic Press, New York, 43-66.

Licari, L., Mackensen, A., 2005. Benthic foraminifera between 1°N and 32°S off West Africa: Do live assemblages from the topmost sediment reliably record environmental variability? Marine Micropaleontology 55 (3-4), 205-233.

Licari, L.N., Schumacher, S., Wenzhöfer, F., Zabel, M., Mackensen, A., 2003. Communities and microhabitats of living benthic foraminifera from the tropical East Atlantic: impact of different productivity regimes. Journal of Foraminiferal Research 33 (1), 10-31.

Linke, P., Lutze, G.F., 1993. Microhabitat preferences of benthic foraminifera - a static concept or a dynamic adaptation to optimize food aquisition? Marine Micropaleontology 20, 215-234.

Lipps, J.H., 1983. Biotic interactions in benthic foraminifera. In: Tevez, M.J.J., McCall (Eds.), Biotic interactions in recent and fossil communities. Plenum, New York, 331-376.

Llinás, O., Rueda, M.J., Marrero, J.P., Pérez-Martell, E., Santana, R., Villagarcía, M.G., Cianca, A., Maroto, L., 2002. Variability of the Antarctic intermediate waters in the northern Canary box. Deep-Sea Research II 49, 3441-3453.

Loeblich, A.R.J., Tappan, H., 1988. Foraminiferal genera and their classification. Van Norstrand Reinhold Company, New York, 869 pp.

Loubere, P., 1987. Late Pliocene variations in the carbon isotope values of North Atlantic benthic foraminifera: biotic control of the isotopic record? Marine Geology 76, 45-56.

Loubere, P., 1991. Deep-sea benthic foraminiferal assemblage response to a surface ocean productivity gradient: a test. Paleoceanography 6 (2), 193-204.

Loubere, P., Gary, A., Lagoe, M., 1993. Generation of the benthic foraminiferal assemblage: theory and preliminary data. Marine Micropaleontology 20, 165-181.

Loubere, P., 1994. Quantitative estimation of surface ocean productivity and bottom water oxygen concentration using benthic foraminifera. Paleoceanography 9, 723-737.

Loubere, P., Meyers, P., Gary, A., 1995. Benthic foraminiferal microhabitat selection, carbon isotope values, and association with larger animals: a test with *Uvigerina peregrina*. Journal of Foraminiferal Research 25 (1), 83-95.

Loubere, P., 1997. Benthic foraminiferal assemblage formation, organic carbon flux and oxygen concentrations on the outer continental shelf and slope. Journal of Foraminiferal Research 27 (2), 93-100.

Loubere, P., 1998. The impact of seasonality on the benthos as reflected in the assemblages of deep-sea foraminifera. Deep-Sea Research I 45, 409-432.

Loubere, P., 1999. A multiproxy reconstruction of biological productivity and oceanography in the eastern equatorial Pacific for the past 30,000 years. Marine Micropaleontology 37, 173-198.

Loubere, P., Fariduddin, M., 1999. Quantitative estimation of global patterns of surface ocean biological productivity and its seasonal variation on timescales from centuries to millennia. Global Biogeochemical Cycles 13 (1), 115-133.

Lutze, G.F., 1980. Depth distribution of benthic foraminifera on the continental margin off NW Africa. *Meteor* Forschungsergebnisse 32 (C), 31-80.

Lutze, G.F., Coulbourn, W.T., 1984. Recent benthic foraminifera from the continental margin off Northwest Africa: community structure and distribution. Marine Micropaleontology 8, 361-401.

Lutze, G.F., 1986. *Uvigerina* species of the Eastern North Atlantic. In: van der Zwaan, B., Jorissen, F.J., Verhallen, P.J.J.M., Daniels, C.H.v. (Eds.), Atlantic European Oligocene to recent Uvigerina, Utrecht, 21-46.

Lutze, G.F., Thiel, H., 1989. Epibenthic foraminifera from elevated microhabitats: *Cibicidoides wuellerstorfi* and *Planulina ariminensis*. Journal of Foraminiferal Research 19 (2), 153-158.

Mackensen, A., 1987. Benthische Foraminiferen-Artengruppen auf dem Island-Schottland-Rücken: Umweltanzeiger an der Grenze zweier ozeanischer Räume. Paläontologische Zeitschrift 61, 149-179.

Mackensen, A., Hald, 1988. *Cassidulina teretis* Tappan and *C. laevigata* d'Orbigny: their living and late Quaternary distribution in northern seas. Journal of Foraminiferal Research 18 (1), 16-24.

Mackensen, A., Douglas, M., 1989. Down-core distribution of live and dead deep-water benthic foraminifera in box cores from the Weddell Sea and California continental borderland. Deep-Sea Research I 36 (6), 879-900.

Mackensen, A., Grobe, H., Kuhn, G., Fütterer, D.K., 1990. Benthic foraminiferal assemblages from the eastern Weddell Sea between 68° and 73° S: distribution, ecology and fossilization potential. Marine Micropaleontology 16, 241-283.

Mackensen, A., Fütterer, D.K., Grobe, H., Schmiedl, G., 1993a. Benthic foraminiferal assemblages from the eastern South Atlantic Polar Front region between 35° and 57° S: distribution, ecology and fossilization potential. Marine Micropaleontology 22, 33-69.

Mackensen, A., Hubberten, H.-W., Bickert, T., Fischer, G., Fütterer, D.K., 1993b. The $\delta^{13}C$ in benthic foraminiferal tests of *Fontbotia wuellerstorfi* (Schwager) relative to the $\delta^{13}C$ of dissolved inorganic carbon in southern ocean deep water: implications for glacial ocean circulation models. Paleoceanography 8 (5), 587-610.

Mackensen, A., Schmiedl, G., Harloff, J., Giese, M., 1995. Deep-sea foraminifera in the South Atlantic Ocean: ecology and assemblage generation. Micropaleontology 41 (4), 342-358.

Mackensen, A., Schumacher, S., Radke, J., Schmidt, D.N., 2000. Microhabitat preferences and stable carbon isotopes of endobenthic foraminifera: clue to quantitative reconstruction of oceanic new production. Marine Micropaleontology 40, 233-258.

Mackensen, A., Rudolph, M., Kuhn, G., 2001. Late Pleistocene deep-water circulation in the subantarctic eastern Atlantic. Global and Planetary Change 30, 197-229.

Mackensen, A., Licari, L., 2004. Carbon isotopes of live benthic foraminifera from the South Atlantic: Sensitivity to bottom water carbonate saturation state and organic matter rain rates. In: Wefer, G., Mulitza, S., Ratmeyer, V. (Eds.), The South Atlantic in the Late Quaternary. Reconstruction of material budget and current systems. Springer-Verlag, Berlin.

Mackensen, A., Wollenburg, J.E., Licari, L., 2006. Low $\delta^{13}C$ in tests of live epibenthic and endobenthic foraminifera at a site of active methane seepage. Paleoceanography.

Martinez, P., Bertrand, P., Shimmield, G.B., Cochrane, K., Jorissen, F.J., Foster, J., Dignan, M., 1999. Upwelling intensity and ocean productivity changes off Cape Blanc (northwest Africa) during the last 70000 years: geochemical and micropalaeontological evidence. Marine Geology 158, 57-74.

McCorkle, D.C., Keigwin, L., Corliss, B.H., Emerson, S., 1990. The influence of microhabitats on the carbon isotopic composition of deep-sea benthic foraminifera. Paleoceanography 5 (2), 161-185.

McCorkle, D.C., Keigwin, L., 1994. Depth profiles of $\delta^{13}C$ in bottom water and core top *C. wuellerstorfi* on the Ontong Java Plateau and Emperor Seamounts. Paleoceanography 9 (2), 197-208.

McCorkle, D.C., Veeh, H.H., Heggie, D.T., 1994. Glacial-Holocene paleoproductivity off western Australia: a comparison of proxy records. In: Zahn, R., Pedersen, T.F., Kaminski, M.A., Labeyrie, L. (Eds.), Carbon cycling in the glacial ocean: constraints on the ocean‘s role in global change. NATO ASI Series, Springer, Heidelberg, 443-480.

McCorkle, D.C., Corliss, B.H., Farnham, C.A., 1997. Vertical distribution and stable isotopic compositions of live (stained) benthic foraminifera from the North Carolina and California continental margins. Deep-Sea Research I 44 (6), 983-1024.

Meggers, H., Freudenthal, T., Nave, S., Targarona, J., Abrantes, F., Helmke, P., 2002. Assessment of geochemical and micropaleontological sedimentary parameters as proxies of surface water properties in the Canary Islands region. Deep-Sea Research II 49, 3631-3654.

Mittelstaedt, E., 1991. The ocean boundary along the northwest African coast: Circulation and oceanographic properties at the sea surface. Progress in Oceanography 26, 307-355.

Mix, A.C., Bard, E., Schneider, R., 2001. Environmental processes of the ice age: land, oceans, glaciers (EPILOG). Quaternary Science Reviews 20, 627-657.

Moreno, A., Nave, S., Kuhlmann, H., Canals, M., Targarona, J., Freudenthal, T., Abrantes, F., 2002. Productivity response in the North Canary Basin to climate changes during the last 250000 yr: a multi-proxy approach. Earth and Planetary Science Letters 196, 147-159.

Morigi, C., Jorissen, F.J., Gervais, A., Guichard, S., Borsetti, A.M., 2001. Benthic foraminiferal faunas in surface sediments off NW Africa: relationship with organic flux to the ocean floor. Journal of Foraminiferal Research 31, 350-368.

Murray, J.W., Weston, J.F., Haddon, C.A., Powell, A.D.J., 1986. Miocene to recent bottom water masses of the north-east Atlantic: an analysis of benthic foraminifera. In: Summerhays, C.P., Shackleton, N.J. (Eds.), North Atlantic Palaeoceanography. Geological Society Special Publication, 219-230.

Murray, J.W., 1991. Ecology and palaeoecology of benthic foraminifera. Longman Scientific & Technical, Harlow, 397 pp.

Murray, J.W., Bowser, S.S., 2000. Mortality, protoplasm decay rate, and reliability of staining techniques to recognize ‚living‘ foraminifera: a review. Journal of Foraminiferal Research 30 (1), 66-70.

Nave, S., Freitas, P., Abrantes, F., 2001. Coastal upwelling in the Canary Island region: spatial variability reflected by the surface sediment diatom record. Marine Micropaleontology 42, 1-23.

Nykjaer, L., van Camp, L., 1994. Seasonal and interannual variability of coastal upwelling along northwest Africa and Portugal from 1981 to 1991. Journal of Geophysical Research 99 (C7), 14,197-14,207.

Parrilla, G., Siedler, G., Niell, X., Wefer, G., Ambar, I., paricipants, 1999. CANIGO (MAS3-CT96-0060) Final Scientific Report, Instituto Espanol de Oceanografia/EU Mast Office.

Pelegrí, J.L., Marrero-Díaz, A., Ratsimandresy, A.W., Antoranz, A., Cisneros-Aguirre, J., Gordo, C., Grisolía, D., Hernández-Guerra, A., Láiz, I., Martínez, A., Parrilla, G., Pérez-Rodríguez, P., Rodríguez-Santana, A., Sangrà, P., 2005. Hydrographic cruises off northwest Africa: the Canary Current and the Cape Ghir region. Journal of Marine Systems 54, 39-63.

Phleger, 1960. Ecology and distribution of recent foraminifera, John Hopkins Press, Baltimore, 297 pp.

Phleger, F.B., Parker, F.L., 1951. Ecology of foraminifera, northwest Gulf of Mexico (part I. Foraminifera distribution (Phleger), part II. Foraminifera Species (Phleger & Parker). Geol. Soc. Am. Mem. 46, part I: 1-88, part II: 1-64.

Phleger, F.B., Parker, F.L., Peirson, J.F., 1953. North Atlantic Foraminifera. Reports Swedish Deep Sea Expedition, 7, 122 pp.

Rathburn, A.E., Corliss, B.H., 1994. The ecology of living (stained) deep-sea benthic foraminifera from the Sulu Sea. Paleoceanography 9 (1), 87-150.

Rathburn, A.E., Corliss, B.H., Tappa, K.D., Lohmann, K.C., 1996. Comparisons of the ecology and stable isotopic compositions of living (stained) benthic foraminifera from the Sulu and South China Seas. Deep-Sea Research I 43 (10), 1617-1646.

Rathburn, A.E., Levin, L.A., Held, Z., Lohmann, K.C., 2000. Benthic foraminifera associated with cold methane seeps on the northern California margin: ecology and stable isotopic composition. Marine Micropaleontology 38, 247-266.

Rathburn, A.E., Perez, M.E., Martin, J.B., Day, S.A., Mahn, C., Gieskes, J., Ziebis, W., Williams, D., Bahls, A., 2003. Relationships between the distribution and stable isotopic composition of living benthic foraminifera and cold methane seep biogeochemistry in Monterey Bay, California. Geochemistry, Geophysics, Geosystems 4, doi:1110.1029/2003GC000595.

Sarnthein, M., Tetzlaff, G., Koopmann, B., Wolter, K., Pflaumann, U., 1981. Glacial and interglacial wind regimes over the eastern subtropical Atlantic and North-West Africa. Nature 193, 193-196.

Sarnthein, M., Thiede, J., Pflaumann, U., Erlenkeuser, H., Fütterer, D.K., Koopmann, B., Lange, H., Seibold, E., 1982. Atmospheric and oceanic circulation patterns off Northwest Africa during the past 25 million years. In: von Rad, U., Hinz, K., Sarnthein, M., Seibold, E. (Eds.), Geology of the Northwest African Continental Margin. Springer, Berlin, Heidelberg, New York, 545-604.

Sarnthein, M., Winn, K., Duplessy, J.-C., Fontugne, M.R., 1988. Global variations of surface ocean productivity in low and mid latitudes: influence on CO_2 reservoirs of the deep ocean and atmosphere during the last 21000 years. Paleoceanography 3 (3), 361-399.

Sarnthein, M., Winn, K., Jung, S.J.A., Duplessy, J.-C., Labeyrie, L., Erlenkeuser, H., Ganssen, G.M., 1994. Changes in east Atlantic deepwater circulation over the last 30,000 years: Eight time slice reconstructions. Paleoceanography 9 (2), 209-267.

Schiebel, R., 1992. Rezente benthische Foraminiferen in Sedimenten des Schelfes und oberen Kontinentalhanges im Golf von Guinea (Westafrika). PhD Thesis, Christian-Albrecht-Universität, Kiel, 179 pp.

Schmiedl, G., 1995. Rekonstruktion der spätquartären Tiefenwasserzirkulation und Produktivität im östlichen Südatlantik anhand von benthischen Foraminiferenvergesellschaftungen, Berichte zur Polarforschung, Alfred Wegener Institut, Bremerhaven, Nr. 160, 207 pp.

Schmiedl, G., Mackensen, A., Müller, P.J., 1997. Recent benthic foraminifera from the eastern South Atlantic Ocean: dependence on food supply and water masses. Marine Micropaleontology 32, 249-287.

Schmiedl, G., De Bovee, F., Buscail, R., Charriere, B., Hemleben, C., Medernach, L., Picon, P., 2000. Trophic control of benthic foraminiferal abundance and microhabitat in the bathyal Gulf of Lions, western Mediterranean Sea. Marine Micropaleontology 40, 167-188.

Schmiedl, G., Pfeilsticker, M., Hemleben, C., Mackensen, A., 2004. Environmental and biological effects on the stable isotope composition of recent deep-sea benthic foraminifera from the Western Mediterranean Sea. Marine Micropaleontology 51, 129-152.

Schmiedl, G., Mackensen, A. in press. Multispecies stable isotopes of benthic foraminifers reveal past changes of organic matter decomposition and deep-water oxygenation in the Arabian Sea. Paleoceanography, Vol.21, doi 10.1029/2006PA001284.

Schnitker, D., 1974. West Atlantic abyssal circulation during the past 120.000 years. Nature 248, 385-387.

Schnitker, D., 1979. The deep waters of the western North Atlantic during the past 24,000 years, and the re-initiation of the western boundary undercurrent. Marine Micropaleontology 4, 265-280.

Schnitker, D., 1980. Quaternary deep-sea benthic foraminifers and bottom water masses. In: Donanth, F.A., Stehli, F.G., Wetherill, G.W. (Eds.), Annual review of earth and planetary sciences, 343-370.

Schönfeld, J., 2001. Benthic foraminifera and pore-water oxygen profiles: a re-assessment of species boundary conditions at the western Iberian Margin. Journal of Foraminiferal Research 31 (2), 86-107.

Schumacher, S., 2001. Mikrohabitatansprüche benthischer Foraminiferen in Sedimenten des Südatlantiks. Berichte zur Polarforschung, Alfred Wegener Institut, Bemerhaven, Nr. 403, 151 pp.

Sen Gupta, B.K., 1989. Morphology and generic placement of the foraminifer „*Anomalina*“ *wuellerstorfi* Schwager. Journal of Paleontology 63 (5), 706-713.

Sen Gupta, B.K., Machain-Castillo, M.L., 1993. Benthic foraminifera in oxygen-poor habitats. Marine Micropaleontology 20, 183-201.

Sen Gupta, B.K., 1999. Systematics of modern foraminifera. In: Gupta, B.K.S. (Ed.), Modern foraminifera. Kluwer Academic Publishers, pp. 7-36.

Sicre, M.-A., Ternois, Y., Paterne, M., Boireau, A., Beaufort, L., Martinez, P., Bertrand, P., 2000. Biomarker stratigraphic records over the last 150 kyears off the NW African coast at 25°N. Organic Geochemistry 31, 577-588.

Sicre, M.-A., Ternois, Y., Paterne, M., Martinez, A., Bertrand, P., 2001. Climatic changes in the upwelling region off Cap Blanc, NW Africa, over the last 70 kyrs: a multi-biomarker approach. Organic Geochemistry 32, 981-990.

Smart, C.W., King, S.C., Gooday, A.J., Murray, J.W., Thomas, E., 1994. A benthic foraminiferal proxy of pulsed organic matter paleofluxes. Marine Micropaleontology 23, 89-99.

Smart, C.W., Gooday, A.J., 1997. Recent benthic foraminifera in the abyssal northeast Atlantic Ocean: relation to phytodetrital inputs. Journal of Foraminiferal Research 27 (2), 85-92.

Stevens, I., Johnson, J., 2003. A numerical modelling study of upwelling filaments off the NW African coast. Oceanologica Acta 26, 549-564.

Stramma, L., Siedler, G., 1988. Seasonal changes in the North Atlantic subtropical gyre. Journal of Geophysical Research 93 (C7), 8111-8118.

Streeter, S.S., 1973. Bottom water and benthonic foraminifera in the Northern Atlantic - Glacial-Interglacial contrasts. Quaternary Research 3, 131-141.

Summerhayes, C.P., Milliman, J.D., Briggs, S.R., Bee, A.G., Hogan, C., 1976. Northwest African shelf sediments: influence of climate and sedimentary processes. Journal of Geology 84, 277-300.

Ter Braak, C.J.F., 1986. Canonical correspondence analysis: a new eigenvector technique for multivariate direct gradient analysis. Ecology 67 (5), 1167-1179.

Ternois, Y., Sicre, M.-A., Paterne, M., 2000. Climatic changes along the northwestern African continental margin over the last 30 kyrs. Geophysical Research Letters 27 (1), 133-136.

Thomas, E., Gooday, A.J., 1996. Cenozoic deep-sea benthic foraminifers: tracers for changes in oceanic productivity? Geology 24 (4), 355-358.

Timm, S., 1992. Rezente Tiefsee-Benthosforaminiferen aus Oberflächensedimenten des Golfes von Guinea (Westafrika) - Taxonomie, Verbreitung, Ökologie und Korngrössenfraktionen, Christian-Albrecht-Universität, Kiel, 192 pp.

Van Camp, L., Nykjaer, L., Mittelstaedt, E., Schlittenhardt, P., 1991. Upwelling and boundary circulation off Northwest Africa as depicted by infrared and visible satellite observations. Progress in Oceanography 26, 357-402.

Van Leeuwen, R.J.W., 1989. Sea-floor distributions and Late Quaternary faunal patterns of planktonic and benthic foraminifers in the Angola Basin. Utrecht Micropaleontological Bulletins 38, 1-287.

Vergnaud Grazzini, C., Pierre, C., 1991. High fertility in the Alboran Sea since the Last Glacial Maximum. Paleoceanography 6 (4), 519-536.

Walton, W.R., 1952. Techniques for recognition of living Foraminifera. Contribution Cushman Foundation of Foraminiferal Research 3, 55-60.

Wefer, G., Heinze, P.-M., Berger, W.H., 1994. Clues to ancient methane release. Nature 369, 282.

Wefer, G., Segl, M., Bassek, D., Buhlmann, K., Deeken, A., Dehning, K., Diekamp, V., Drünert, F., Eberwein, A., Franke, P., Freudenthal, T., Geisen, M., Godoy, J., Gonzales-Davila, M., Günther, L., Hayn, C., Henderiks, J., Irmisch, A., Jeronimo, D., Kotte, N., Koy, U., Kretschmar, F., Langer, J., Makaoui, A., Maroto, L., Meggers, H., Meinecke, G., Metzler, W., Moreno, A., Nave, S., Neuer, S., Nowald, N., Ratmeyer, V., Rieß, W., Rosiak, U., Schroeter, M., Sprengel, C., Taragarona, J., Thiele, J., Thierstein, H., von Oppen, V., Waldmann, C., 1999. Report and preliminary results of *Meteor*-Cruise M 42/4, Las Palmas - Las Palmas - Viena do Castelo, 26.09.1998 - 26.10.1998. Berichte Fachbereich Geowissenschaften, Universität Bremen, 132, 104 pp.

Wollenburg, J.E., 1992. Zur Taxonomie von rezenten benthischen Foraminiferen aus dem Nansen Becken, Woodruff, F., Savin, S.M., Douglas, R.G., 1980. Biological fractionation of oxygen and carbon isotopes by recent benthic foraminifera. Marine Micropaleontology 5, 3-11.

Wooster, W.S., Bakun, A., McLain, D.R., 1976. The seasonal upwelling cycle along the eastern boundary of the North Atlantic. Journal of Marine Research 34 (2), 131-141.

Zahn, R., Winn, K., Sarnthein, M., 1986. Benthic foraminiferal $\delta^{13}C$ and accumulation rates of organic carbon: *Uvigerina peregrina* group and *Cibicidoides wuellerstorfi*. Paleoceanography 1 (1), 27-42.

Zahn, R., Sarnthein, M., Erlenkeuser, H., 1987. Benthic isotope evidence for changes of the Mediterranean outflow during the Late Quaternary. Paleoceanography 2 (6), 543-559.

Zahn, R., Mix, A.C., 1991. Benthic foraminiferal δ^{18}O in the ocean‘s temperature-salinity-density field: constraints on ice age thermohaline circulation. Paleoceanography 6 (1), 1-20.

Zhao, M., Eglington, G., Haslett, S.K., Jordan, R.W., Sarnthein, M., Zhang, Z., 2000. Marine and terrestrial biomarker records for the last 35000 years at ODP site 658C off NW Africa. Organic Geochemistry 31, 919-930.

APPENDIX

Taxonomic list

All dominant species described and discussed within this PhD thesis are listed. The taxonomic classification of benthic foraminiferal species is based on the work by Loeblich & Tappan (1988) and Jones (1994). The original name is given with an asteriks to facilitate the locating within Ellis & Messina (1949). Scanning Electron Microscope pictures of selected species are presented in two plates.

Order **FORAMINIFERIDA** Eichwald 1830

Suborder **TEXTULARIINA** Delage & Hérouard 1896

Bigeneria cylindrica Cushman 1922
*1922 *B. cylindrica* Cushman
1994 *B. cylindrica* Cushman – Jones, Pl. 44; Figs. 19-24

Cribrostomoides jeffreysii (Williamson 1858) Plate I, Fig. 8
*1858 *Nonionina jeffreysii* Williamson
1990 *C. jeffreysii* (Williamson) – Mackensen et al., Pl. 4; Fig. 1
1992 *C. jeffreysii* (Williamson) – Wollenburg, Pl. 5; Figs. 1,4
1994 *Veleroninoides jeffreysii* (Williamson) – Jones, Pl. 35; Figs. 1-3,5
2001 *C. jeffreysii* (Williamson) – Schumacher, Pl. 3; Fig. 10

Reophax dentaliniformis Brady 1881 Plate II, Fig. 8
*1881 *R. dentaliniformis* Brady
1990 *R. dentaliniformis* Brady – Mackensen et al., Pl. 6; Fig. 3
1992 *R. dentaliniformis* Brady – Timm, Pl. 2; Fig. 4
1994 *R. dentaliniformis* Brady – Jones, Pl. 30; Figs. 21,22

Suborder **ROBERTININA** Loeblich & Tappan 1984

Hoeglundina elegans (d'Orbigny 1826) Plate I, Fig. 14
*1826 *Rotalia (Turbinulina) elegans* d'Orbigny
1960 *H. elegans* (d'Orbigny) – Barker, Pl. 105; Figs. 3-6
1993a *H. elegans* (d'Orbigny) – Mackensen et al., Pl. 1; Figs. 9,10
1994 *H. elegans* (d'Orbigny) – Jones, Pl. 105; Figs. 3-6
2001 *H. elegans* (d'Orbigny) – Schumacher, Pl. 5; Figs. 11,12

Suborder **MILIOLINA** Delage & Hérouard 1896

Pyrgoella irregularis (d’Orbigny 1839) Plate II, Fig. 7
*1884 *Biloculina irregularis* d’Orbigny
1960 *Nummoloculina irregularis* (d’Orbigny) – Barker, Pl. 1; Figs. 17,18
1994 *P. irregularis* (d’Orbigny) – Jones, Pl. 1; Figs. 17,18

Suborder **ROTALIINA** Delage & Hérouard 1896

Bolivina albatrossi Cushman 1922 Plate I, Fig. 1
*1922 *B. albatrossi* Cushman
1992 *B. albatrossi* Cushman – Schiebel, Pl. 1; Fig. 1a,b
1992 *B. albatrossi* Cushman – Timm, Pl. 5; Fig. 2

Brizalina spathulata (Williamson 1858) Plate I, Fig. 2
*1858 *Textularia variabilis* var *spathulata* Williamson
1994 *B. spathulata* (Williamson) – Jones, Pl. 52; Figs. 20,21

Bulimina aculeata d’Orbigny 1826 Plate I, Fig. 3
*1826 *B. aculeata* d’Orbigny
1960 *B. aculeata* d’Orbigny – Barker, Pl. 51; Figs. 7–9
1990 *B. aculeata* d’Orbigny – Mackensen et al., Pl. 2; Figs. 1-3
1993a *B. aculeata* d’Orbigny – Mackensen et al., Pl. 1; Figs. 3,4
1994 *B. aculeata* d’Orbigny – Jones, Pl. 51; Figs. 7-9
1995 *B. aculeata* d’Orbigny – Schmiedl, Pl. 2; Fig. 11
2001 *B. aculeata* d’Orbigny – Schumacher, Pl. 6; Figs. 5,6

Bulimina marginata d’Orbigny 1826 Plate I, Fig. 4
*1826 *B. marginata* d’Orbigny
1960 *B. marginata* d’Orbigny – Barker, Pl. 51; Figs. 3-5
1994 *B. marginata* d’Orbigny – Jones, Pl. 51; Figs. 3-5
1995 *B. marginata* d’Orbigny – Schmiedl, Pl. 2; Fig. 10

Bulimina mexicana (Cushman 1922) Plate I, Fig. 5
*1922 *Bulimina inflata* var *mexicana* Cushman
1994 *B. mexicana* (Cushman) – Jones, Pl. 51; Figs. 10-13
1995 *B. mexicana* (Cushman) – Schmiedl, Pl. 2; Fig. 13
1997 *B. mexicana* (Cushman) – Schmiedl, Pl. 1; Fig. 12
2001 *B. mexicana* (Cushman) – Schumacher, Pl. 6; Figs. 7,8
2005 *B. mexicana* (Cushman) – Licari, Pl. 1; Figs. 12,13

Cassidulina laevigata d'Orbigny 1826

*1826 *C. laevigata* d'Orbigny
1960 *C. carinata* Silvestri 1896 – Barker, Pl. 54; Figs. 2,3
1988 *C. laevigata* d'Orbigny – Mackensen & Hald, Pl. 1; Figs. 1-7
1992 *C. laevigata* d'Orbigny – Schiebel, Pl. 2; Fig. 11
1994 *C. laevigata* var *carinata* Silvestri 1896 – Jones, Pl. 54; Figs. 2-3
1997 *C. laevigata* d'Orbigny – Schmiedl, Pl. 1; Figs. 13,14

Chilostomella oolina Schwager 1878 Plate I, Fig. 6

*1878 *C. oolina* Schwager
1985 *C. oolina* Schwager – Corliss, Pl. 1; Figs. 7
1994 *C. oolina* Schwager – Jones, Pl. 55; Figs. 12-14, 17-18
2001 *C. oolina* Schwager – Schumacher, Pl. 6; Fig. 11
2005 *C. oolina* Schwager – Licari, Pl. 2; Fig. 11

Cibicidoides kullenbergi Parker 1953 Plate I, Fig. 7

*1953 *Cibicidoides kullenbergi* Parker
1989 *Cibicides kullenbergi* (Parker) – van Leeuwen, Pl. 9; Figs. 1-3
1995 *C. kullenbergi* Parker – Schmiedl, Pl. 4; Figs. 5,6
1997 *C. kullenbergi* Parker – Schmiedl, Pl. 3; Figs. 16,17
2001 *C. kullenbergi* Parker – Schumacher, Pl. 8; Figs. 7-9

Cibicidoides wuellerstorfi (Schwager 1866)

*1866 *Anomalina wuellerstorfi* Schwager
1960 *Planulina wuellerstorfi* Schwager – Barker, Pl. 93; Fig. 9
1987 *Cibicidoides wuellerstorfi* (Schwager) – Mackensen, Fig. 11 n
1988 *Fontbotia wuellerstorfi* (Schwager) – Loeblich & Tappan, Pl. 634; Figs. 10-12 / Pl. 635; Figs. 1-3
1989 *Cibicides wuellerstorfi* (Schwager) – van Leeuwen, Pl. 10; Figs. 1-9
1989 *Cibicides wuellerstorfi* (Schwager) – Sen Gupta, Figs. 1-3
1993a *Cibicidoides wuellerstorfi* (Schwager) – Mackensen et al., Pl. 2; Figs. 4,5
1994 *C. wuellerstorfi* (Parker) – Jones, Pl. 93; Figs. 8,9
1995 *Fontbotia wuellerstorfi* (Parker) – Schmiedl, Pl. 4; Figs. 7-9
2001 *C. wuellerstorfi* (Parker) – Schumacher, Pl. 8; Figs. 10-12

Epistominella exigua (Brady 1884) Plate I, Fig. 9

*1884 *Pulvinulina exigua* Brady
1960 *E. exigua* (Brady) – Barker, Pl. 103; Figs. 13,14
1987 *E. exigua* (Brady) – Mackensen, Figs. 11 h-i
1990 *E exigua* (Brady) – Mackensen et al., Pl. 7; Figs. 1,2
1992 *E. exigua* (Brady) – Timm, Pl. 7; Fig. 6
1993a *E exigua* (Brady) – Mackensen et al., Pl. 7; Figs. 1,2
1994 *Alabaminoides exiguus* (Brady) – Jones, Pl. 103; Figs. 13,14
1995 *E. exigua* (Brady) – Schmiedl, Pl. 5; Figs. 7-9
1997 *E. exigua* (Brady) – Schmiedl, Pl. 2; Figs. 7-9
2001 *E. exigua* (Brady) – Schumacher, Pl. 7; Figs. 11-13
2005 *E. exigua* (Brady) – Licari, Pl. 2; Figs. 12-14

Eponides pusillus Parr 1950

*1950 *E. pusillus* Parr
1960 *E. pusillus* Parr – Phleger et al., Pl. 9; Figs. 5,6
1989 *Nuttallides pusillus pusillus* (Parker) – van Leeuwen, Pl. 14; Figs. 4-12
1992 *Epistominella pusilla* (Parr) – Timm, Pl. 7; Fig. 9

Gavelinopsis translucens (Phleger & Parker 1951) Plate I, Figs. 10,11

*1951 *„Rotalia“ translucens* Phleger & Parker
1992 *G. translucens* (Phleger & Parker) – Timm, Pl. 7; Fig. 12
1995 *G. translucens* (Phleger & Parker) – Schmiedl, Pl. 6; Figs. 17,18
2005 *G. translucens* (Phleger & Parker) – Licari, Pl. 1; Figs. 5-7

Globobulimina affinis (d'Orbigny 1839) Plate I, Fig. 12

*1839 *Bulimina affinis* d'Orbigny
1947 *G.* sp. a Cushman – Hoeglund, Pl. 20; Figs. 4a-c / Pl. 21; Figs. 1,6 / Pl. 22 / Fig. 2 / Text-Figs. 234-237
?1947 *G.* sp. b Cushman – Hoeglund, Pl. 21; Figs. 2,7 / Pl. 22; Fig. 3 / Text-Figs. 238-242
1953 *G. affinis* (d'Orbigny) – Phleger et al., Pl. 6; Figs. 32
1985 *G. affinis* (d'Orbigny) – Corliss, Pl. 1; Fig. 8
2005 *G. affinis* (d'Orbigny) – Licari, Pl. 2; Fig. 6

Globobulimina hoeglundi (Cushman 1921) Plate I, Fig. 13

*1921 *Bulimina subaffinis* (Cushman)
1947 *G.* sp. c (Cushman) – Hoeglund, Pl. 21; Fig. 3 / Pl. 22; Fig. 4 / Text-Figs. 243-246
*1960 *G. hoeglundi* (Uchio), Pl. 6; Figs. 7,8

Globocassidulina subglobosa (Brady 1881)

*1881 *Cassidulina subglobosa* Brady

1993a *G. subglobosa* (Brady) – Mackensen et al., Pl. 2; Fig. 9

1994 *G. subglobosa* (Brady) – Jones, Pl. 52; Fig. 17

1995 *G. subglobosa* (Brady) – Schmiedl, Pl. 6; Fig. 16

1997 *G. subglobosa* (Brady) – Schmiedl, Pl. 2; Fig. 18

2001 *G. subglobosa* (Brady) – Schumacher, Pl. 7; Fig. 1

Hyalinea balthica (Schröter 1783) Plate II, Fig. 1

*1783 *Nautilus balthicus* Schröter

1960 *H. balthica* (Schröter) – Barker, Pl. 112; Figs. 1,2

1994 *H. balthica* (Schröter) – Jones, Pl. 112; Figs. 1,2

Lobatula lobatula (Walker & Jacob 1798)

*1798 *Nautilus lobatulus* Walker & Jacob

1953 *Cibicides lobatulus* (Walker & Jacob) – Phleger et al., Pl. 11; Figs. 9,14

1960 *C. lobatulus* (Walker & Jacob) – Barker, Pl. 92; Fig. 20 / Pl. 93; Figs. 1,4,5

1987 *C. lobatulus* (Walker & Jacob) – Mackensen, Fig. 10a

1988 *L. vulgaris* (Walker & Jacob) – Loeblich & Tappan, Pl. 637; Figs. 10-13

1994 *C. lobatulus* (Walker & Jacob) – Jones, Pl. 92; Fig. 10 / Pl. 93; Figs. 1,4-5 / Pl. 115; Figs. 4-5

Melonis barleeanum (Williamson 1858) Plate II, Fig. 2

*1858 *Nonionina barleeana* Williamson

1960 *Nonion barleeanum* (Williamson) – Barker, Pl. 109; Figs. 8,9

1989 *M. barleeanus* (Williamson) – van Leeuwen, Pl. 13; Figs. 1,2

1992 *M. barleeanum* (Williamson) – Timm, Pl. 6; Fig. 6

1994 *M. barleeanus* (Williamson) – Jones, Pl. 13; Figs. 1,2

1995 *M. barleeanum* (Williamson) – Schmiedl, Pl. 3; Figs. 9,10

1997 *M. barleeanum* (Williamson) – Schmiedl, Pl. 2; Figs. 10,11

2001 *M. barleeanum* (Williamson) – Schumacher, Pl. 9; Figs. 7,8

2005 *M. barleeanum* (Williamson) – Licari, Pl. 1; Figs. 10,11

Melonis pompiloides (Fichtel & Moll 1798) Plate II, Fig. 3
*1798 *Nautilus pompilioides* Fichtel & Moll
1960 *Nonion pompilioides* (Fichtel & Moll) – Barker, Pl. 109; Figs. 10,11
1993a *M. pompilioides* (Fichtel & Moll) – Mackensen et al., Pl. 3; Figs. 6,7
1994 *M. pompilioides* (Fichtel & Moll) – Jones, Pl. 109; Figs. 10-12
1995 *M. pompilioides* (Fichtel & Moll) – Schmiedl, Pl. 3; Figs. 7,8
1997 *M. pompilioides* (Fichtel & Moll) – Schmiedl, Pl. 2; Figs. 14,15
2001 *M. pompilioides* (Fichtel & Moll) – Schumacher, Pl. 9; Figs. 5,6

Nonion asterizans (Fichtel & Moll 1798) Plate II, Figs. 4,5
*1798 *Nautilus asterizans* Fichtel & Moll
1953 *N. asterizans* (Fichtel & Moll) – Phleger et al., Pl. 6; Fig. 3
1960 *N.* cf *asterizans* (Fichtel & Moll) – Barker, Pl. 109; Figs. 12,13
1980 *N. asterizans* (Fichtel & Moll) – Haake, Pl. 3; Fig. 18
1992 *N. asterizans* (Fichtel & Moll) – Schiebel, Pl. 5; Fig. 14

Nonionella iridea Heron-Allen & Earland 1932 Plate II, Fig. 6
*1932 *N. iridea* Heron-Allen & Earland
1990 *N. iridea* Heron-Allen & Earland – Mackensen et al., Pl. 1; Figs. 7-9
1992 *N. iridea* Heron-Allen & Earland – Wollenburg, Pl. 19; Figs. 7-8 / Pl. 20; Fig. 1
1995 *N. iridea* Heron-Allen & Earland – Schmiedl, Pl. 3; Figs. 15-16
2001 *N. iridea* Heron-Allen & Earland – Gooday, Fig. 1B

Sphaeroidina bulloides Deshayes 1832 Plate II, Fig. 9
*1832 *S. bulloides* Deshayes
1994 *S. bulloides* Deshayes – Jones, Pl. 84; Figs. 1-5, ?6-7
2001 *S. bulloides* Deshayes – Schumacher, Pl. 6; Fig. 12
2005 *S. bulloides* Deshayes – Licari, Pl. 2; Figs. 9,10

Trifarina bradyi (Cushman 1923) Plate II, Fig. 10
*1884 *Rhabdogonium tricarinata* - Brady
1923 *T. bradyi* (Cushman)
1960 *T. bradyi* (Cushman) – Barker, Pl. 67; Figs. 1-3
1994 *T. bradyi* (Cushman) – Jones, Pl. 67; Figs. 1-3

Uvigerina mediterranea Hofker 1932 Plate II, Fig. 11

*1932 *U. mediterranea* Hofker
*1952 *U. finisterrensis* Colom, Fig. 4
1960 *Euuvigerina peregrina* (Cushman) – Barker, Pl. 74; Figs. 11,12
1980 *U. finisterrensis* Colom – Haake, Pl. 2; Fig. 29
1994 *U. mediterranea* Hofker – Jones, Pl. 74; Figs. 11,12

Uvigerina peregrina Cushman 1923

*1923 *U. peregrina* Cushman
1986 *U. peregrina* Cushman – Lutze, Pl. 1; Figs. 1-6
1986 *U. hollicki* (Thalmann 1950) – Lutze, Pl. 2; Figs. 1-6
1995 *U. peregrina* Cushman – Schmiedl, Pl. 3; Figs. 1,2
1997 *U. peregrina* Cushman – Schmiedl, Pl. 1; Figs. 6,7
2001 *U. peregrina* Cushman – Schumacher, Pl. 6; Fig. 4
2005 *U. peregrina* Cushman – Licari, Pl. 1; Figs. 1,2

Valvulineria laevigata Phleger & Parker 1951 Plate II, Fig. 12

*1951 *V. laevigata* Phleger & Parker
1980 *V. laevigata* Phleger & Parker – Haake, Pl. 3; Fig. 3
1994 *V. laevigata* Phleger & Parker – Timm, Pl. 7; Fig. 14
1995 *V. laevigata* Phleger & Parker – Schmiedl, Pl. 4; Figs. 3,4

PLATE I

Scale bar = 100 µm

Fig. 1 *Bolivina albatrossi* Cushman 1922; GeoB 4237-2, fossil (LGM)

Fig. 2 *Brizalina spathulata* (Williamson 1858); GeoB 6008-2 (0–1 cm), live

Fig. 3 *Bulimina aculeata* d'Orbigny 1826; GeoB 6006-2 (5–6 cm), live

Fig. 4 *Bulimina marginata* d'Orbigny 1826; GeoB 6008-2 (4–5 cm), live

Fig. 5 *Bulimina mexicana* (Cushman 1922); GeoB 4236-2 (0–1 cm), dead

Fig. 6 *Chilostomella oolina* Schwager 1878; GeoB 6005-2, fossil (LGM)

Fig. 7 *Cibicidoides kullenbergi* Parker 1953; GeoB 4207-1 (0–1 cm), live

Fig. 8 *Cribrostomoides jeffreysii* (Williamson 1858); GeoB 4227-1 (0–1 cm), live

Fig. 9 *Epistominella exigua* (Brady 1884); GeoB GeoB 4217-5, fossil (LGM)

Fig. 10 *Gavelinopsis translucens* (Phleger & Parker 1951) – spiral side; GeoB 6006-2 (0–1 cm), dead

Fig. 11 *G. translucens* (Phleger & Parker 1951) – umbilical side; GeoB 6005-1 (0–1 cm), live

Fig. 12 *Globobulimina affinis* (d'Orbigny 1839); GeoB 5546-3 (0–1 cm), dead

Fig. 13 *Globobulimina hoeglundi* (Cushman 1921); GeoB 5546-3 (3–4 cm), live

Fig. 14 *Hoeglundina elegans* (d'Orbigny 1826) - spiral side; GeoB 6005-1 (0–1 cm), live


1


2

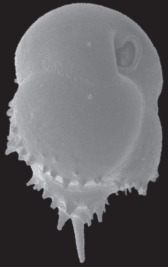
3


4


5

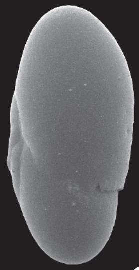
6


7


8

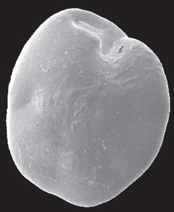
9

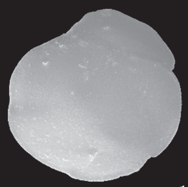
10


11


12


13

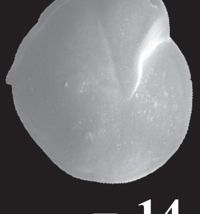
14

PLATE II

Scale bar = 100 µm

Fig. 1 *Hyalinea balthica* (Schröter 1783); GeoB 6007-1 (0–1 cm), dead

Fig. 2 *Melonis barleeanum* (Williamson 1858); GeoB 6006-2 (0–1 cm), dead

Fig. 3 *Melonis pompiloides* (Fichtel & Moll 1798) - apertural view; GeoB 4221-1, fossil (LGM)

Fig. 4 *Nonion asterizans* (Fichtel & Moll 1798); GeoB 6008-2 (0–1 cm), live

Fig. 5 *N. asterizans* (Fichtel & Moll 1798) - apertural view; GeoB 6008-2 (1–2 cm), live

Fig. 6 *Nonionella iridea* Heron-Allen & Earland 1932; GeoB 5540-2, fossil (LGM)

Fig. 7 *Pyrgoella irregularis* (d'Orbigny 1839); GeoB 4226-1 (0–1 cm), live

Fig. 8 *Reophax dentaliniformis* Brady 1881; GeoB 5542-3 (1–2 cm), live

Fig. 9 *Sphaeroidina bulloides* Deshayes 1832; GeoB 6005-1 (0–1 cm), dead

Fig. 10 *Trifarina bradyi* (Cushman 1923); GeoB 6006-2 (0–1cm), live

Fig. 11 *Uvigerina mediterranea* Hofker 1932; GeoB 6006-2 (5–6 cm), live

Fig. 12 *Valvulineria laevigata* Phleger & Parker 1951 - umbilical side; GeoB 5541-2 (2–3 cm), live

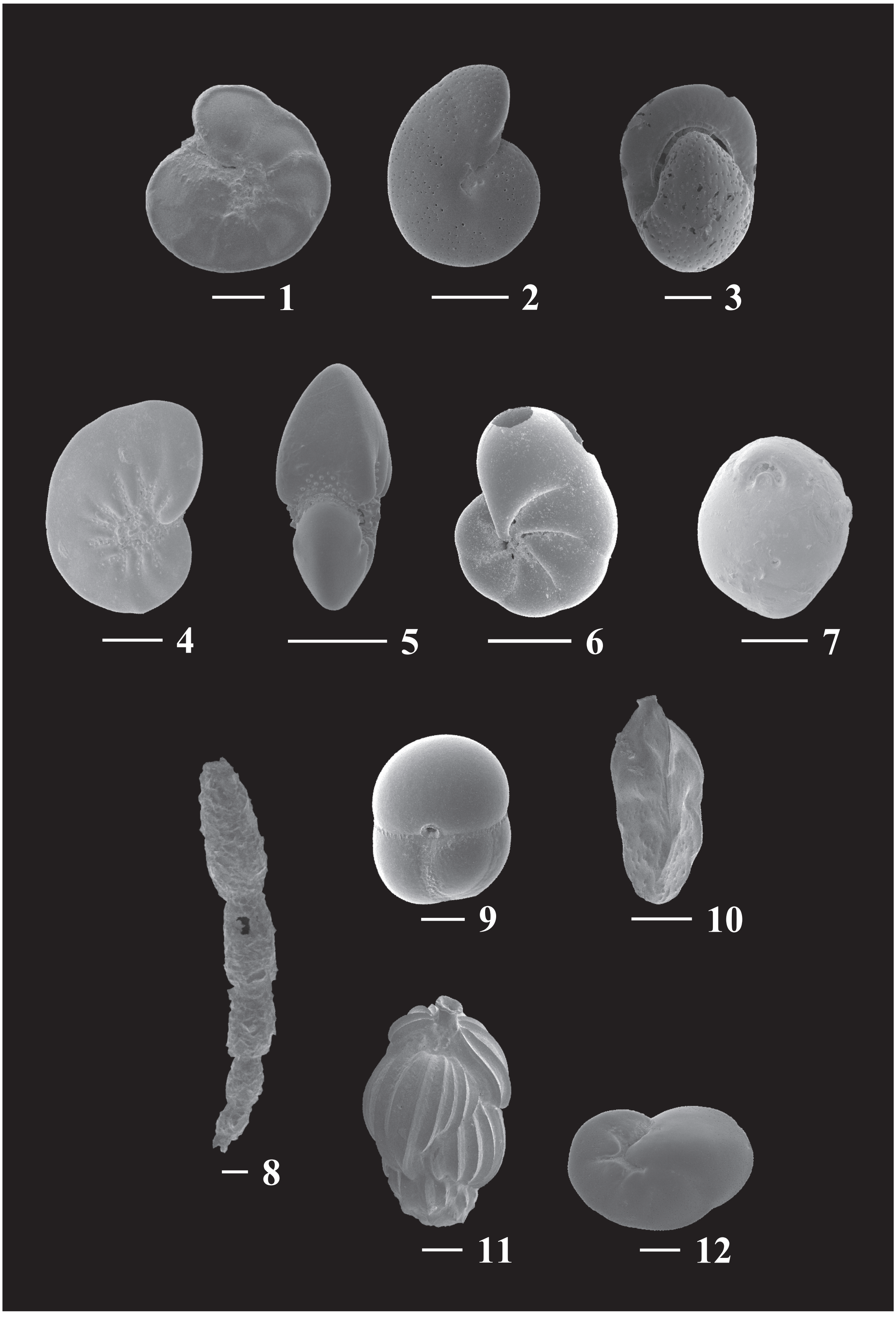
1
2
3
4
5
6
7
8
9
10
11
12